Electronic Supplementary Material (ESI) for Photochemical & Photobiological Science

Supplement

for

Sterically congested quinone methides in photodehydration reactions of 4-hydroxybiphenyl derivatives, and investigation of their antiproliferative activity

By

Nikola Basarić,*[a] Nikola Cindro,[a] Damir Bobinac,[a] Kata Mlinarić-Majerski,[a] Lidija Uzelac,[b] Marijeta Kralj[b] and Peter Wan,*[c]

[a] Department of Organic Chemistry and Biochemistry, Bijenička cesta 54, 10 000 Zagreb, Croatia. Fax: + 385 1 4680 195; Tel: +385 1 4561 141; E-mail: nbasaric@irb.hr

[b] Department of Molecular Medicine, Ruđer Bošković Institute, Bijenička cesta 54, 10 000 Zagreb, Croatia

[c] Department of Chemistry, University of Victoria, Box 3065 Stn CSC, Victoria BC, V8W3V6, Canada, Fax: + 1 (250) 721-7147, Tel: + 1 (250) 721-8976; E-mail: pwan@uvic.ca

Table of contents:

1. Experimental procedures and characterization of compounds

Suzuki reaction, general procedure

A two neck flask (100 mL) equipped with a condenser and a nitrogen inlet was charged with a methanol solution (15 mL) of 2-methoxyphenyl boronic acid (1.50 g, 10 mmol) and a toluene solution (35 mL) of dibromobenzene (2.33 g, 10 mmol). To the mixture was added anhydrous potassium carbonate (2.73 g, 19.72 mmol) and *tetrakis*-triphenylphosphine palladium $Pd(PPh_3)_4$ (0.17 g, 0.148 mmol), and the mixture was heated at the temperature of reflux for 24 h. The next day, to the cooled mixture H_2O (50 mL) was added and the layers were separated. The aqueous layer was extracted with CH_2Cl_2 (3 × 30 mL), the organic layers were combined and dried over anhydrous $MgSO_4$. After filtration, the solvent was removed on a rotary evaporator to afford crude product that was purified on a column of silica gel using hexane-CH_2Cl_2 (2:1) as an eluent.

2-bromo-4'-methoxybiphenyl

From 4-methoxyphenyl boronic acid (1.52 g, 10 mmol) and *o*-dibromobenzene (2.35 g, 10 mmol), in the presence of potassium carbonate (2.74 g, 19.79 mmol) and $Pd(PPh_3)_4$ (0.15 g, 0.13 mmol), the reaction furnished 1.88 g (71 %) of the product in the form of yellowish oil.

^{1}H NMR ($CDCl_3$, 300 MHz) δ/ppm: 7.65 (d, 1H, J = 8.0 Hz), 7.28-7.38 (m, 4H), 7.16 (ddd, 1H, J = 1.0 Hz, J = 6.1 Hz, J = 8.0 Hz), 6.96 (d, 2H, J = 8.8 Hz), 3.85 (s, 3H).

3-bromo-4'-methoxybiphenyl.

From 4-methoxyphenyl boronic acid (1.51 g, 10 mmol) and *m*-dibromobenzene (2.34 g, 10 mmol), in the presence of potassium carbonate (2.73 g, 19.71 mmol) and $Pd(PPh_3)_4$ (0.124 g, 0.107 mmol), the reaction furnished 1.69 g (64 %) of the product in the form of yellowish oil.

^{1}H NMR ($CDCl_3$, 600 MHz) δ/ppm: 7.69 (t, 1H, J = 1.7 Hz), 7.48 (d, 2H, J = 8.7 Hz), 7.38-7.48 (m, 2H), 7.26 (t, 1H, J = 7.9 Hz), 6.97 (d, 2H, J = 8.7 Hz), 3.85 (s, 3H).

4-bromo-4'-methoxybiphenyl

From 4-methoxyphenyl boronic acid (1.52 g, 10 mmol) and *p*-dibromobenzene (2.59 g, 11 mmol), in the presence of potassium carbonate (2.74 g, 20.0 mmol) and $Pd(PPh_3)_4$ (0.15 g, 0.13 mmol), the reaction furnished 1.62 g (62%) of the product in the form of yellowish oil.

^{1}H NMR ($CDCl_3$, 300 MHz) δ/ppm: 7.52 (d, 2H, J = 8.5 Hz), 7.47 (d, 2H, J = 8.8 Hz), 7.39 (d, 2H, J = 8.5 Hz), 6.97 (d, 2H, J = 8.8 Hz), 3.84 (s, 3H).

4-methoxy-4'-methylbiphenyl

From 4-methoxyphenyl boronic acid (2.0 g, 13.2 mmol) and *p*-bromtoluene (2.26 g, 13.25 mmol), in the presence of potassium carbonate (3.65 g, 26.5 mmol) and $Pd(PPh_3)_4$ (0.15 g, 0.13 mmol), the reaction furnished 2.25 g (86%) of the product in the form of yellowish oil.

^{1}H NMR ($CDCl_3$, 300 MHz) δ/ppm: 7.50 (d, 2H, J = 8.8 Hz), 7.43 (d, 2H, J = 8.0 Hz), 7.21 (d, 2H, J = 8.0 Hz), 6.95 (d, 2H, J = 8.8 Hz), 3.83 (s, 3H), 2.37 (s, 3H); ^{13}C NMR ($CDCl_3$, 75 MHz) δ/ppm: 158.85 (s), 137.88 (s), 136.22 (s), 133.67 (s), 129.32 (d), 127.83 (d), 126.47 (d), 114.07 (d), 55.22 (q), 20.91 (q).

4-methoxy-4'-hydroxymethylbiphenyl

A two neck round bottom flask (250 mL) equipped with a condenser was charged with a solution of 4-methoxy-4'-methylbiphenyl (1.80 g, 9.1 mmol) in carbon tetrachloride (100 mL). To the solution NBS (1.77 g, 10 mmol) and AIBN (0.15 g, 0.91mmol) were added. The mixture was heated at the temperature of reflux until all NBS disappeared. The mixture was filtered to remove succinimide and the solvent was removed on a rotary evaporator. To the residue, calcium carbonate (4.0 g, 40 mmol) was added and suspended in a mixture of dioxane (50 mL) and water (50 mL). The suspension was refluxed for 24 h. Solvent was removed on a rotary evaporator. To the residue HCl (3M, 50 mL) was slowly added and resulting suspension extracted with methylene chloride (3 × 50 mL). Organic extracts were dried over anhydrous $MgSO_4$. After filtration and evaporation of the solvent the residue was chromatographed on a column of SiO_2

using CH_2Cl_2 as eluent and with increasing polarity by use of ethyl acetate. Reaction furnished 1.4 g (72%) of the pure product.

Colorless crystals, mp 164-166 °C; ^{1}H NMR ($CDCl_3$, 300 MHz) δ/ppm: 7.54 (d, 2H, J = 8.2 Hz), 7.52 (d, 2H, J = 8.8 Hz), 7.41 (d, 2H, J = 8.2 Hz), 6.97 (d, 2H, J = 8.8 Hz), 4.72 (s, 2H), 3.85 (s, 3H), 1.68 (s, 1H, OH); ^{13}C NMR ($CDCl_3$, 75 MHz) δ/ppm: 159.13 (s), 140.19 (s), 139.20 (s), 133.28 (s), 127.99 (d, 2C), 127.37 (d, 2C), 126.78 (d, 2C), 114.15 (d, 2C), 66.06 (t), 55.25 (q).

4-hydroxymethyl-4'-hydroxybiphenyl (10)

From 4-methoxy-4'-hydroxymethylbiphenyl (1.00 g, 4.7 mmol), sodium hydride (0.86 g, 18.8 mmol) and ethyl mercaptane (1.35 mL, 18.8 mmol) in DMF (10 mL) the reaction gave 1.58 g of the crude product that was purified by chromatography on silica gel using dichlormethane-ethyl acetate (7:3) to afford 0.22 g (23%) of the pure product in the form of colorless crystals. Besides product reaction gave thioether 0.80 g.

mp 195-196 °C; ^{1}H NMR (DMSO-d_6, 300 MHz), δ/ppm: 9.50 (s, 1H, OH), 7.51 (d, 2H, J = 8.5 Hz), 7.46 (d, 2H, J = 8.5 Hz), 7.33 (d, 2H, J = 8.5 Hz), 6.83 (d, 2H, J = 8.6 Hz), 5.15 (br s, 1H, OH), 4.50 (s, 2H); ^{13}C NMR (DMSO-d_6, 75 MHz), δ/ppm: 156.96 (s), 140.62 (s), 138.64 (s), 130.88 (s), 127.58 (d, 2C), 126.99 (d, 2C), 125.63 (d, 2C), 115.69(d, 2C), 62.67 (t).

2. Irradiations of 5-8 in CH_3OH-H_2O under different conditions.

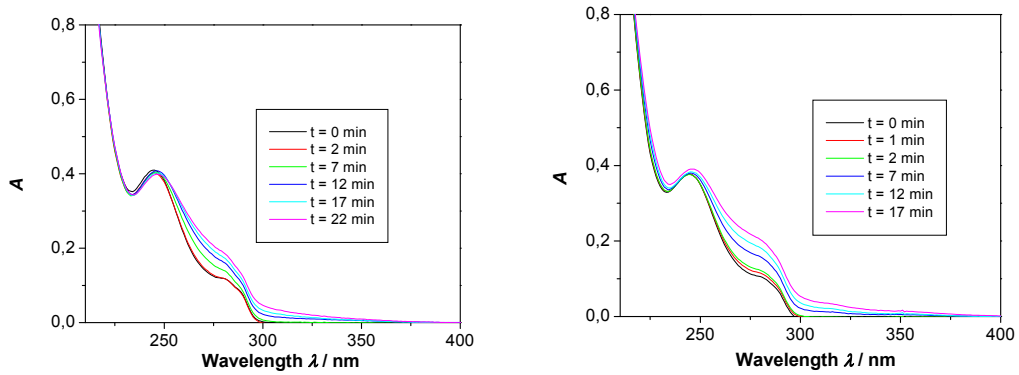

Fig 1. UV-Vis spectra after photolyses (16 lamps 254 nm) of **5** in a UV-vis cuvette in CH_3CN (left) and CH_3CN-H_2O (1:1) (right).

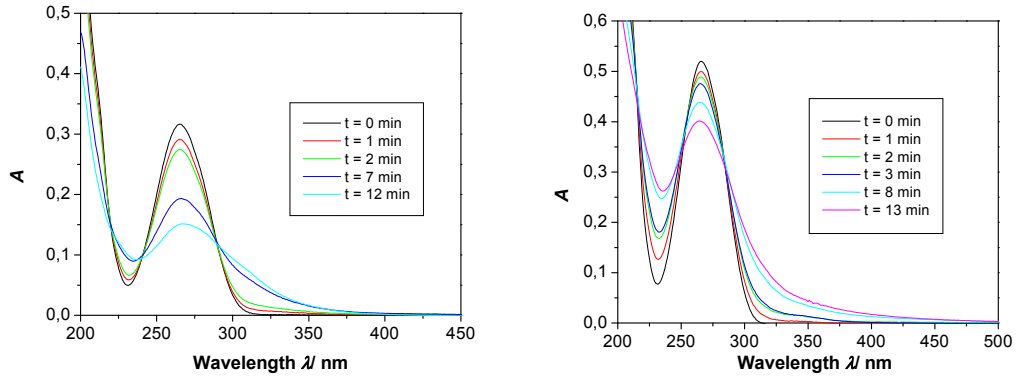

Fig 2. UV-Vis spectra after photolyses (16 lamps 254 nm) of **7** in a UV-vis cuvette in CH_3CN (left) and CH_3CN-H_2O (1:1) (right).

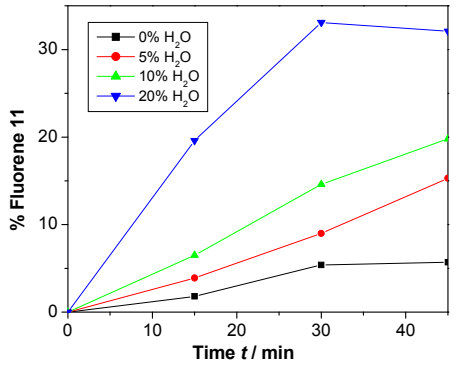

Fig. 3. Conversion of **5** to **11** on photolysis (8 lamps, 254 nm) in CH_3OH-H_2O with different H_2O content.

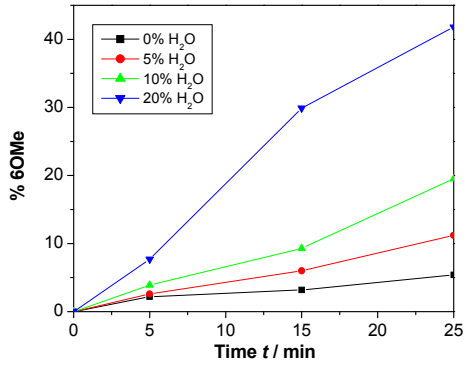

Fig. 4. Conversion of **6** to **6OM**e on photolysis (8 lamps, 254 nm) in CH_3OH-H_2O with different H_2O content.

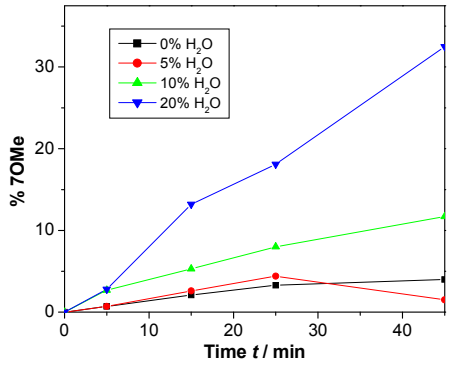

Fig. 5. Conversion of **7** to **7OMe** on photolysis (8 lamps, 254 nm) in CH_3OH-H_2O with different H_2O content.

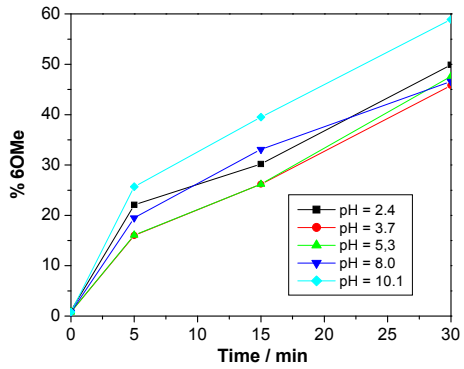

Fig. 6. Conversion of **6** to **6OMe** on photolysis (8 lamps, 254 nm) in CH_3OH-H_2O (20%) at different pH.

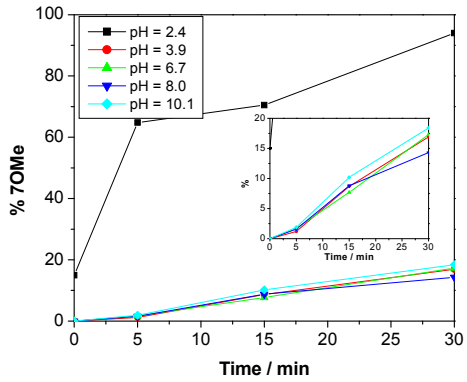

Fig. 7. Conversion of **7** to **7OM**e on photolysis (8 lamps, 254 nm) in CH_3OH-H_2O (20%) at different pH.

3. UV-vis and Fluorescence Spectra of 5-9.

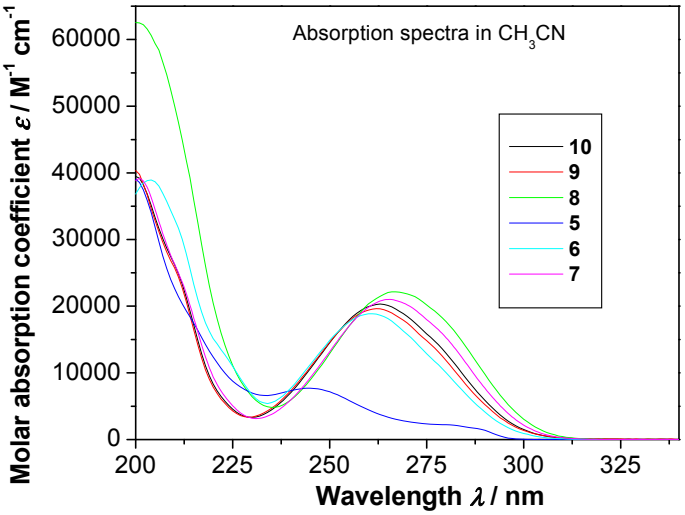

Fig. 8. Absorption spectra of **5**-**10** in CH_3CN.

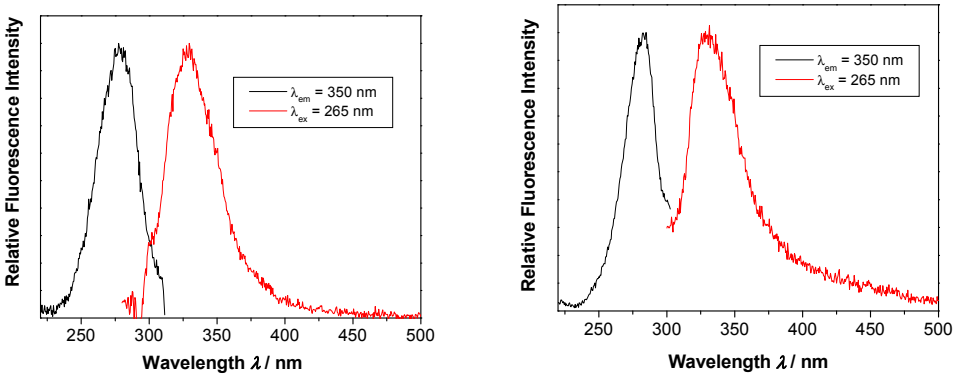

Fig. 9. Normalized excitation and emission spectra of **5** in CH_3CN (left) and CH_3CN-H_2O (1:4) (right).

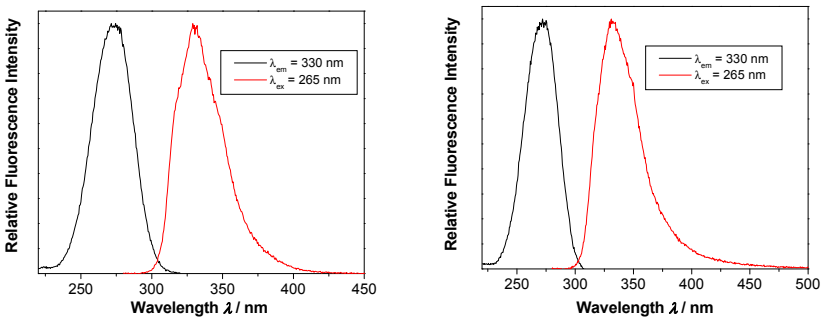

Fig. 10. Normalized excitation and emission spectra of **6** in CH_3CN (left) and CH_3CN-H_2O (1:4) (right).

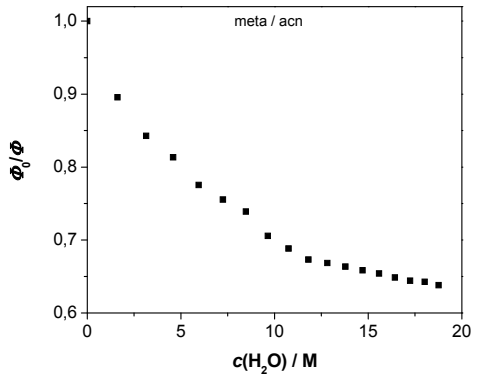

Fig. 11. Stern-Volmer quenching plot of fluorescence of **6** in CH_3CN by addition of H_2O.

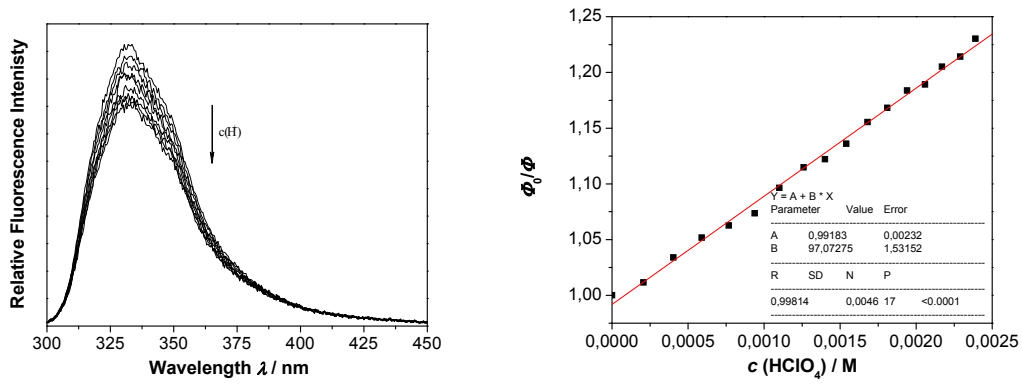

Fig. 12. Fluorescence spectra of **6** in CH_3CN-H_2O (1:4) on addition of $HClO_4$ (left), and Stern-Volmer quenching plot of fluorescence of **6** in CH_3CN-H_2O (1:4)by addition of $HClO_4$ (right).

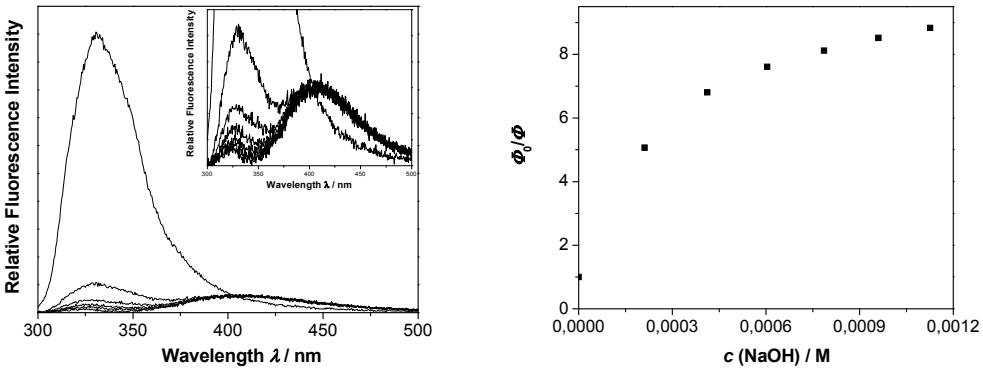

Fig. 13. Fluorescence spectra of **6** in CH_3CN-H_2O (1:4) on addition of NaOH (left), and Stern-Volmer quenching plot of fluorescence of **6** in CH_3CN-H_2O (1:4) by addition of NaOH (right).

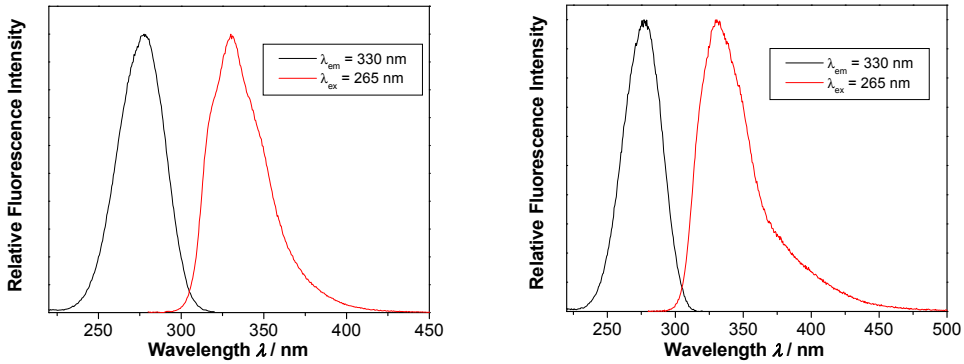

Fig. 14. Normalized excitation and emission spectra of **7** in CH_3CN (left) and CH_3CN-H_2O (1:4) (right).

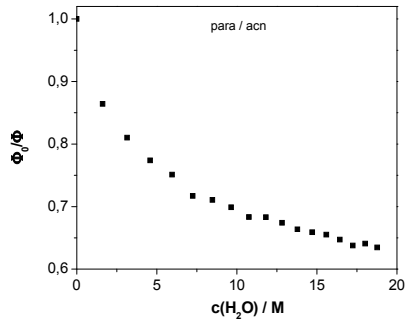

Fig. 15. Stern-Volmer quenching plot of fluorescence of **7** in CH_3CN by addition of H_2O.

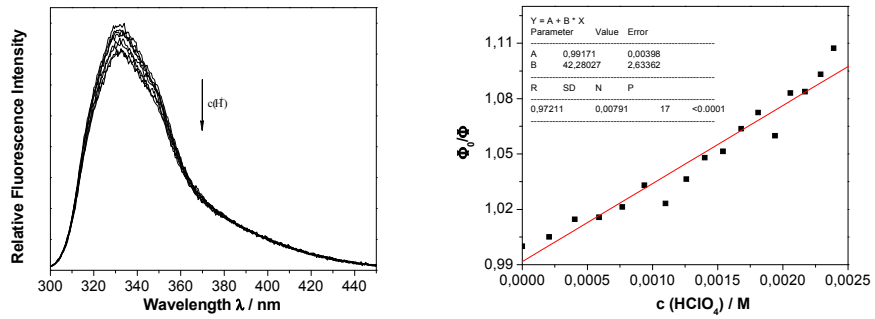

Fig. 16. Fluorescence spectra of **7** in CH_3CN-H_2O (1:4) on addition of $HClO_4$ (left), and Stern-Volmer quenching plot of fluorescence of **7** in CH_3CN-H_2O (1:4)by addition of $HClO_4$ (right).

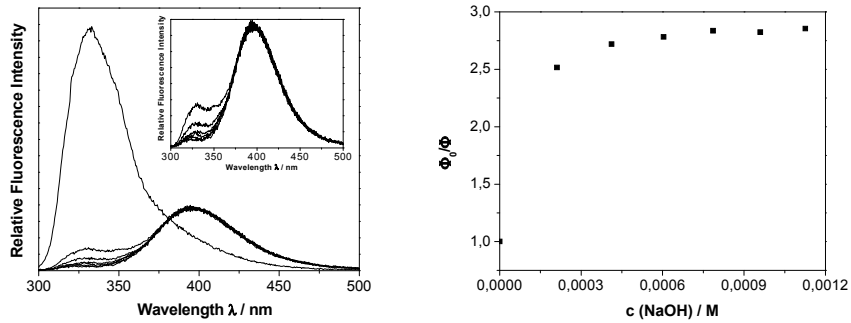

Fig. 17. Fluorescence spectra of **7** in CH_3CN-H_2O (1:4) on addition of NaOH (left), and Stern-Volmer quenching plot of fluorescence of **7** in CH_3CN-H_2O (1:4) by addition of NaOH (right).

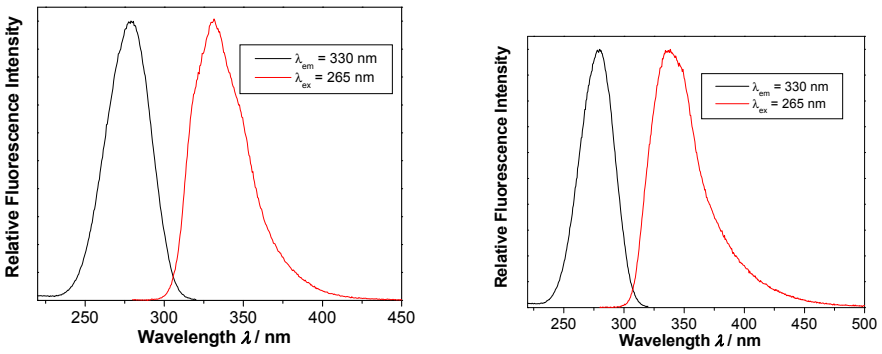

Fig. 18. Normalized excitation and emission spectra of **8** in CH_3CN (left) and CH_3CN-H_2O (1:4) (right).

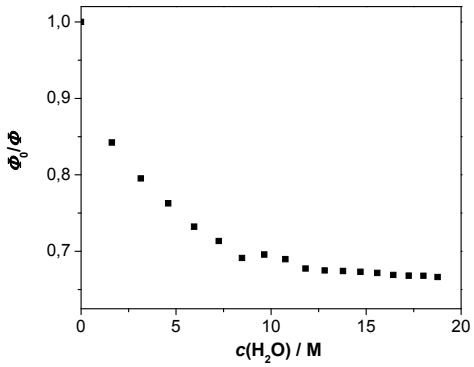

Fig. 19. Stern-Volmer quenching plot of fluorescence of **8** in CH_3CN by addition of H_2O.

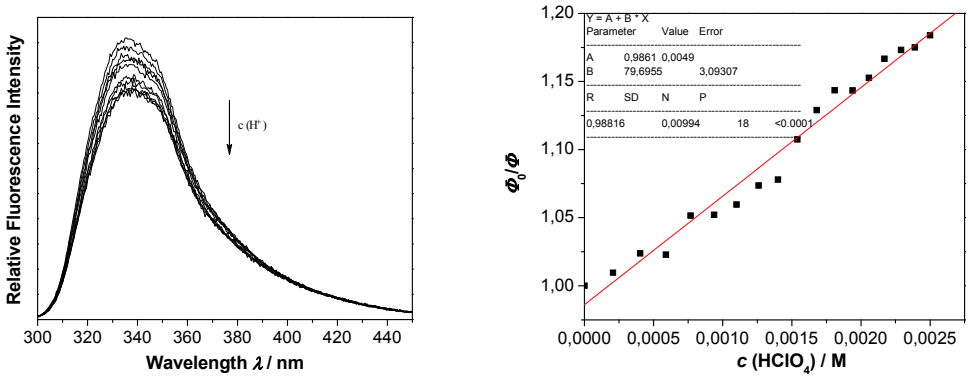

Fig. 20. Fluorescence spectra of **8** in CH_3CN-H_2O (1:4) on addition of $HClO_4$ (left), and Stern-Volmer quenching plot of fluorescence of **8** in CH_3CN-H_2O (1:4) by addition of $HClO_4$ (right).

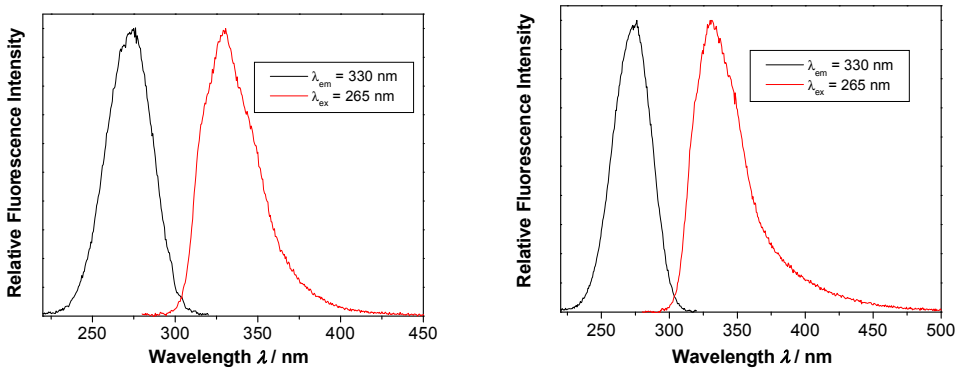

Fig. 21. Normalized excitation and emission spectra of **9** in CH_3CN (left) and CH_3CN-H_2O (1:4) (right).

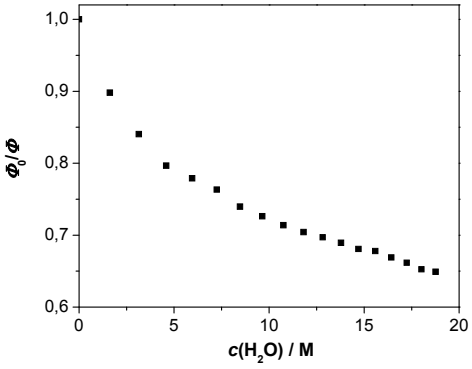

Fig. 22. Stern-Volmer quenching plot of fluorescence of **9** in CH_3CN by addition of H_2O.

3. Laser Flash Photolysis

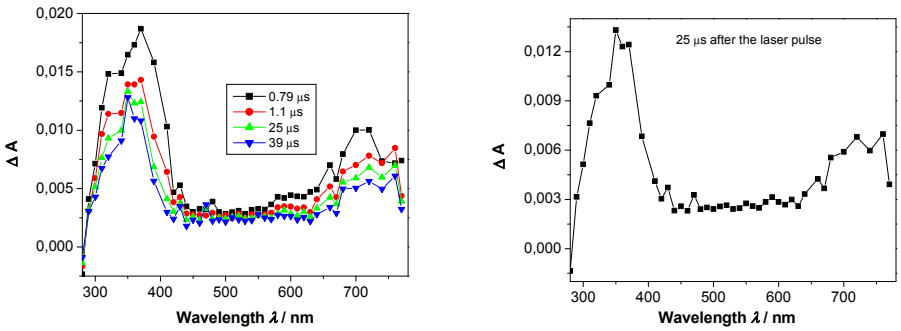

Fig. 23. Transient absorption spectra of N_2-purged CH_3CN-H_2O (1:1) solution of **5**.

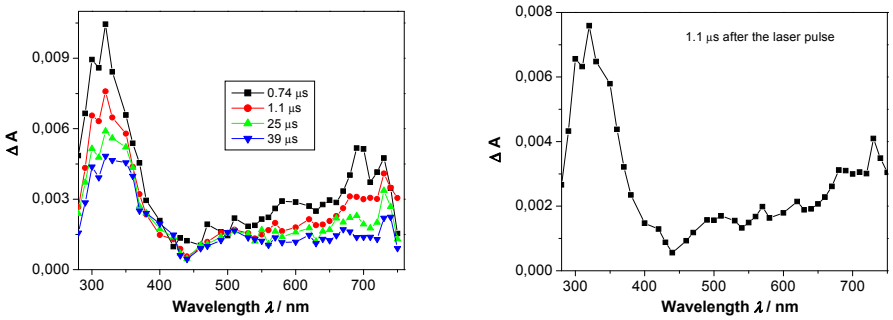

Fig. 24. Transient absorption spectra of O_2-purged CH_3CN-H_2O (1:1) solution of **5**.

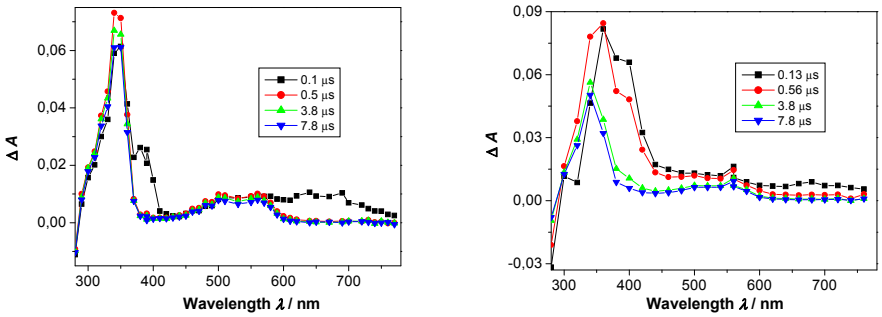

Fig. 25. Transient absorption spectra of O_2-purged CH_3CN solution of **6** (left) and N_2O-purged CH_3CN solution of **6** (right).

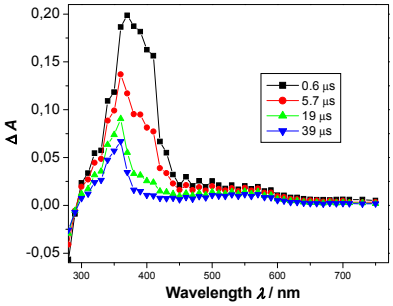

Fig. 25. Transient absorption spectra of N_2-purged CH_3CN-H_2O (1:1) solution of **6**.

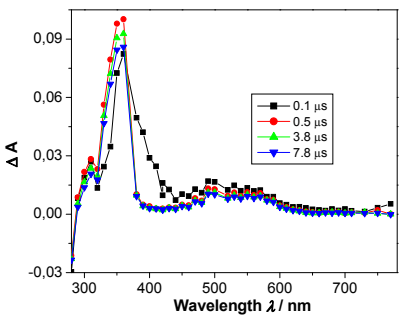

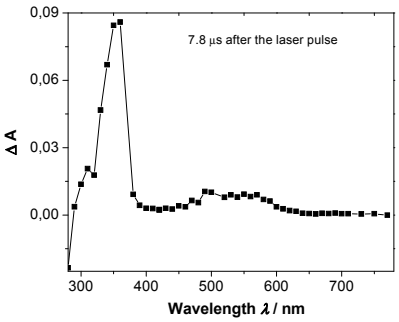

Fig. 26. Transient absorption spectra of O_2-purged CH_3CN-H_2O (1:1) solution of **6**.

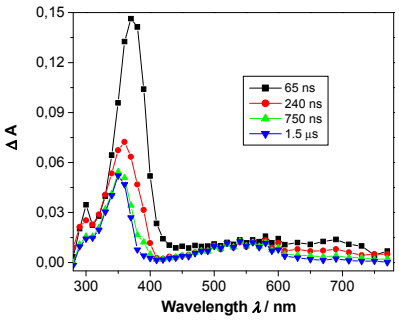

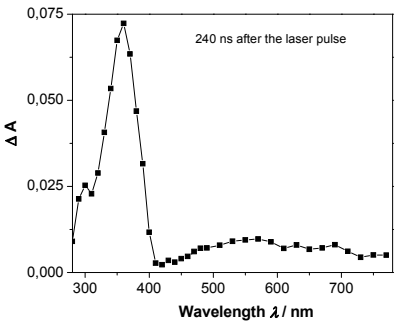

Fig. 27. Transient absorption spectra of O_2-purged TFE solution of **6**.

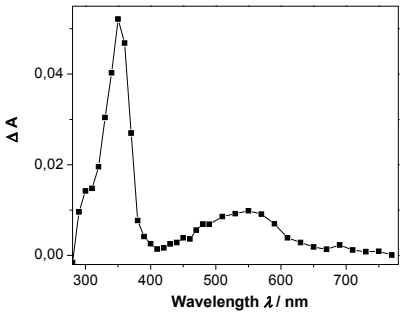

Fig. 28. Transient absorption spectrum of O_2-purged TFE solution of **6** 1.5 μs after the laser pulse.

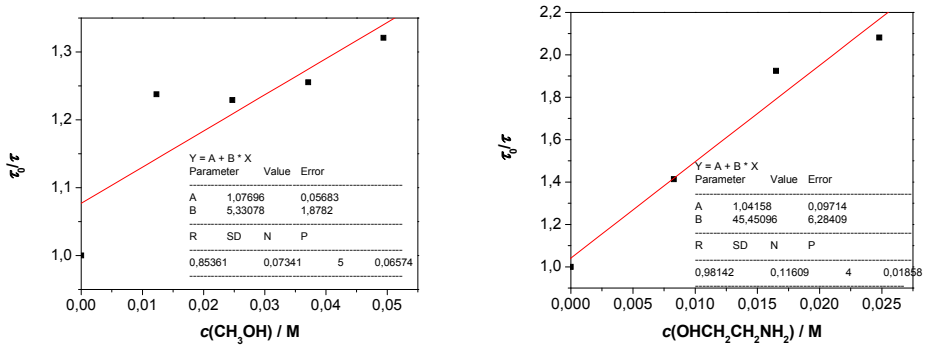

Fig. 29. Stern-Volmer plots for the quenching of the transient absorption at 390 nm of O_2-purged TFE solution of **6** by CH_3OH (left) and ethanolamine (right).

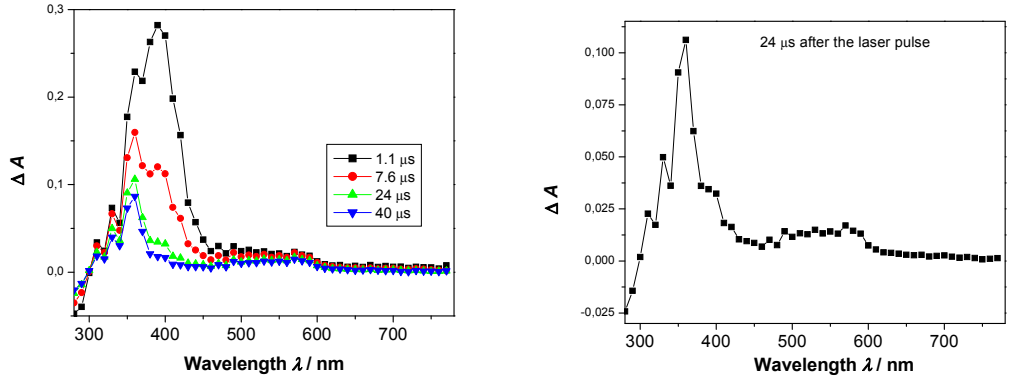

Fig. 30. Transient absorption spectra of N_2-purged CH_3CN solution of **7**.

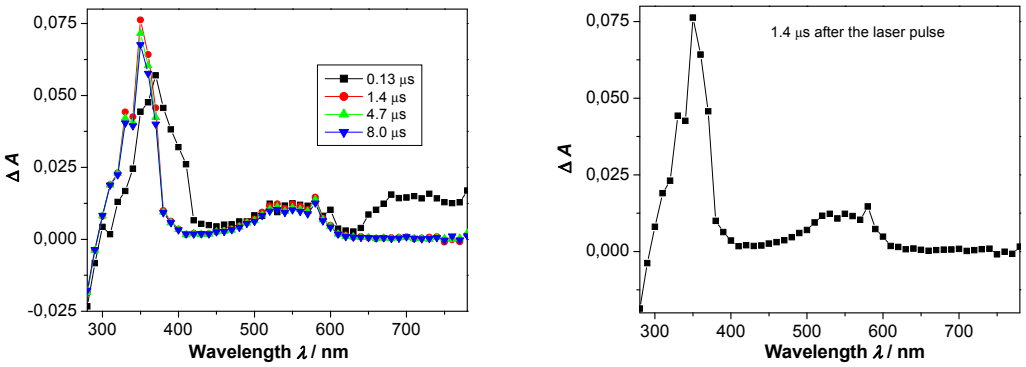

Fig. 31. Transient absorption spectra of O_2-purged CH_3CN solution of **7**.

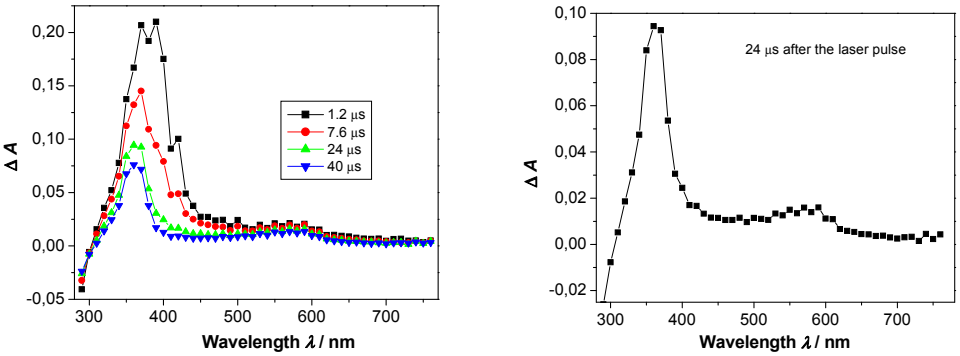

Fig. 32. Transient absorption spectra of N_2-purged CH_3CN-H_2O (1:1) solution of **7**.

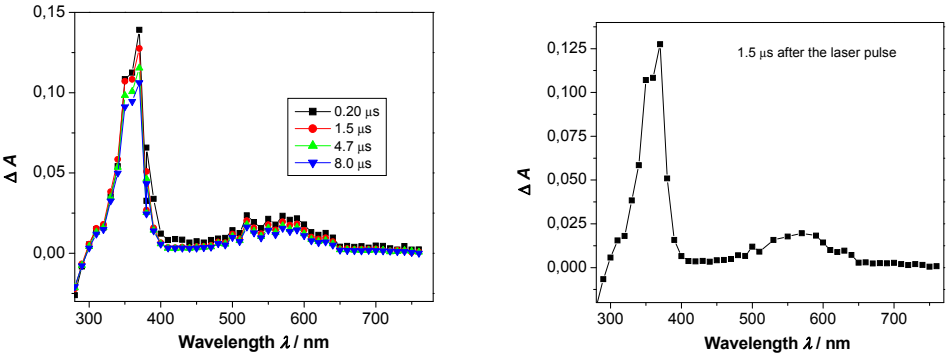

Fig. 33. Transient absorption spectra of O_2-purged CH_3CN-H_2O (1:1) solution of **7**.

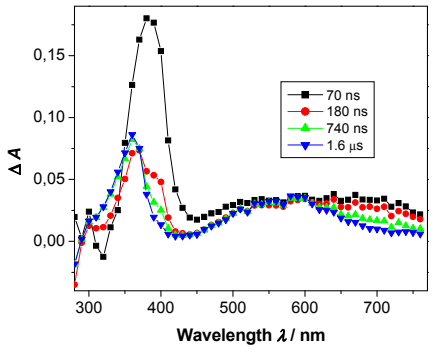

Fig. 34. Transient absorption spectra of O_2-purged TFE solution of **7**.

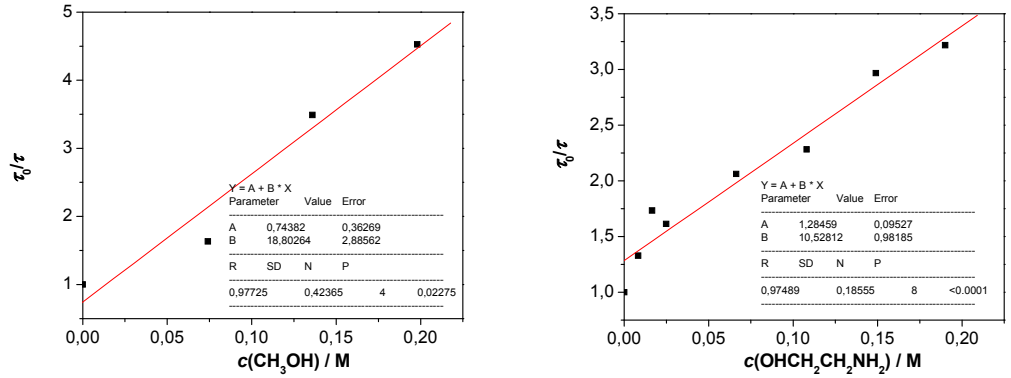

Fig. 35. Stern-Volmer plots for the quenching of the transient absorption at 525 nm of O_2-purged TFE solution of **7** by CH_3OH (left) and ethanolamine (right).

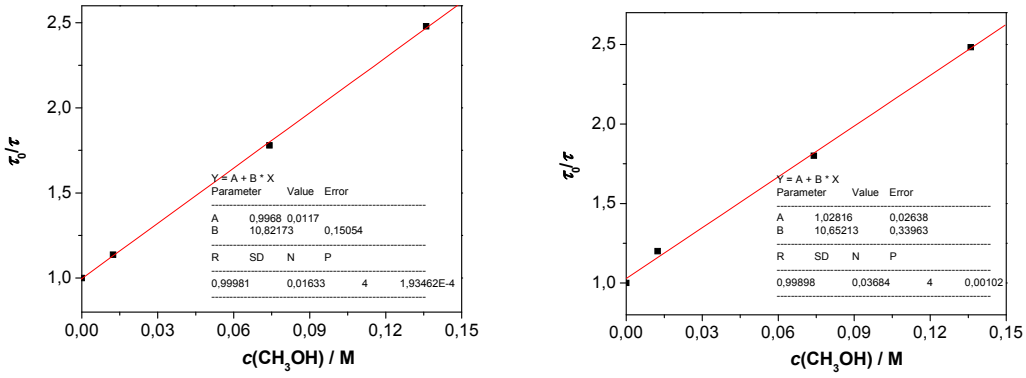

Fig. 36. Stern-Volmer plots for the quenching of the transient absorption at 380 nm (left) and 700 nm (right) of O_2-purged TFE solution of **7** by CH_3OH.

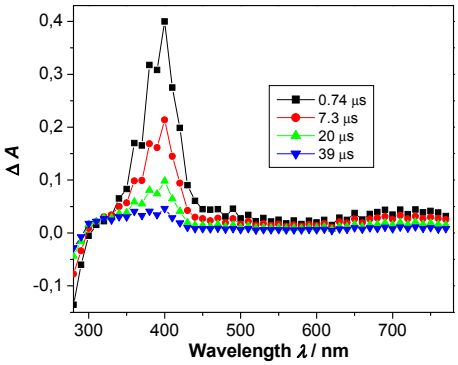

Fig. 37. Transient absorption spectra of N_2-purged CH_3CN-H_2O (1:1) solution of **7'**.

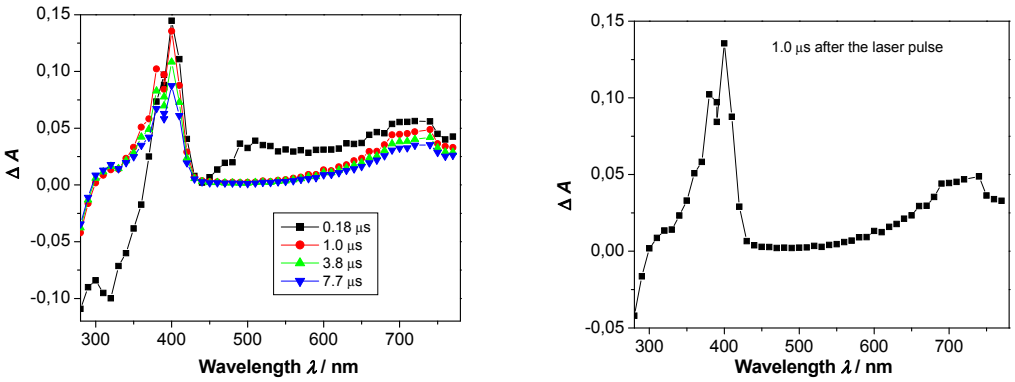

Fig. 38. Transient absorption spectra of O_2-purged CH_3CN-H_2O (1:1) solution of **7'**.

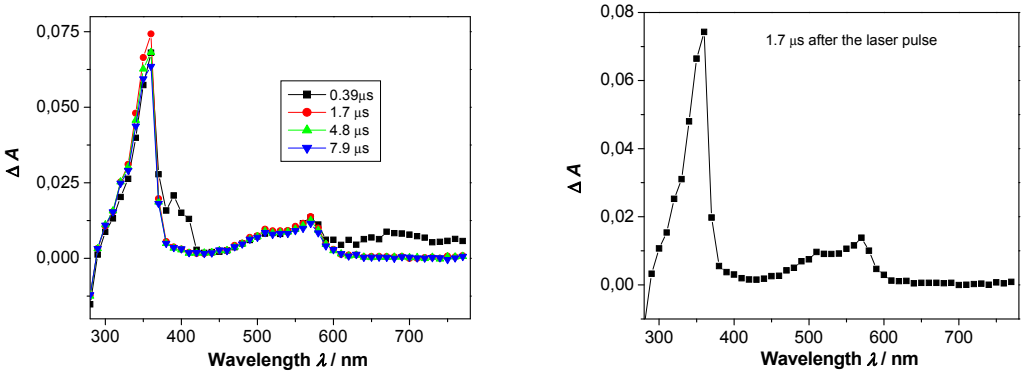

Fig. 39. Transient absorption spectra of O_2-purged CH_3CN solution of **9**.

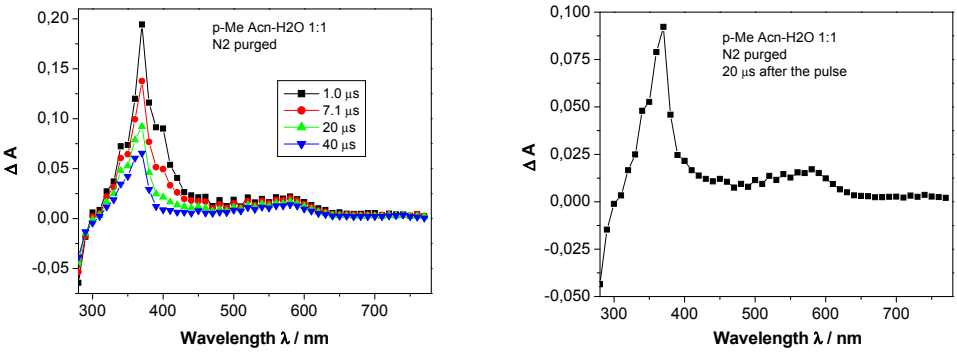

Fig. 40. Transient absorption spectra of N_2-purged CH_3CN-H_2O (1:1) solution of **9**.

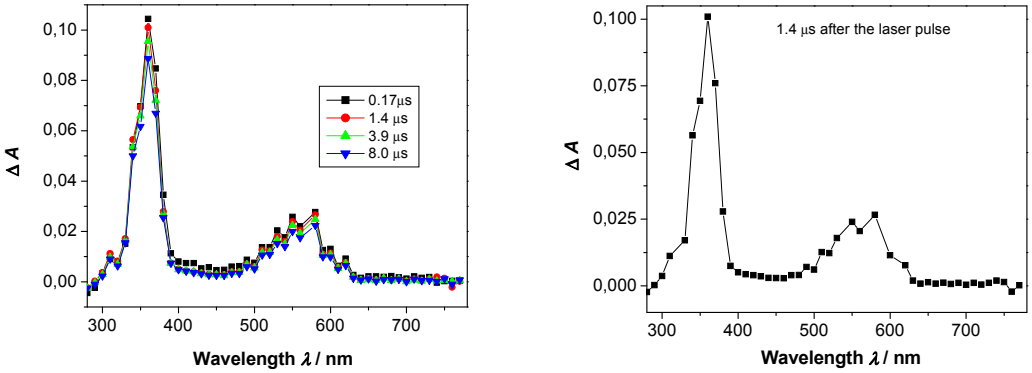

Fig. 41. Transient absorption spectra of O_2-purged CH_3CN-H_2O (1:1) solution of **9**.

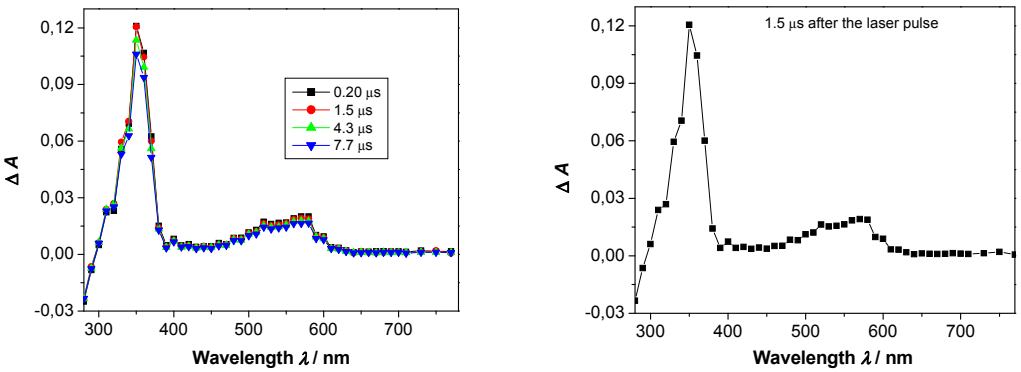

Fig. 42. Transient absorption spectra of O_2-purged CH_3CN-H_2O (1:1) solution of **10**.

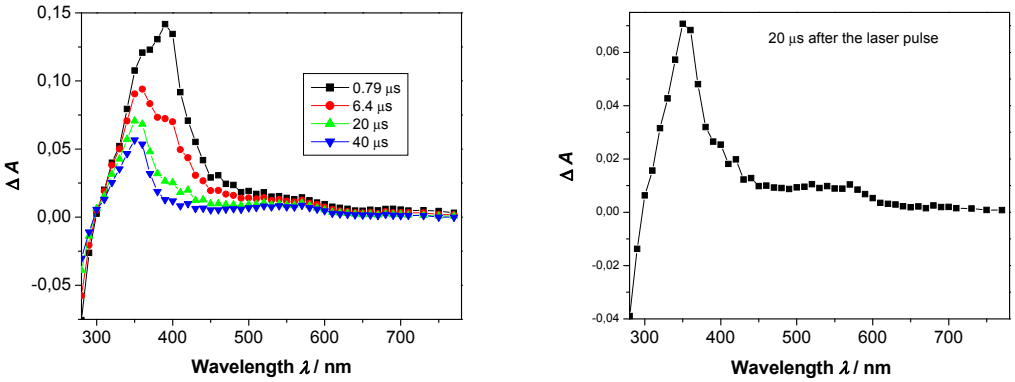

Fig. 43. Transient absorption spectra of N_2-purged CH_3CN solution of **8**.

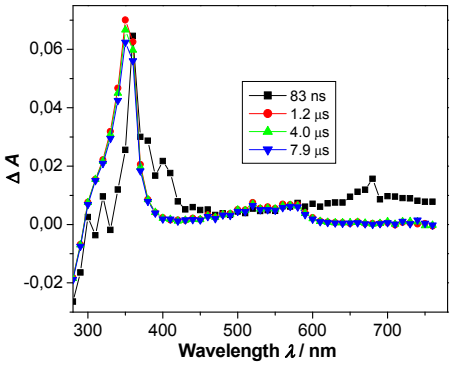

Fig. 44. Transient absorption spectra of O_2-purged CH_3CN solution of **8**

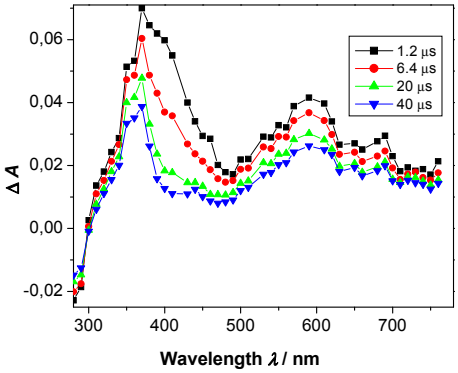

Fig. 45. Transient absorption spectra of N_2-purged CH_3CN-H_2O (1:1) solution of **8**.

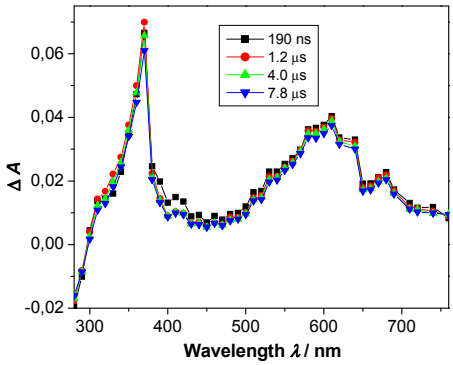

Fig. 46. Transient absorption spectra of O_2-purged CH_3CN-H_2O (1:1) solution of **8**.

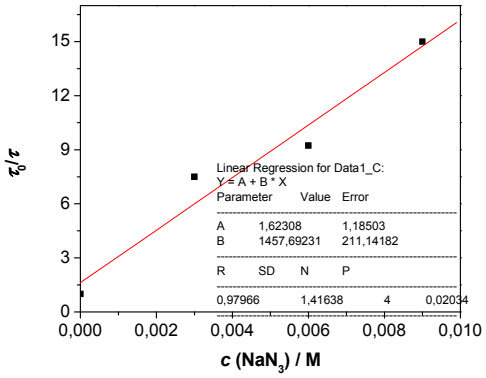

Fig. 47. Stern-Volmer plots for the quenching of the transient absorption at 600 nm of TFE solution of **8** by NaN_3.

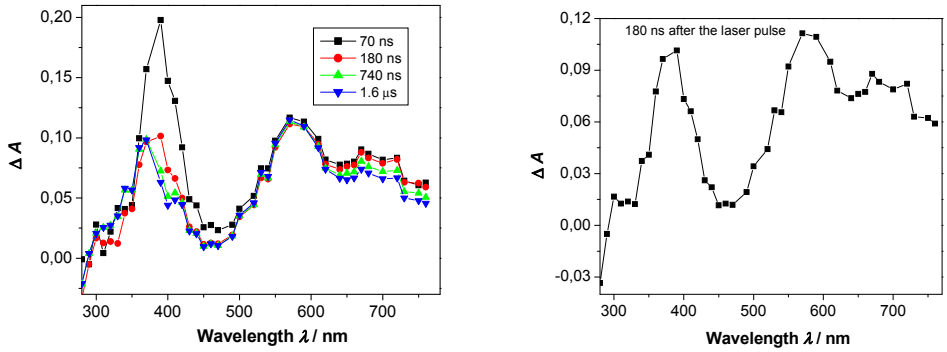

Fig. 48. Transient absorption spectra of O_2-purged TFE solution of **8**

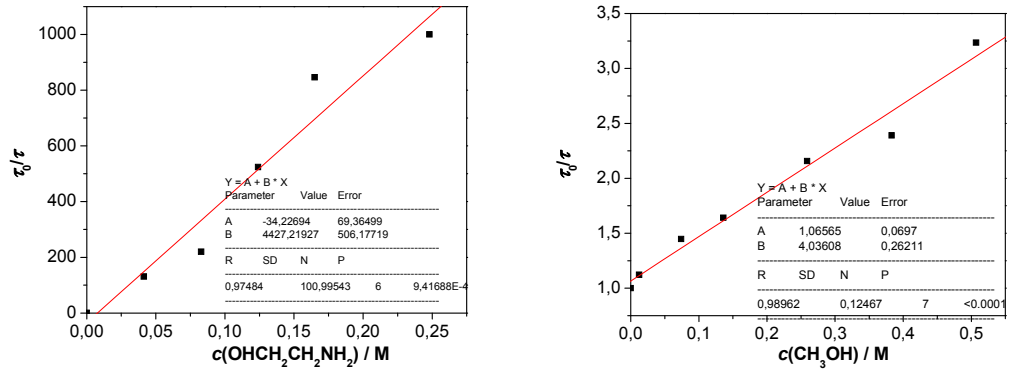

Fig. 49. Stern-Volmer plots for the quenching of the transient absorption of TFE solution of **8** by ethanolamine (left) and CH_3OH (right).

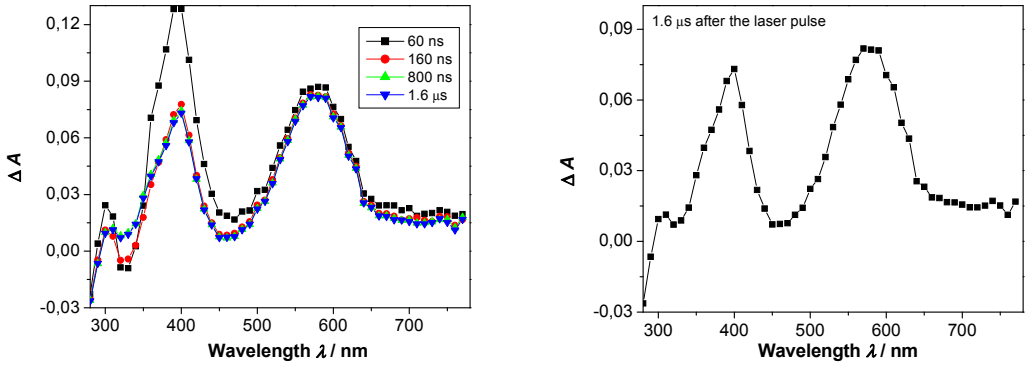

Fig. 50. Transient absorption spectra of O_2-purged TFE solution of **8'**

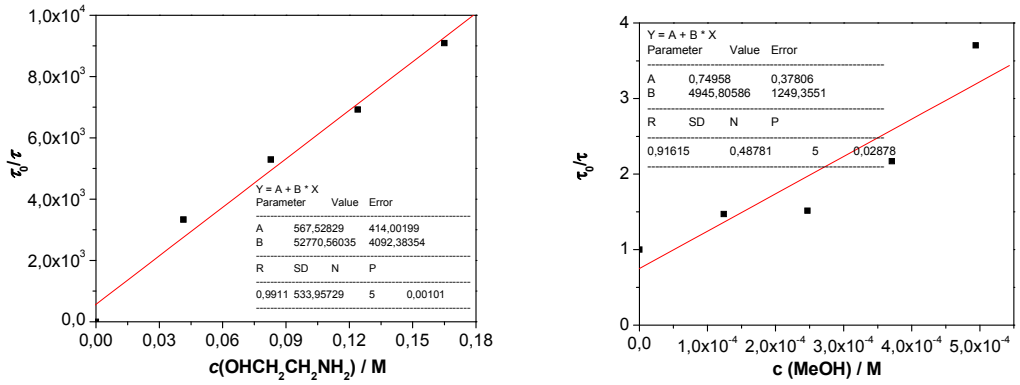

Fig. 51. Stern-Volmer plots for the quenching of the transient absorption of TFE solution of **8'** by ethanolamine (left) and CH_3OH (right).

^{1}H NMR ($CDCl_3$, 300 MHz)

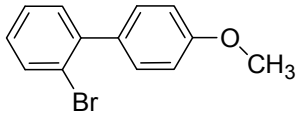

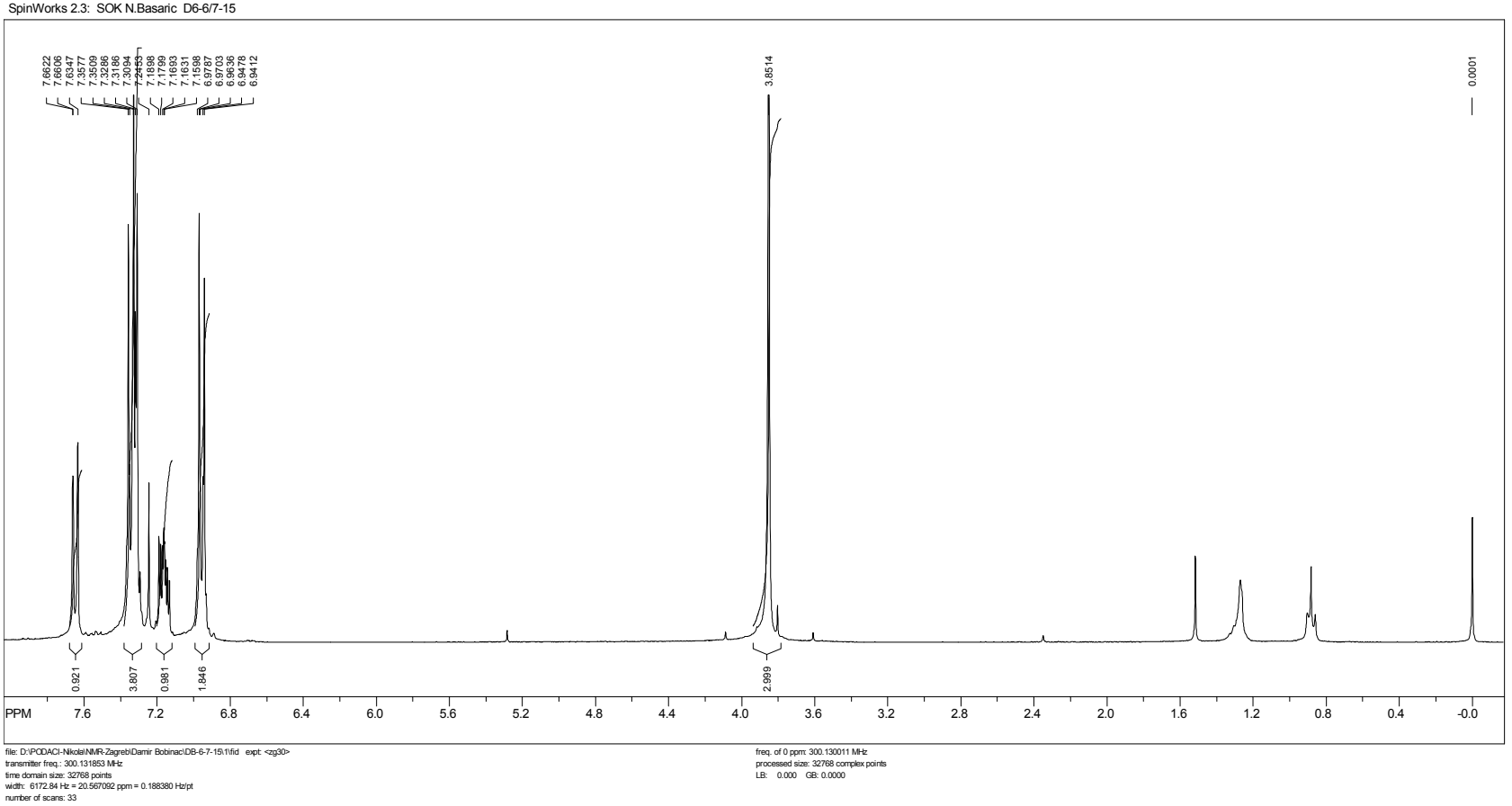

^{1}H NMR ($CDCl_3$, 300 MHz)

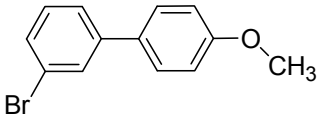

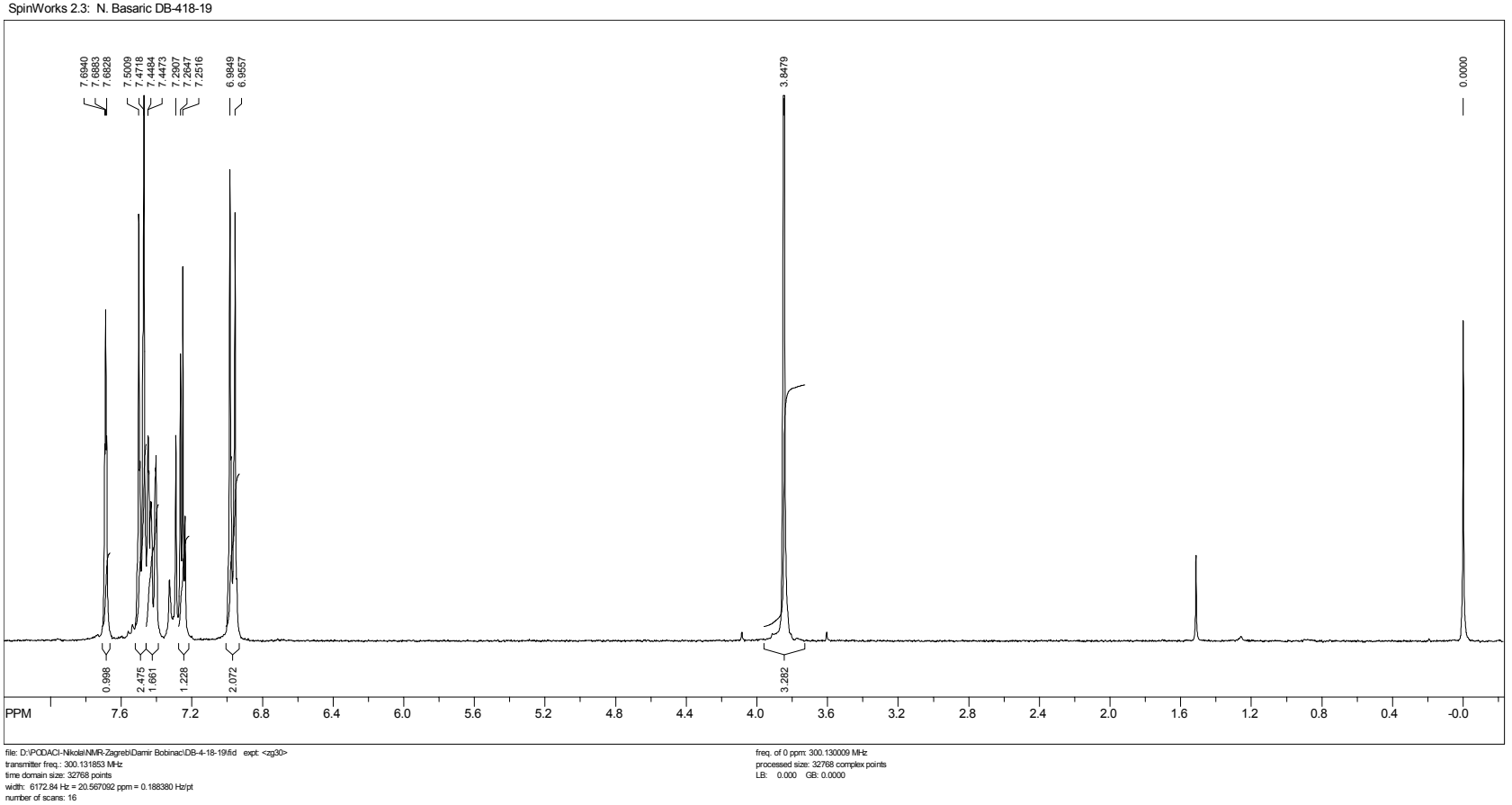

^{1}H NMR ($CDCl_3$, 300 MHz)

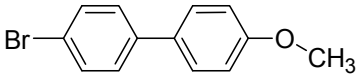

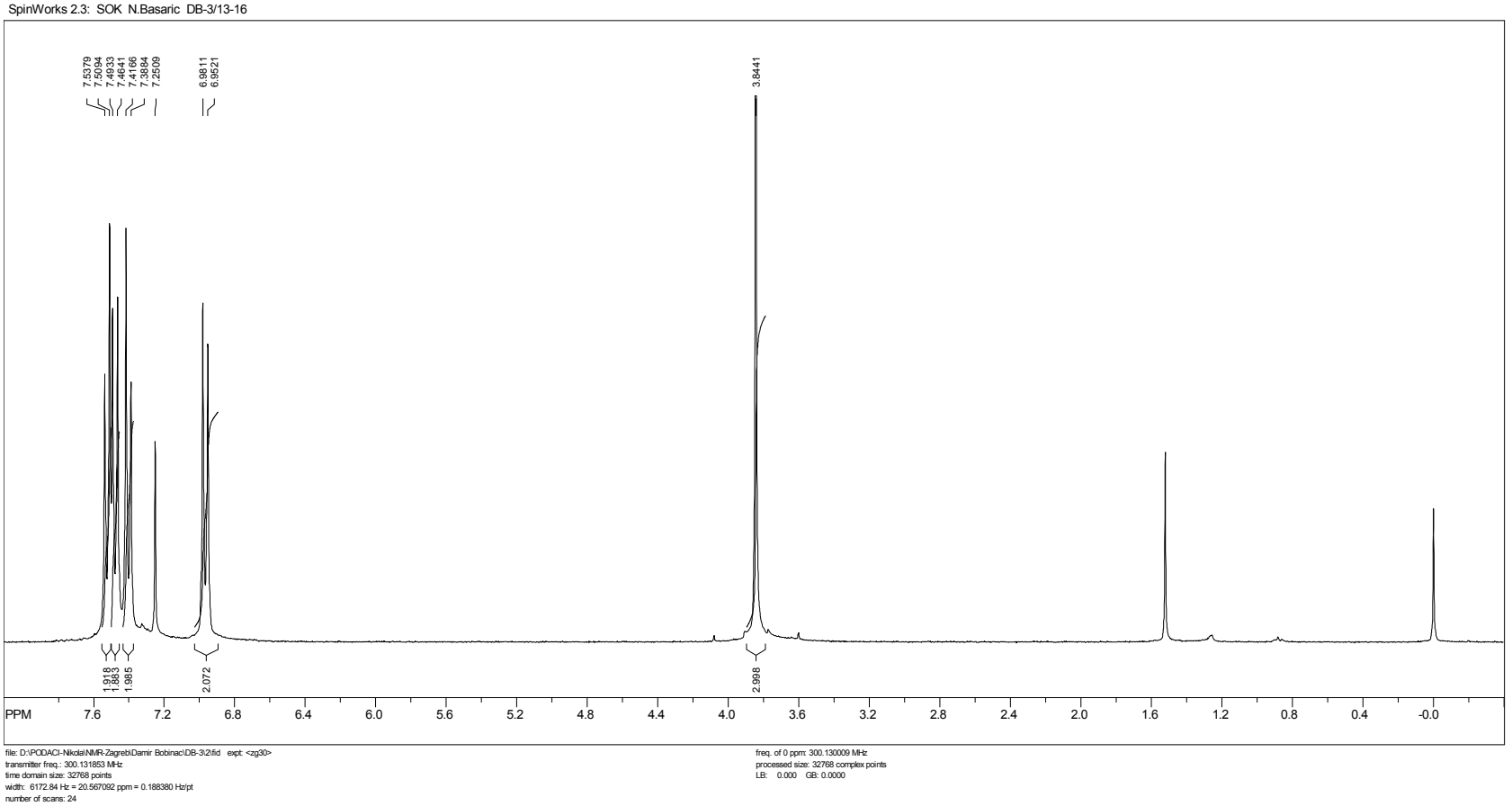

^{1}H NMR ($CDCl_3$, 600 MHz) of **5'**

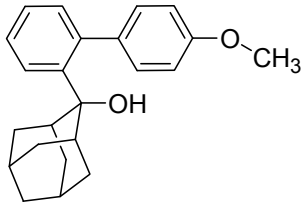

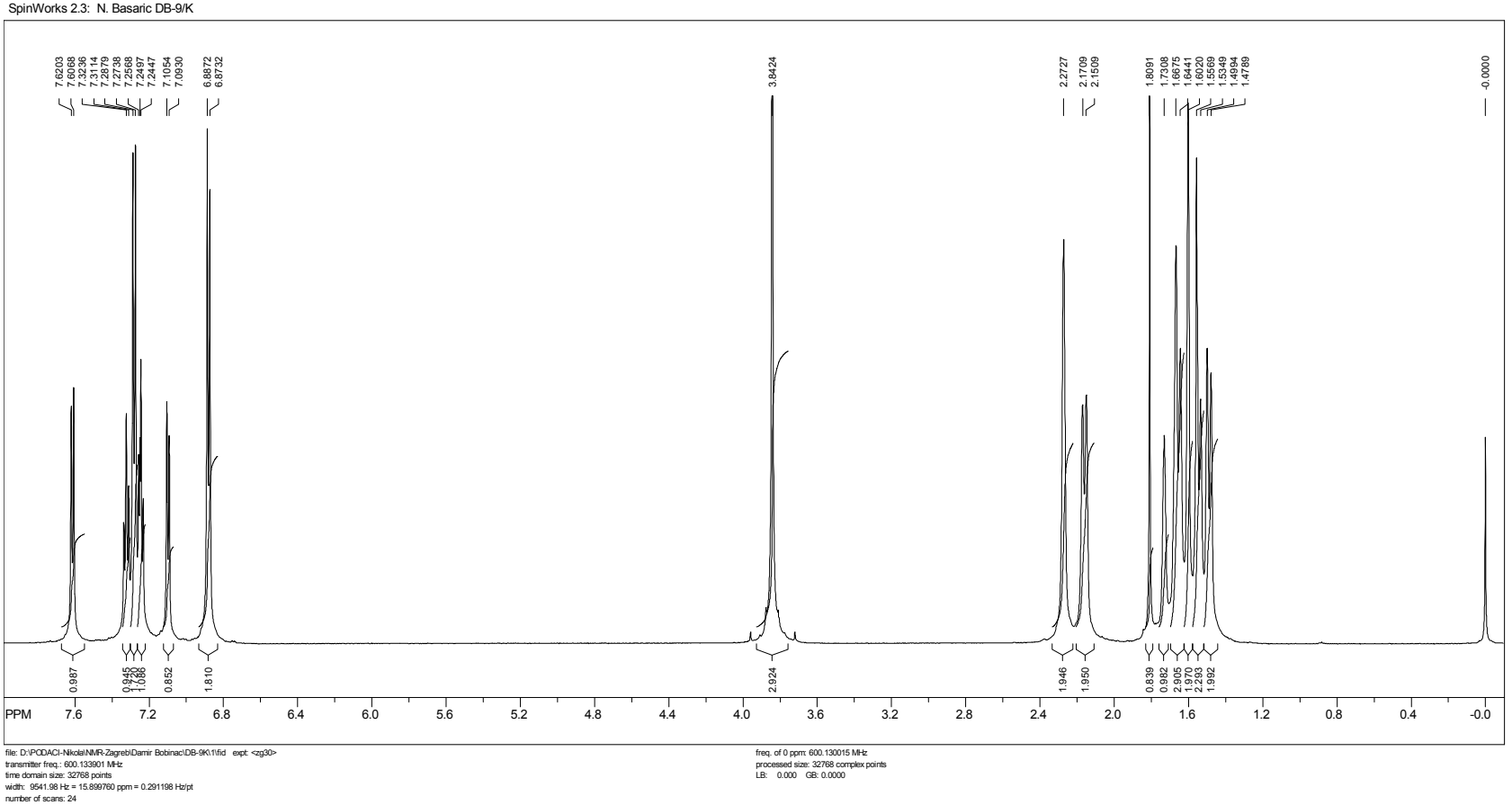

^{13}C NMR ($CDCl_3$, 150 MHz) of **5'**

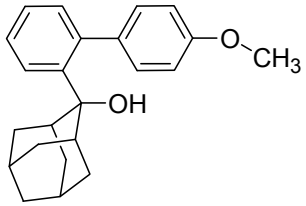

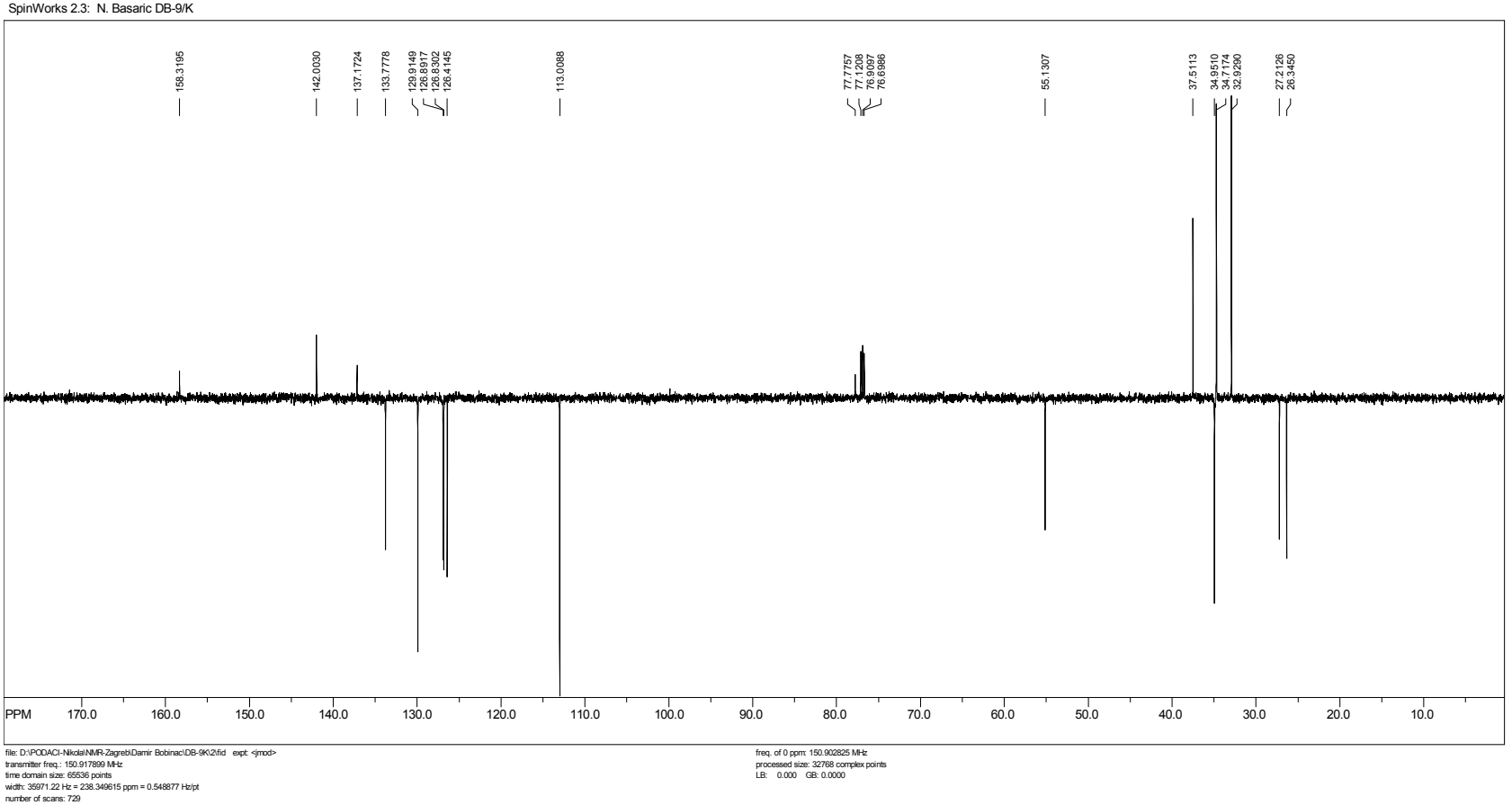

^{1}H NMR ($CDCl_3$, 300 MHz) of **6'**

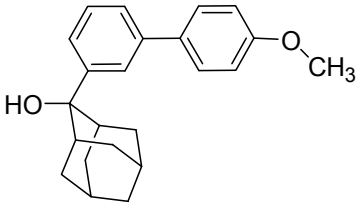

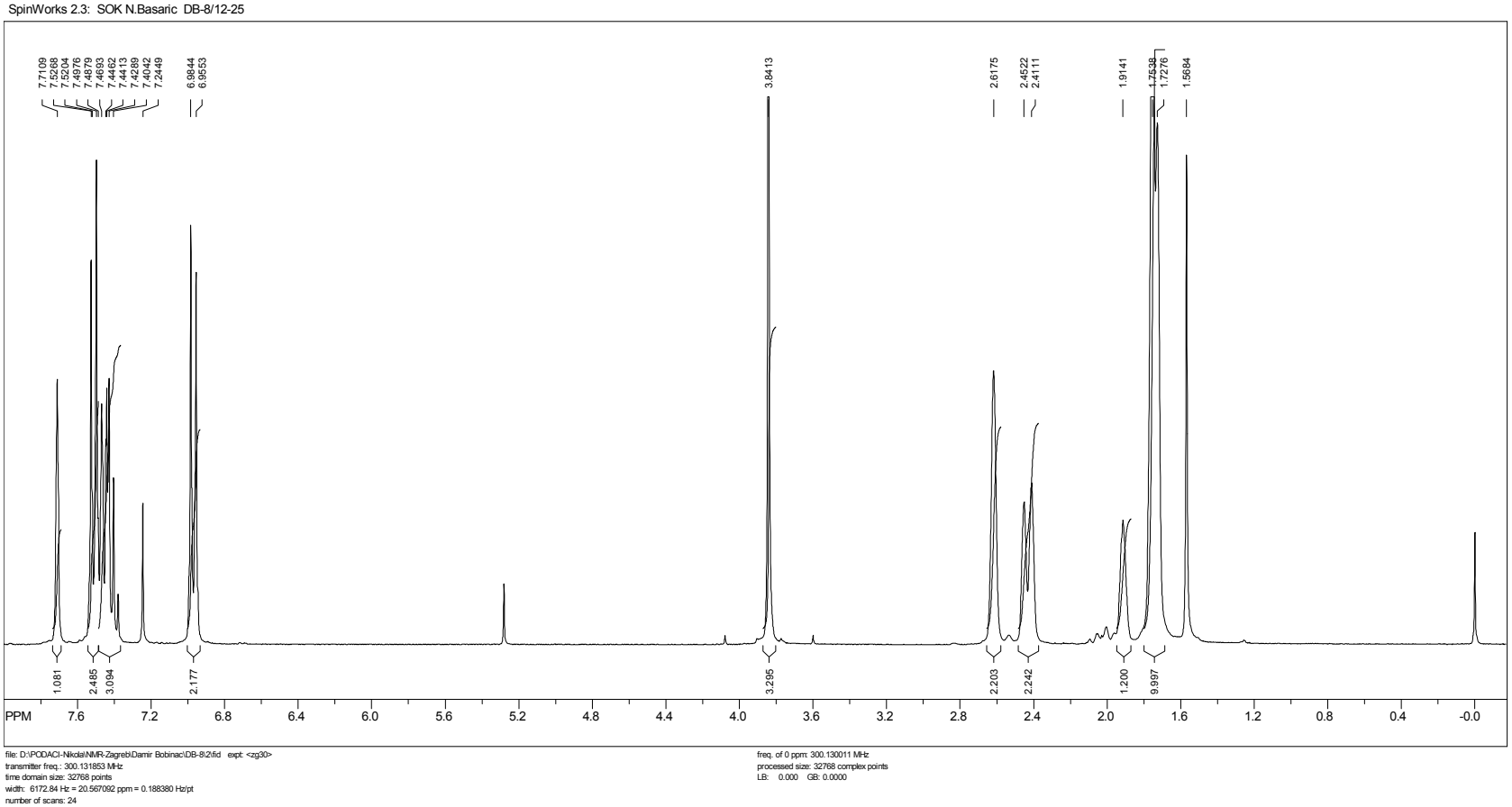

^{13}C NMR ($CDCl_3$, 75 MHz) of **6'**

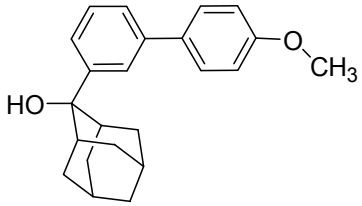

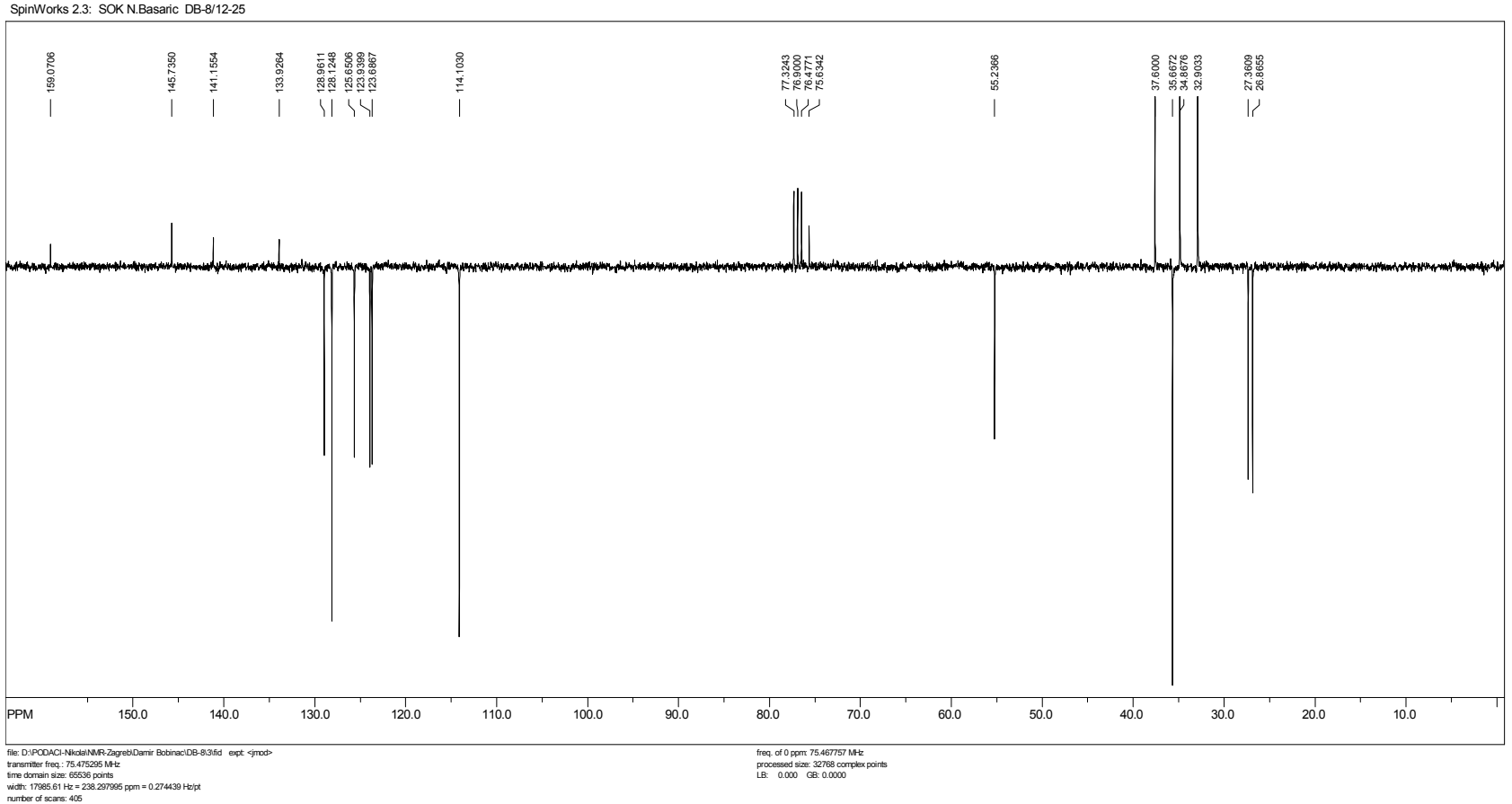

^{1}H NMR ($CDCl_3$, 300 MHz) of **7'**

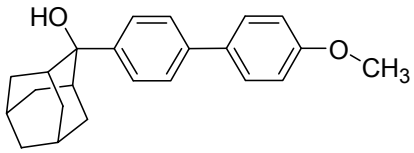

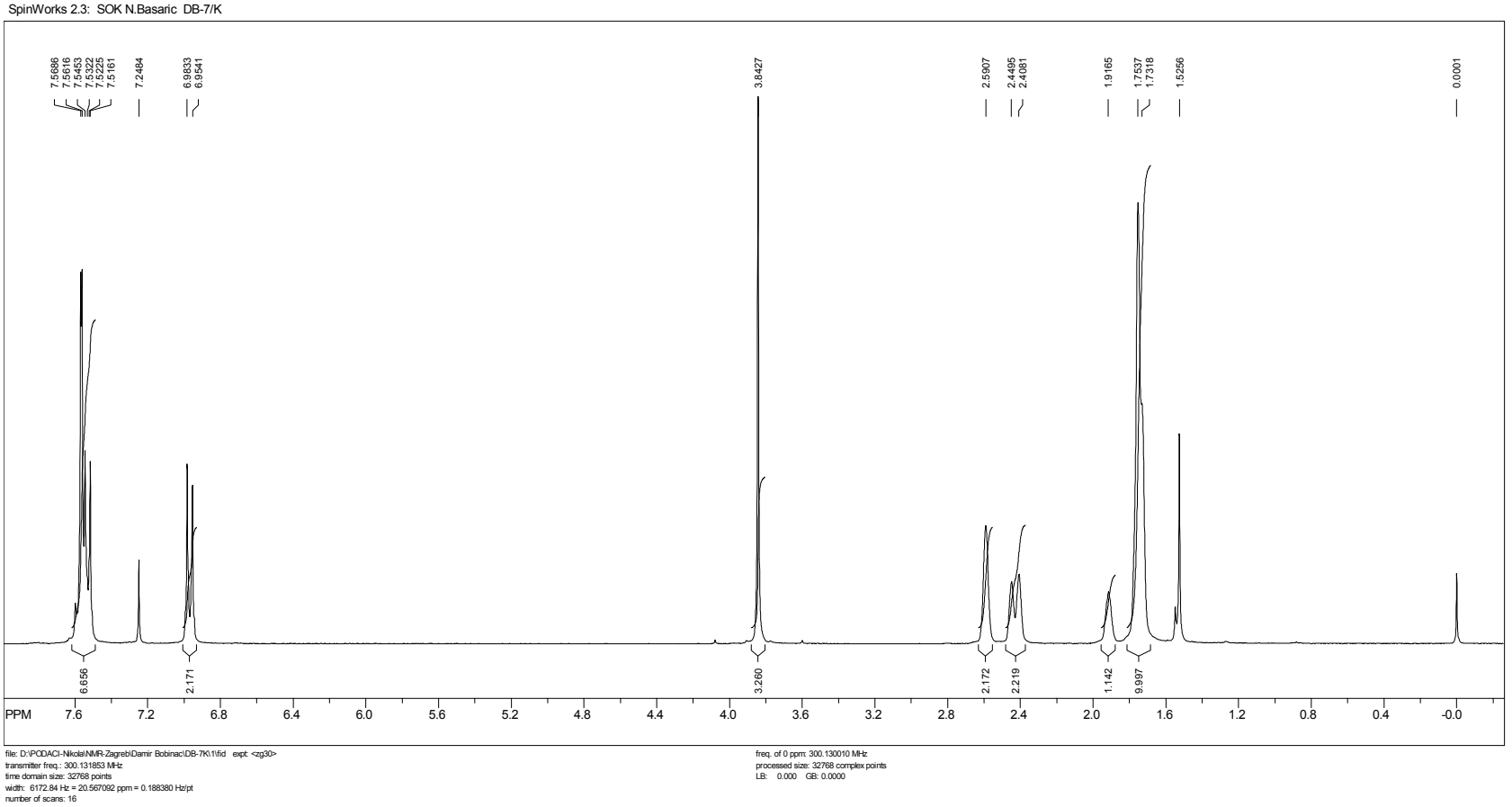

^{13}C NMR ($CDCl_3$, 75 MHz) of **7'**

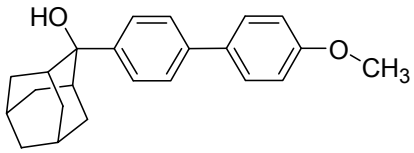

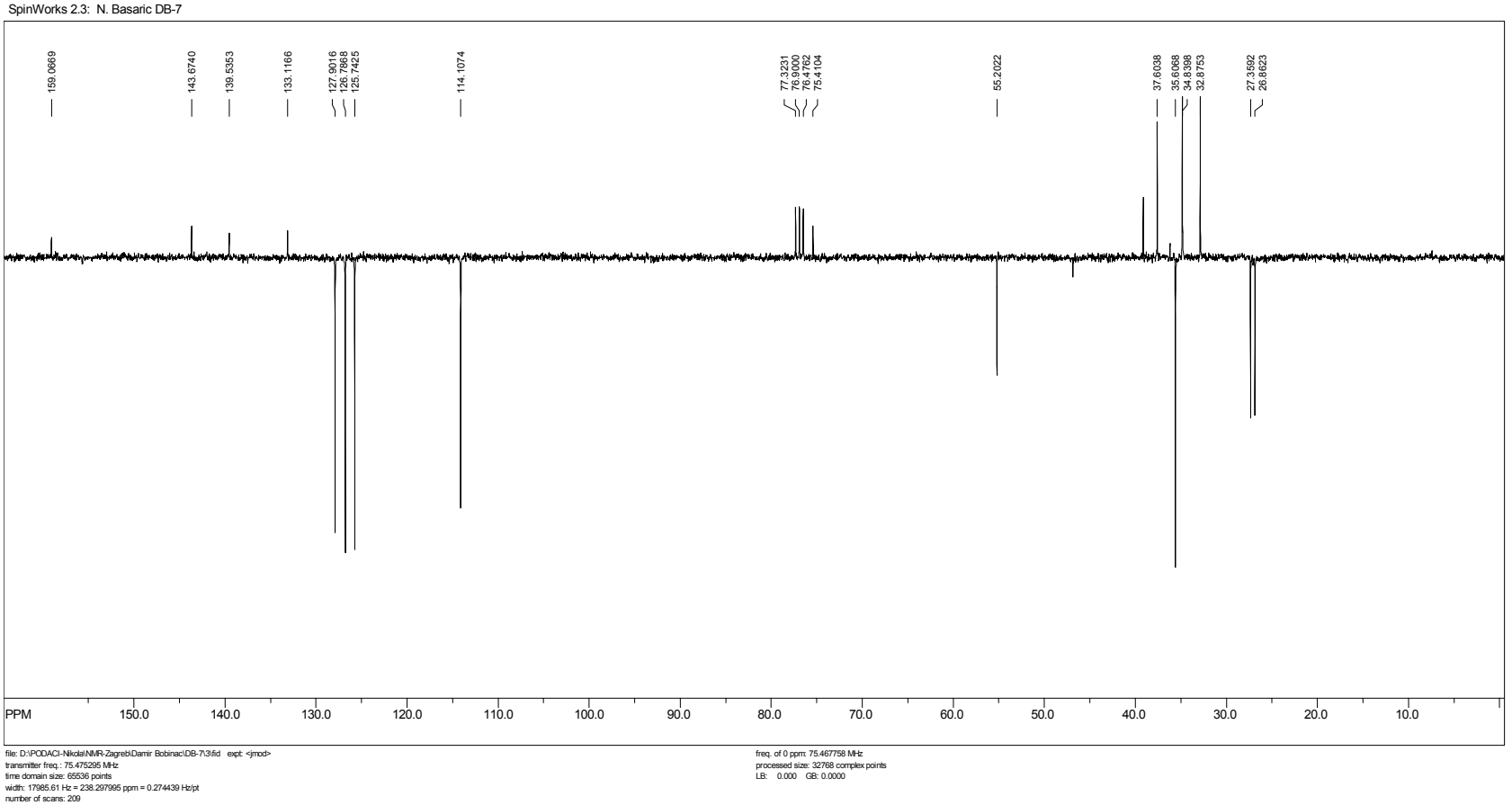

^{1}H NMR ($CDCl_3$, 600 MHz) of **8'**

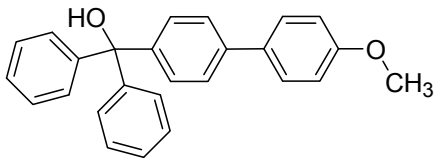

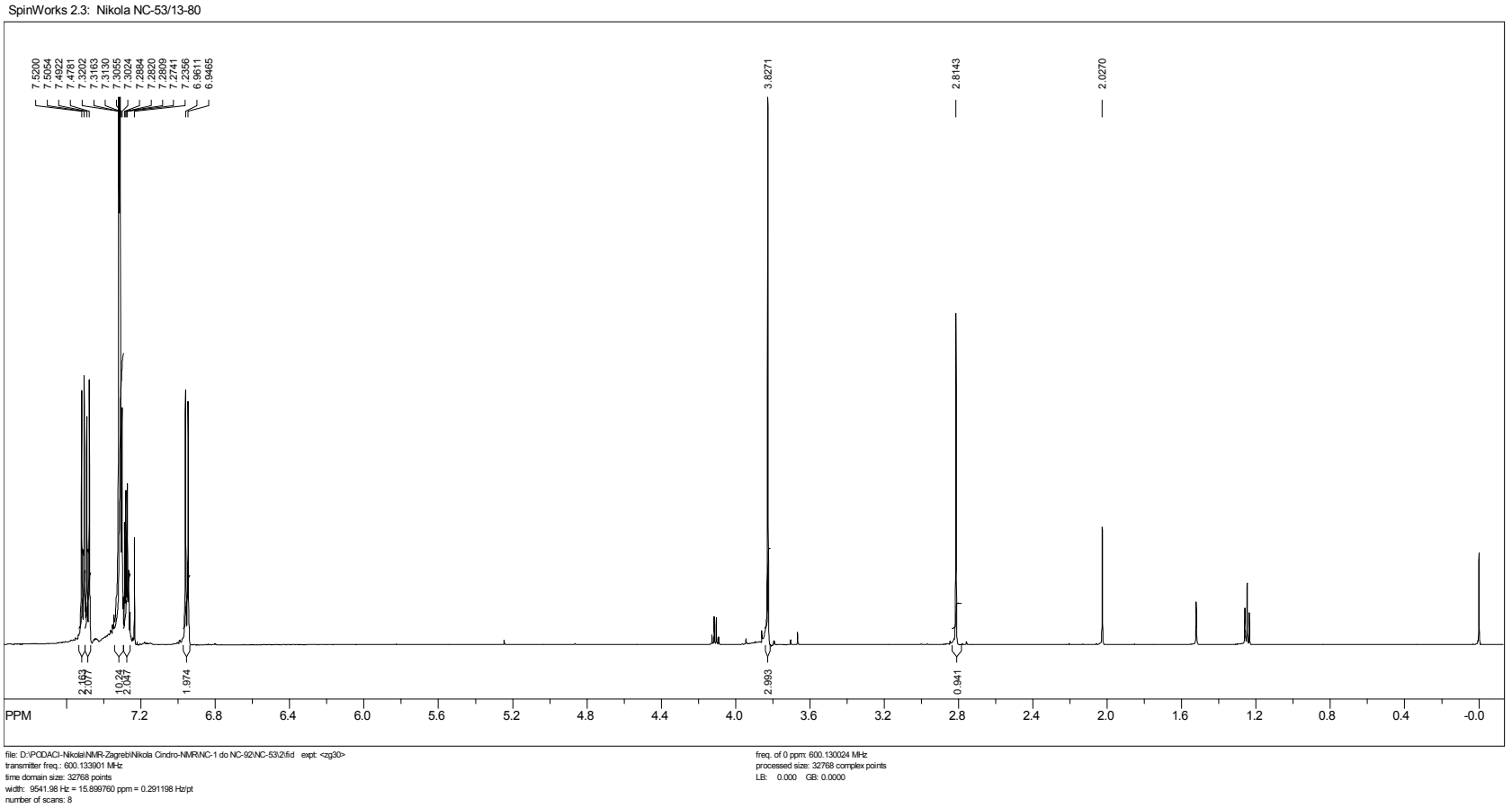

^{13}C NMR ($CDCl_3$, 150 MHz) of **8'**

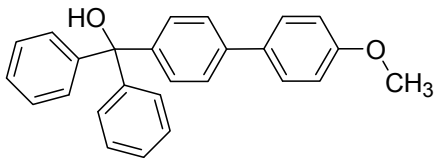

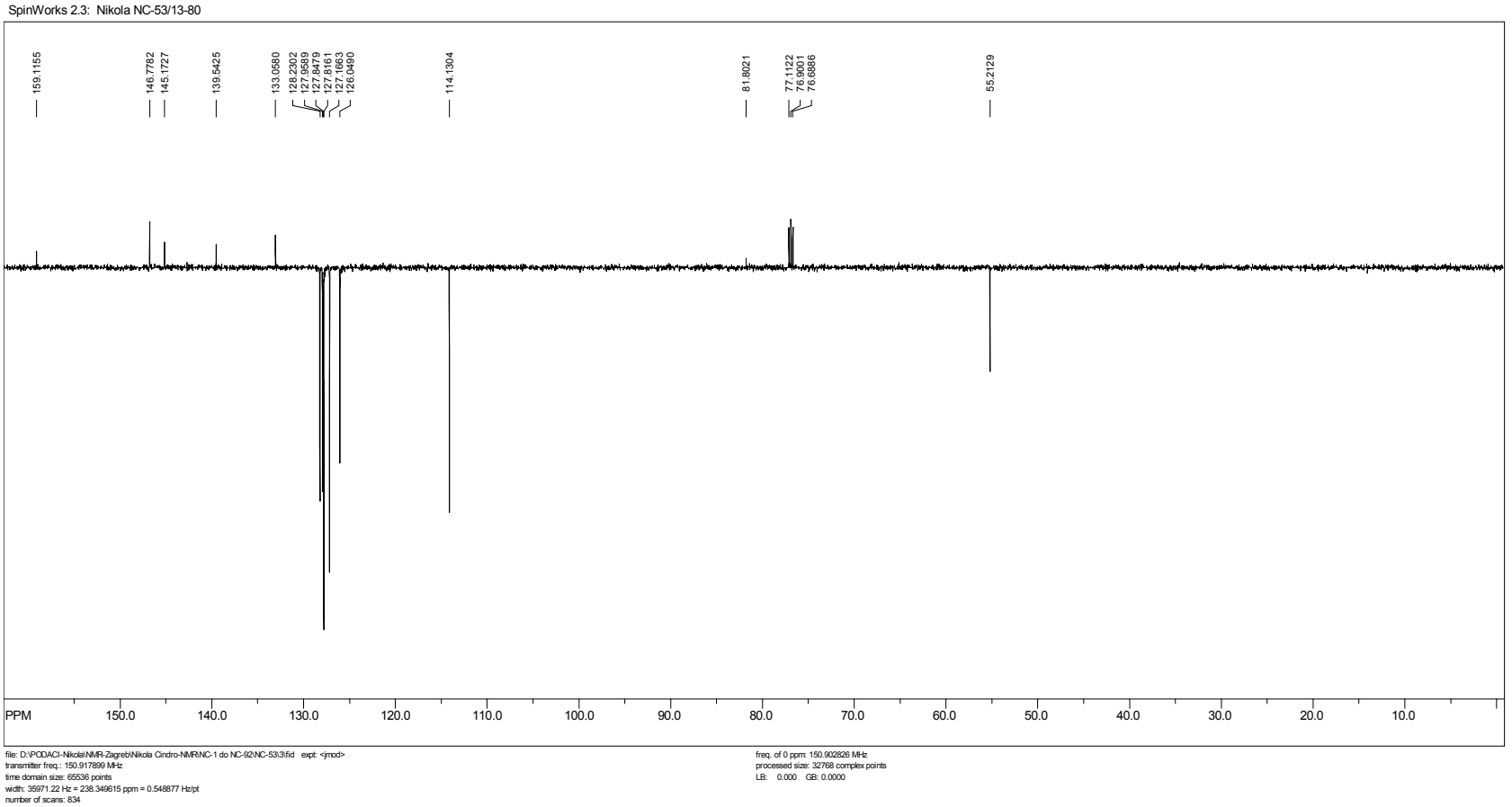

^{1}H NMR ($CDCl_3$, 300 MHz) of **9'**

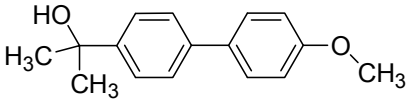

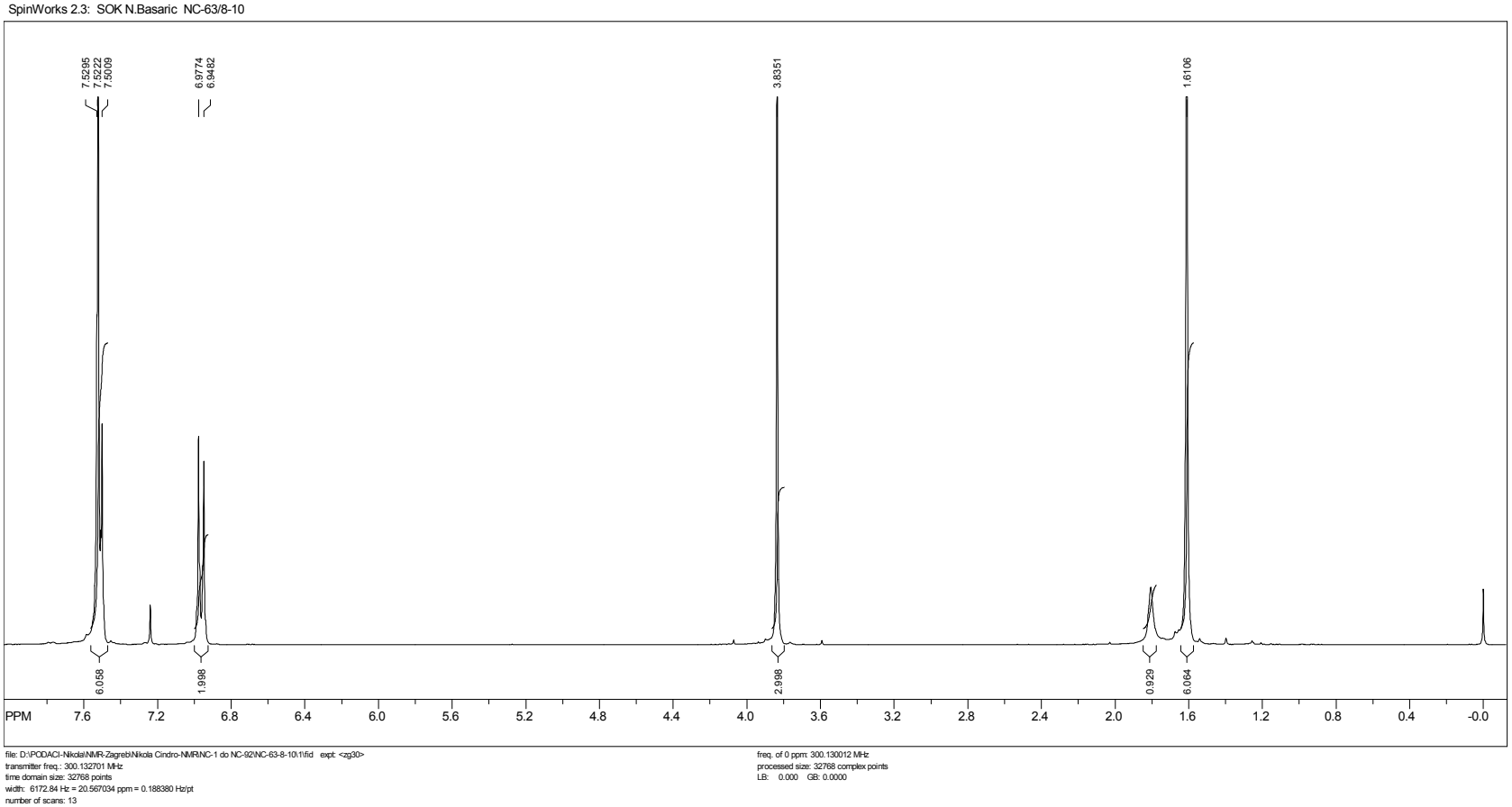

^{13}C NMR ($CDCl_3$, 75 MHz) of **9'**

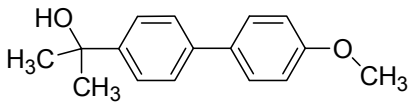

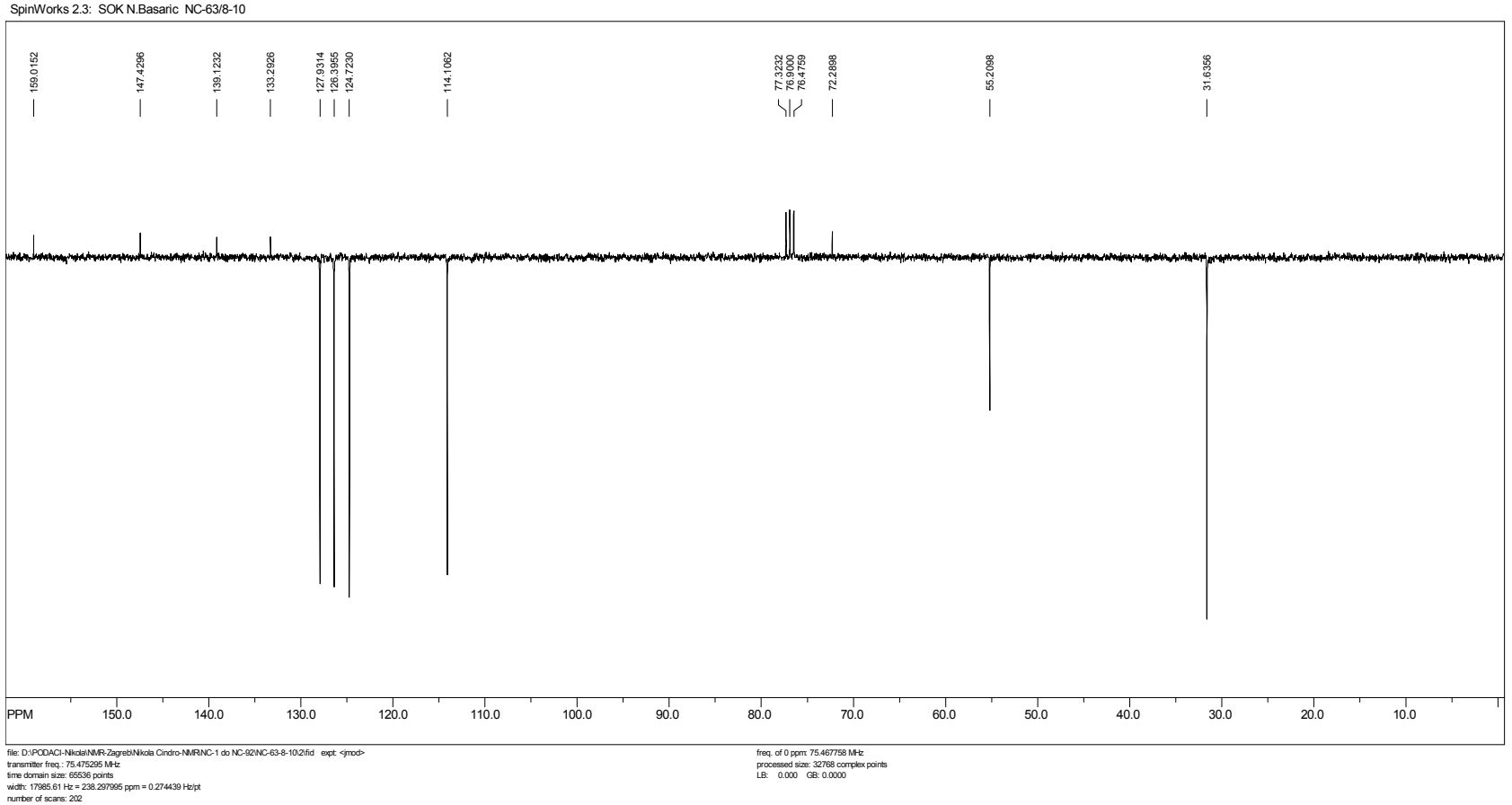

^{1}H NMR ($CDCl_3$, 300 MHz)

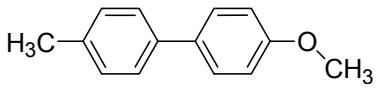

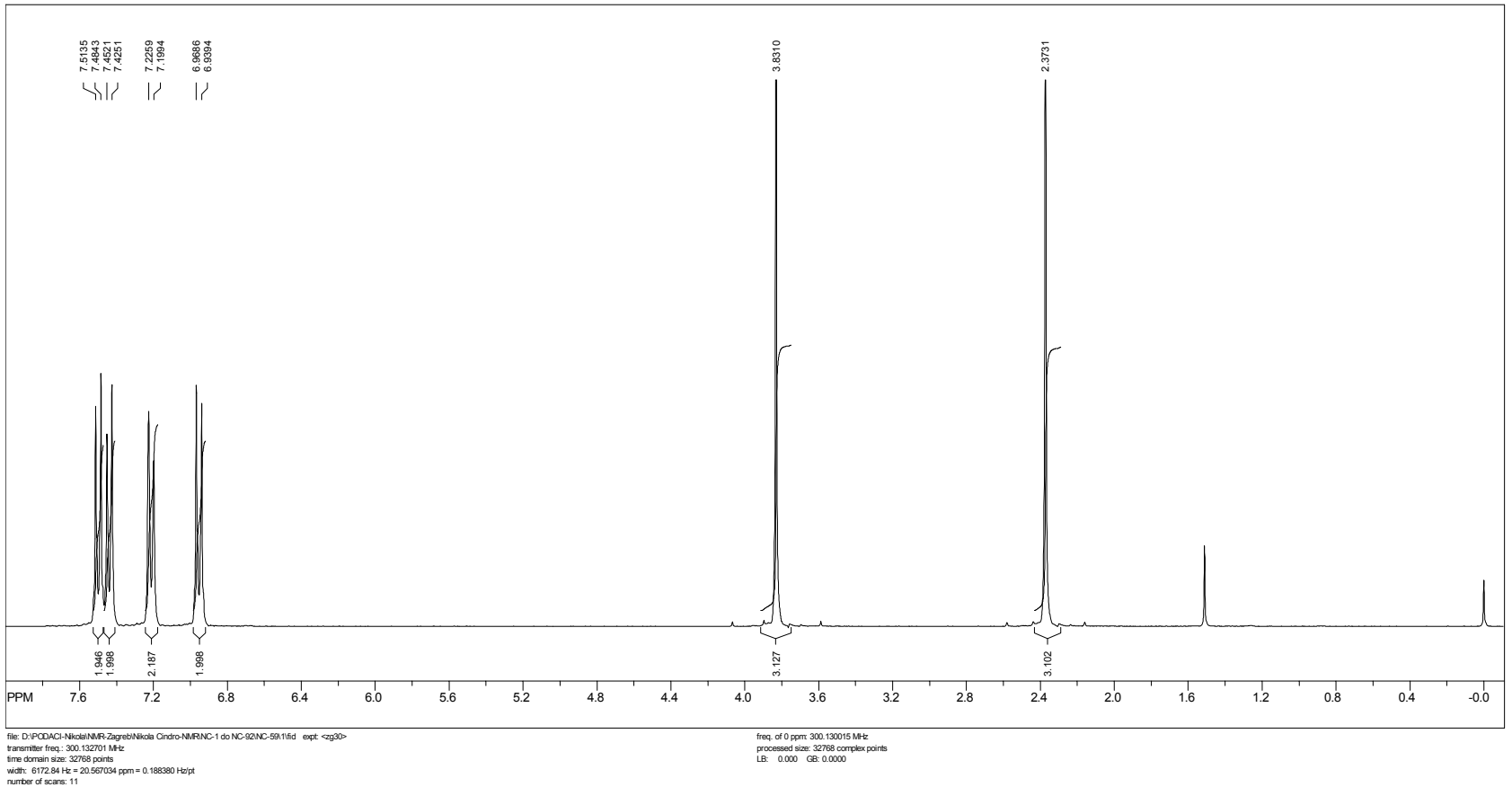

file: D:\PCDACI-Nikola\NMR-Zagreb\Nikola Cindro-NMR\NC-1 do NC-92\NC-59\1\fid expt: <zg30>
transmitter freq.: 300.132701 MHz
time domain size: 32768 points
width: 6172.84 Hz = 20.567034 ppm = 0.188380 Hz/pt
number of scans: 11

freq. of 0 ppm: 300.130015 MHz
processed size: 32768 complex points
LB: 0.000 GB: 0.0000

^{13}C NMR ($CDCl_3$, 75 MHz)

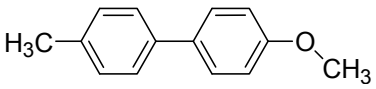

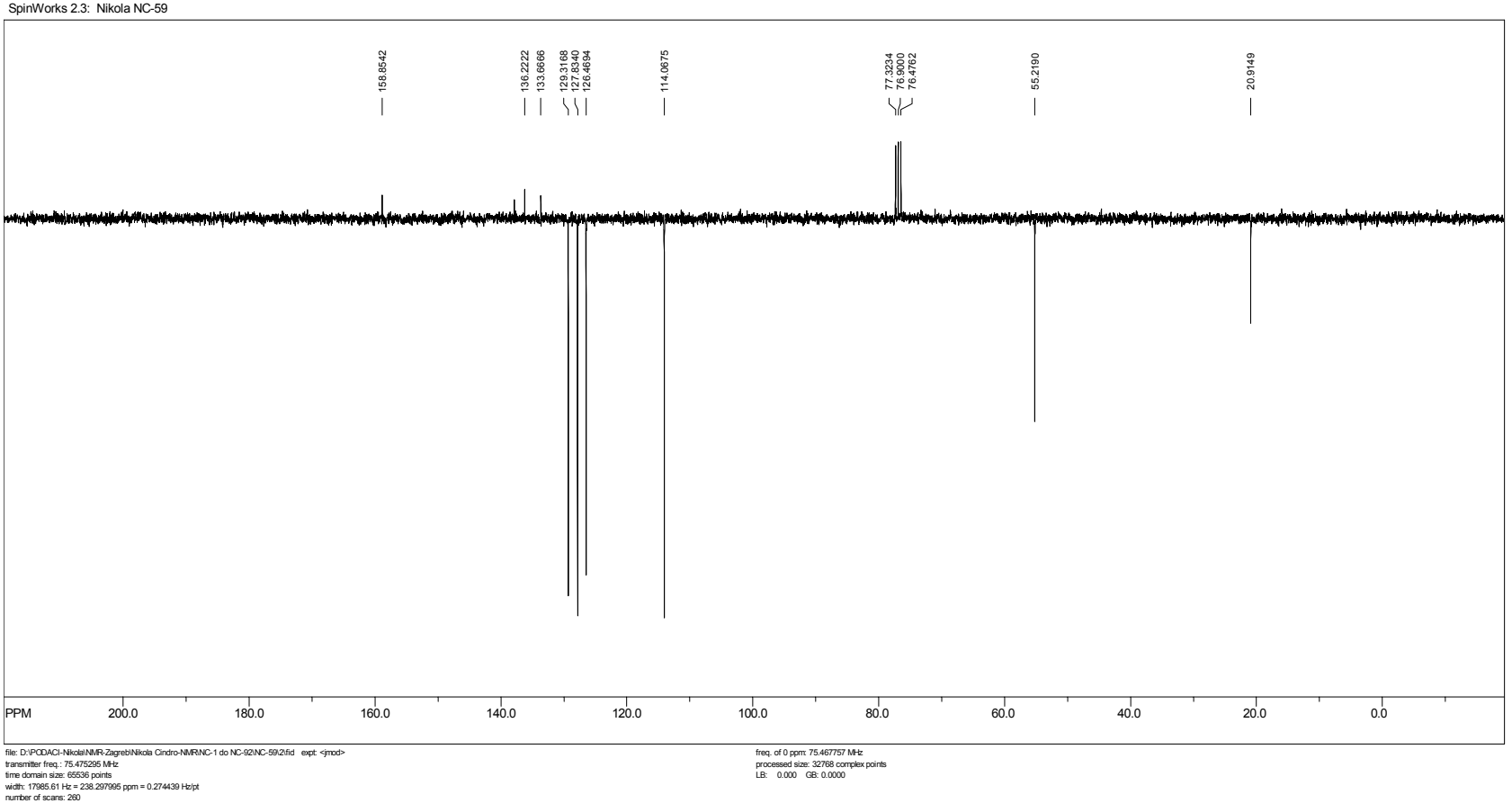

^{1}H NMR ($CDCl_3$, 300 MHz)

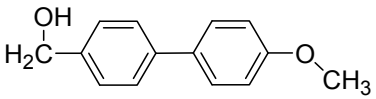

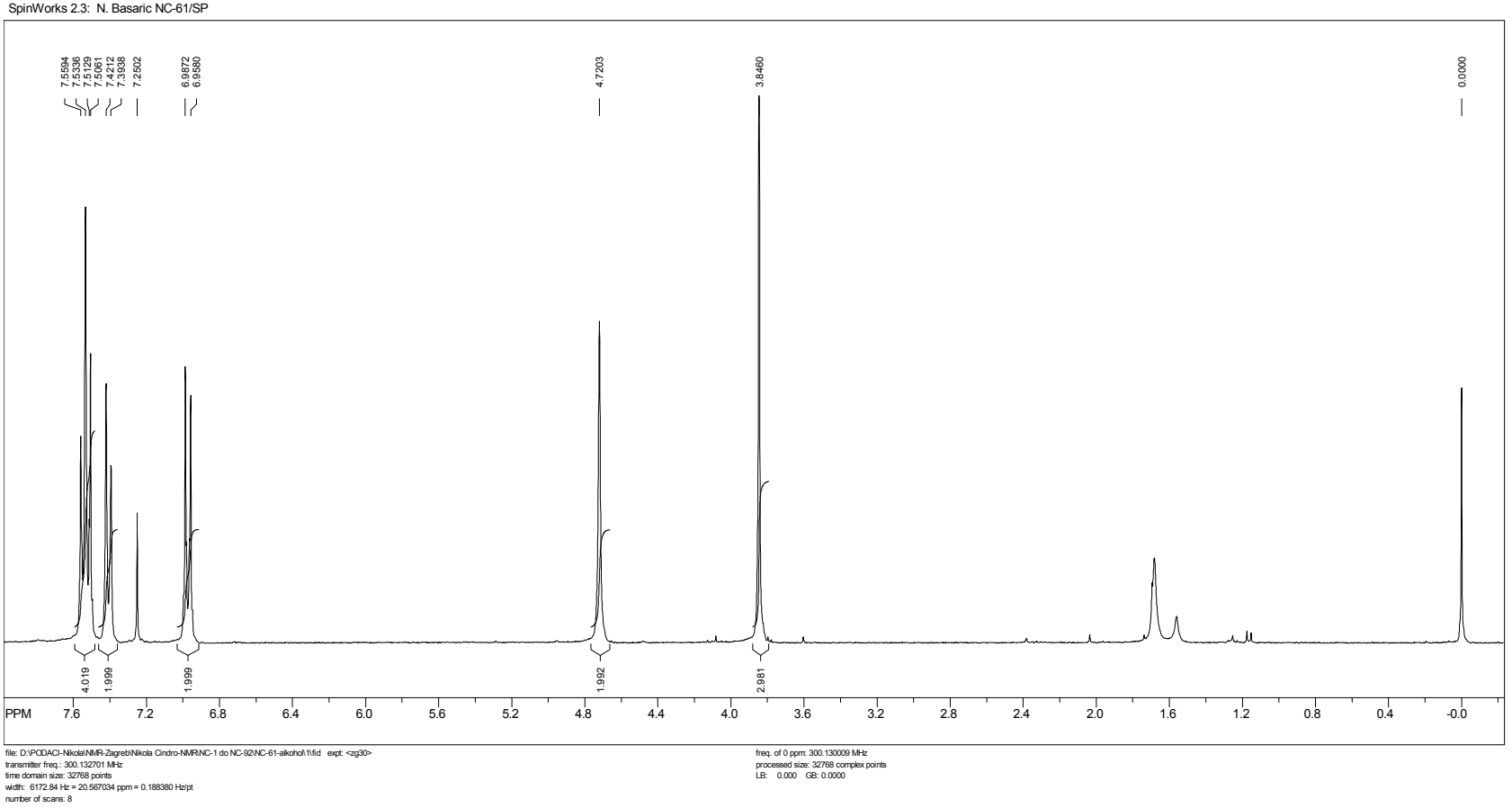

^{13}C NMR ($CDCl_3$, 75 MHz)

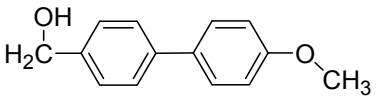

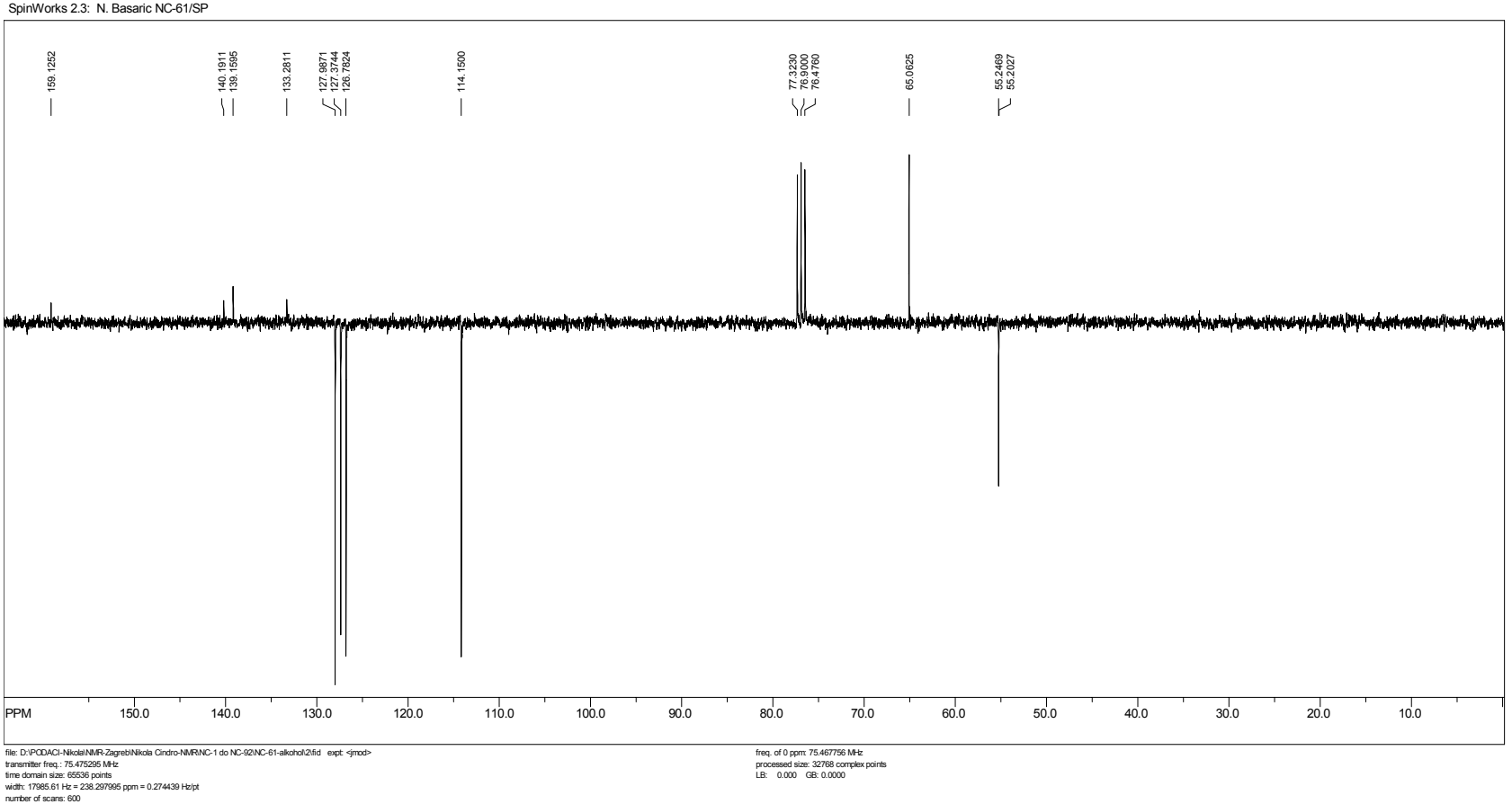

^{1}H NMR (DMSO-d_6, 300 MHz) of **5**

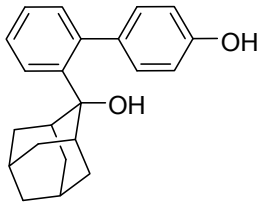

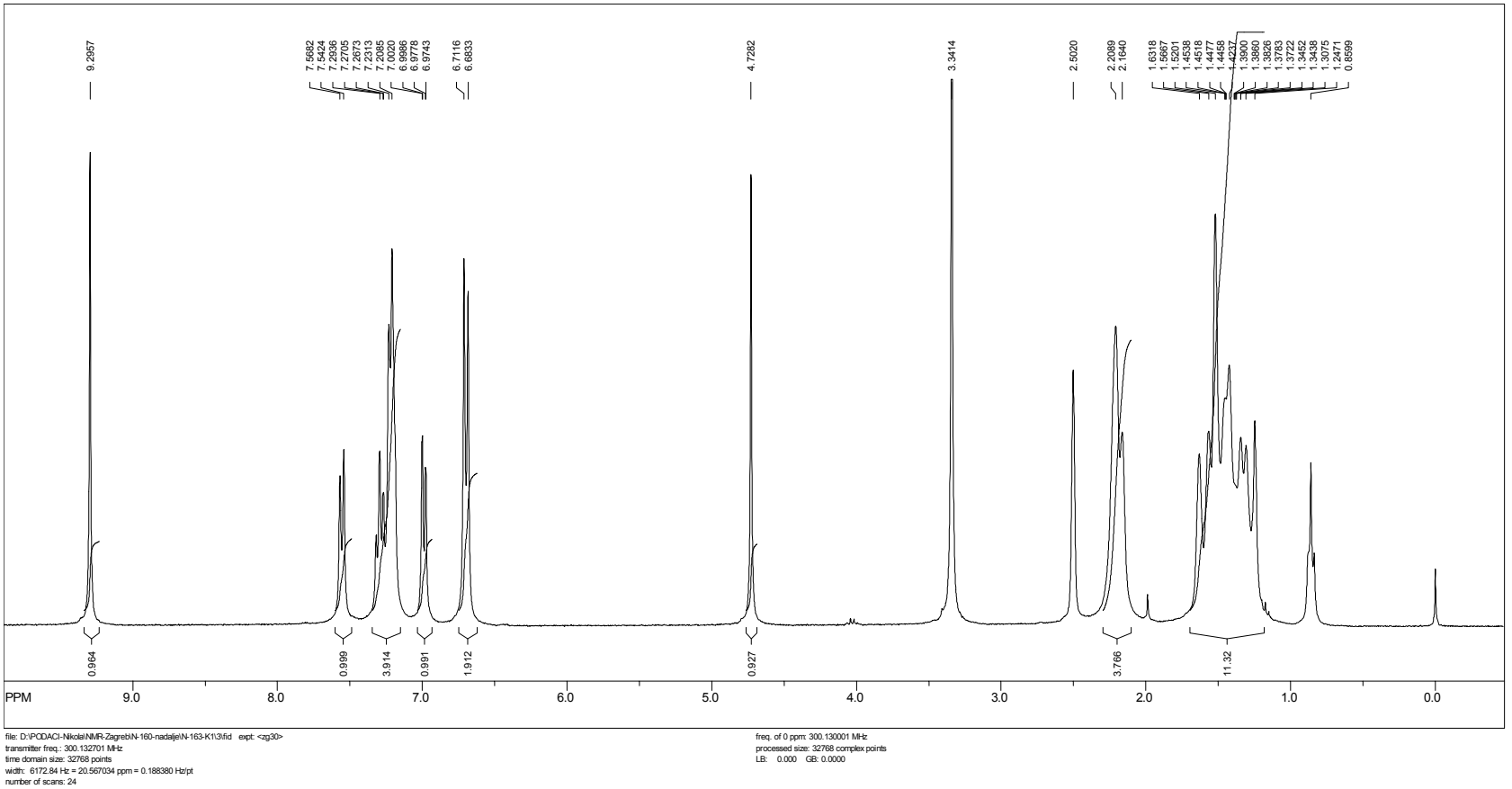

^{13}C NMR (DMSO-d_6, 75 MHz) of **5**

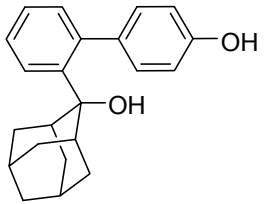

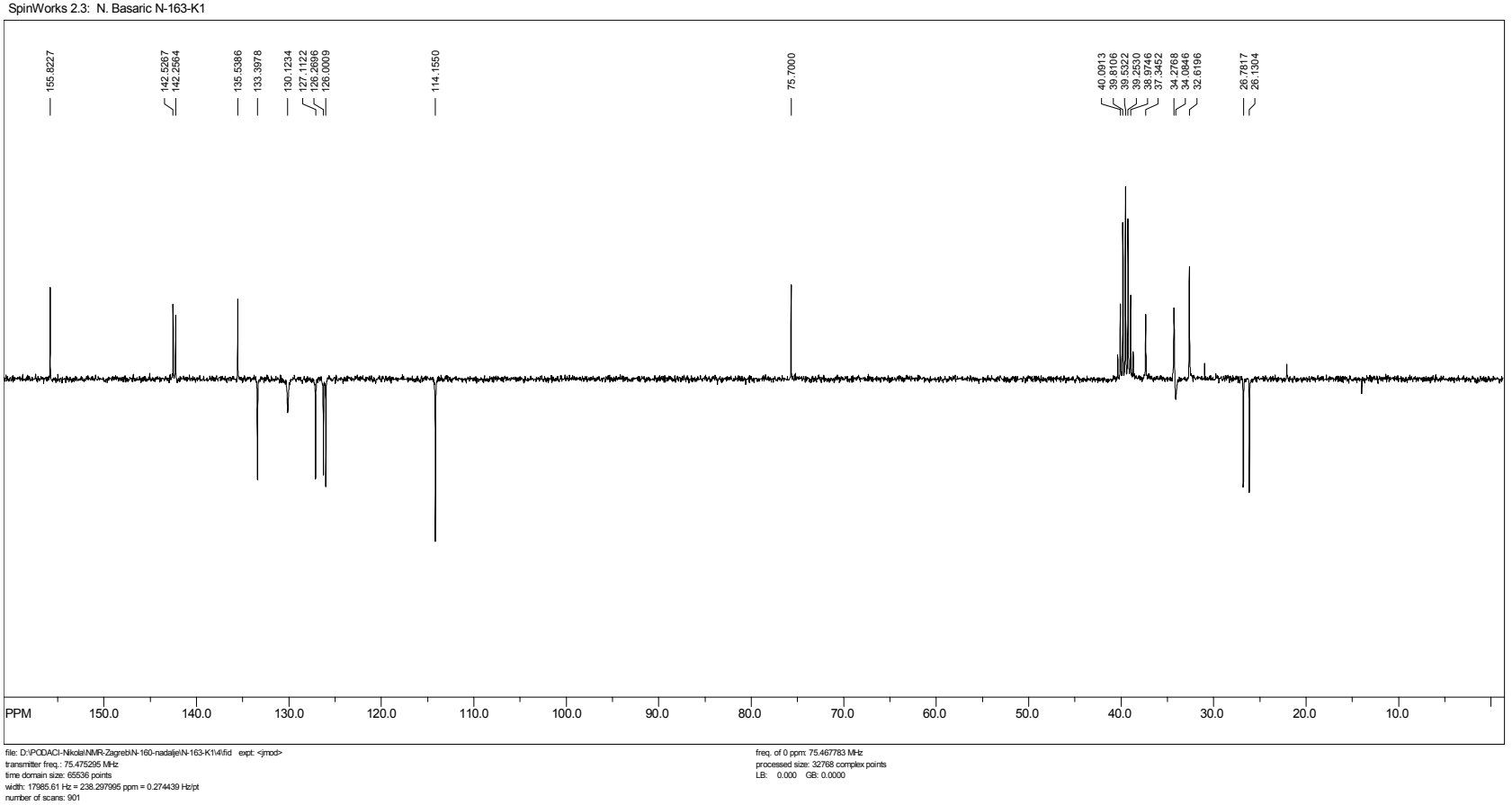

^{1}H NMR (DMSO-d_6, 300 MHz) of **6**

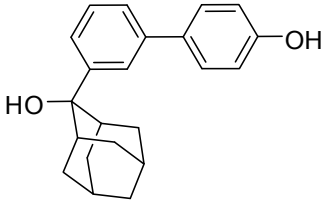

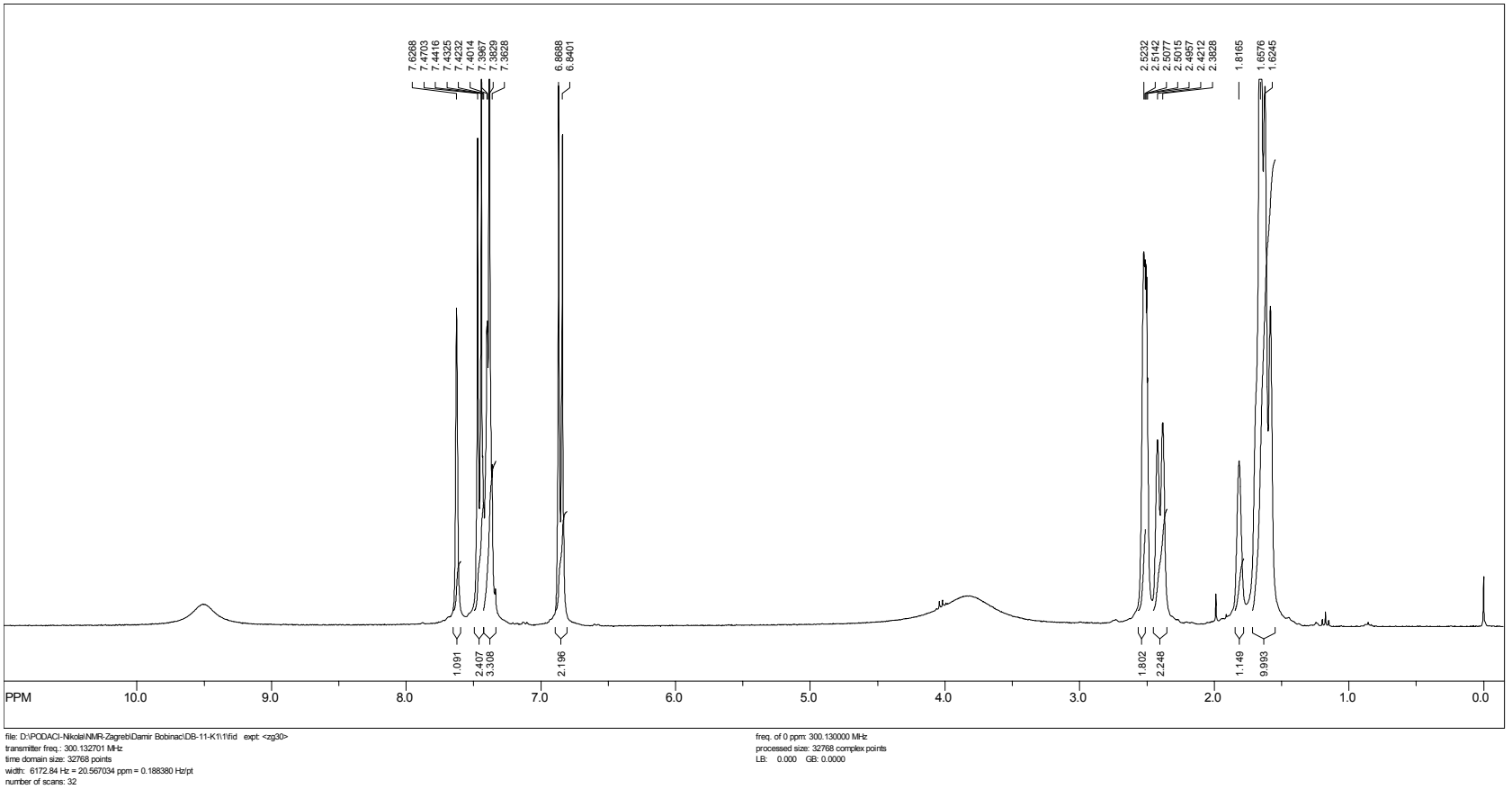

^{13}C NMR (DMSO-d_6, 75 MHz) of **6**

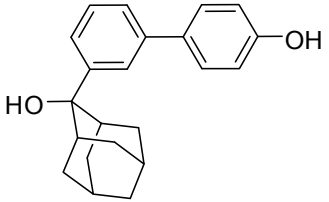

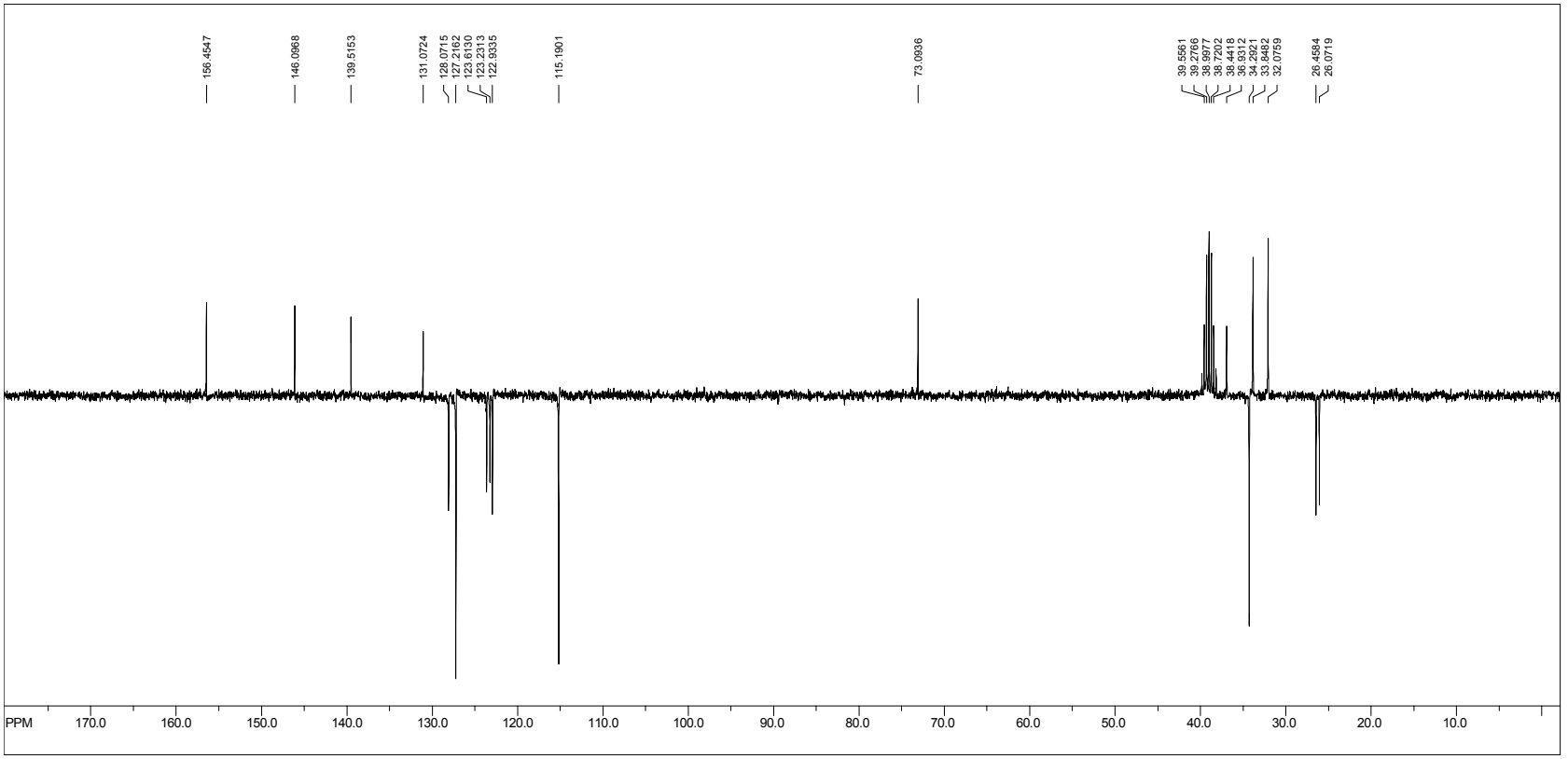

^{1}H NMR (DMSO-d_6, 300 MHz) of **7**

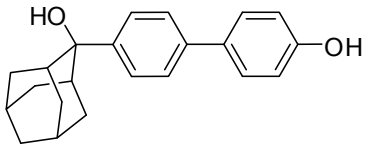

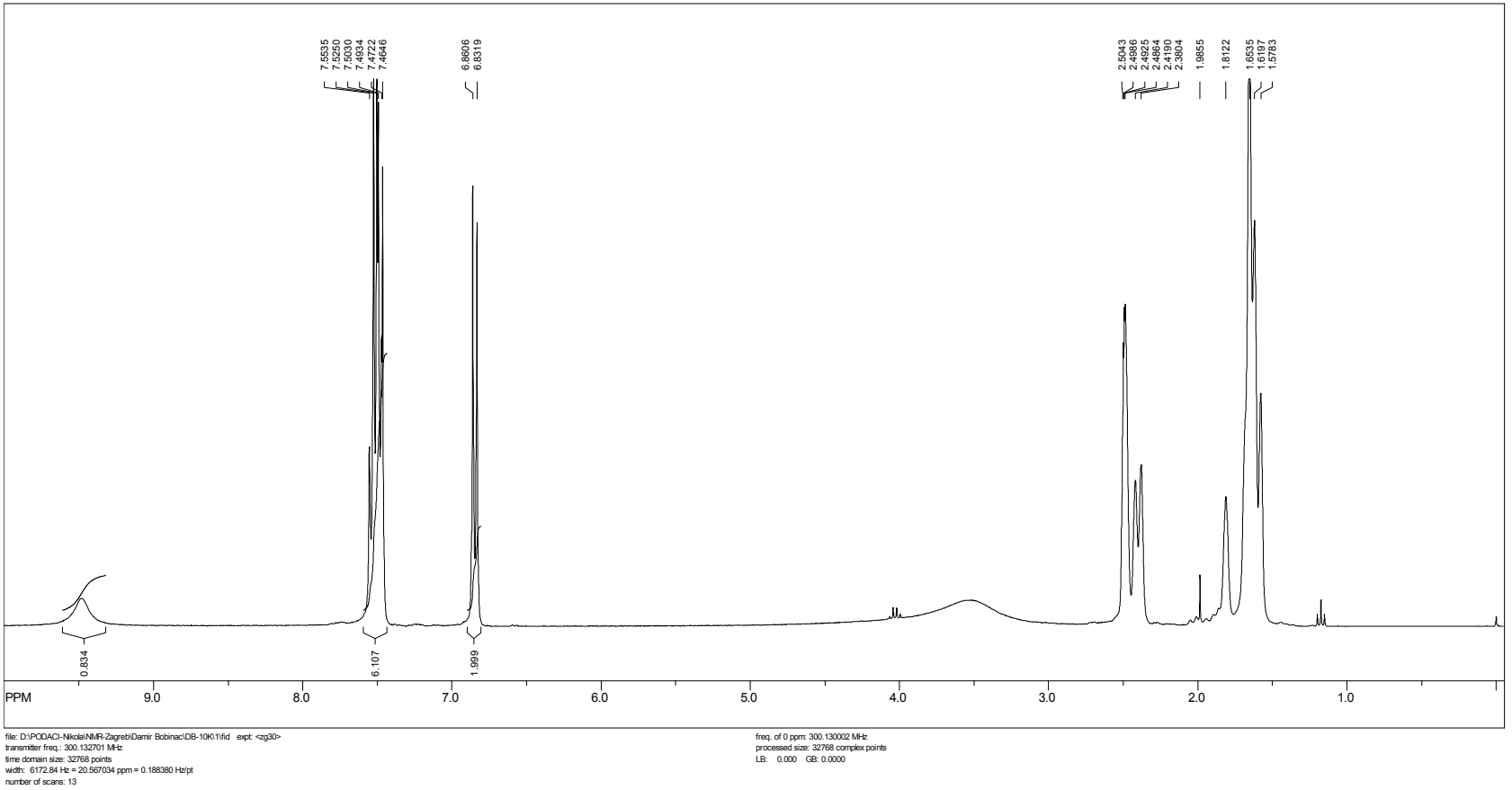

^{13}C (DMSO-d_6, 75 MHz) of **7**

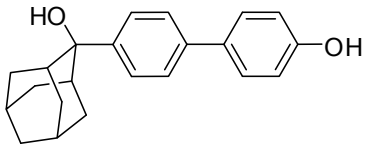

SpinWorks 2.3: SOK N.Basaric DB-10/k

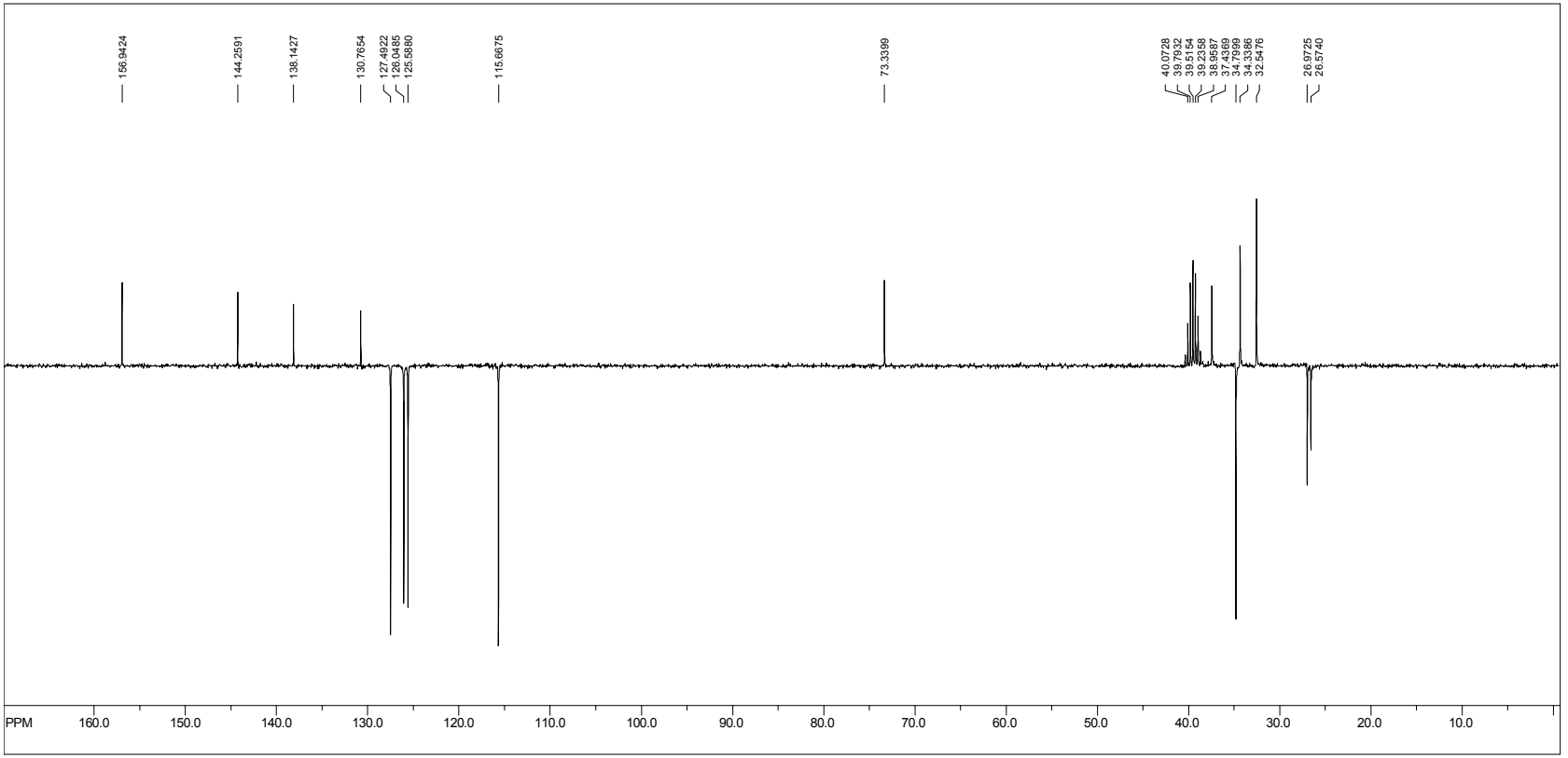

file: D:\PODACI-Nikola\NMR-Zagreb\Damir Bobinac\DB-10K\2\fid expt: <jmod>
transmitter freq.: 75.475295 MHz
time domain size: 65536 points
width: 17985.61 Hz = 238.297995 ppm = 0.274439 Hz/pt
number of scans: 592

freq. of 0 ppm: 75.467786 MHz
processed size: 32768 complex points
LB: 0.000 GB: 0.0000

^{1}H NMR (DMSO-d_6, 300 MHz) of **8**

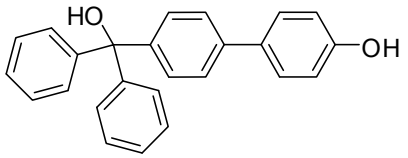

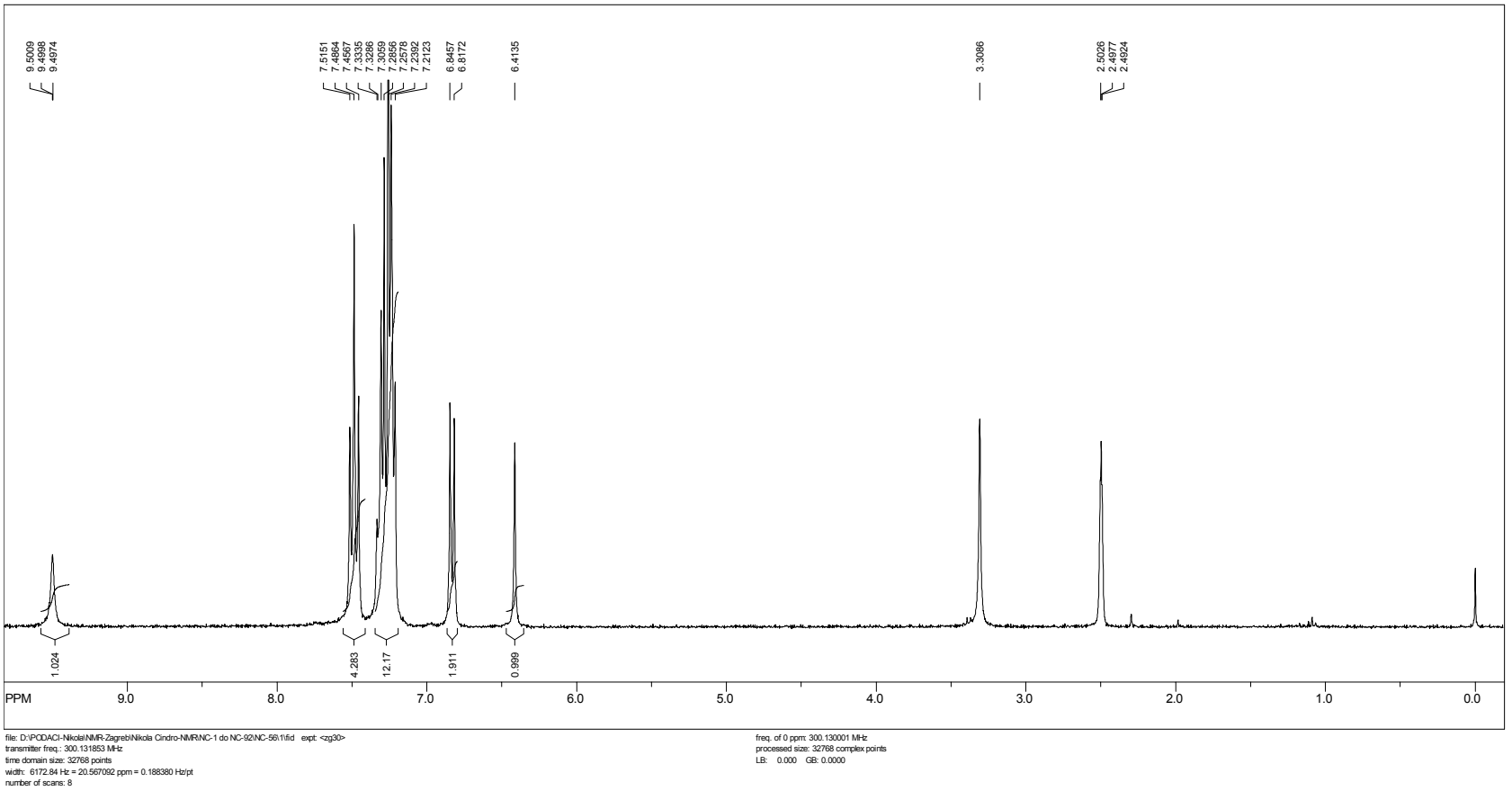

^{13}C NMR (DMSO-d_6, 75 MHz) of **8**

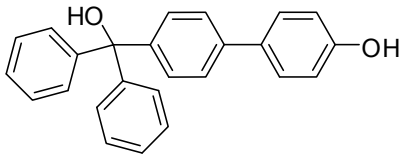

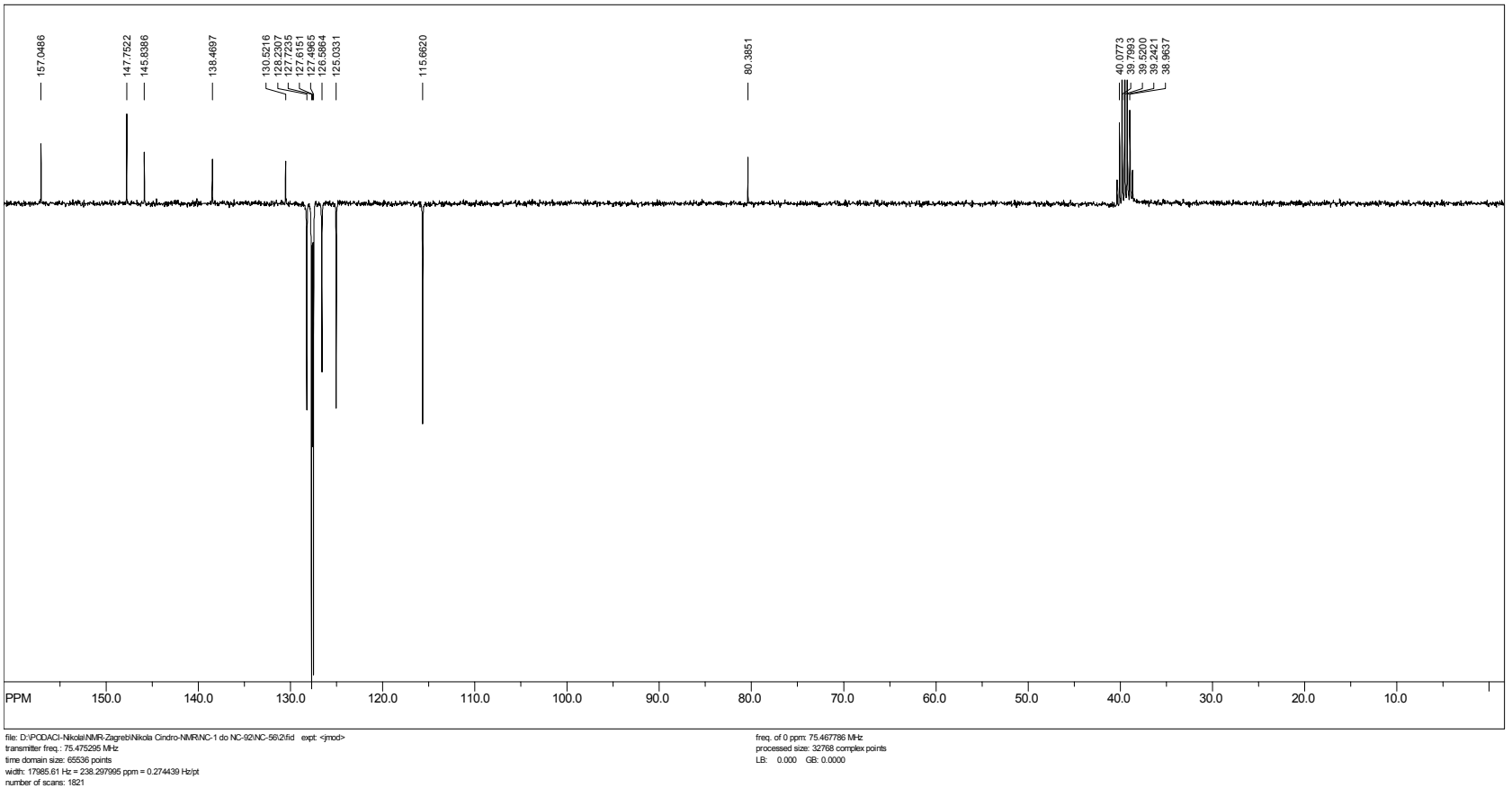

^{1}H NMR (DMSO-d_6, 300 MHz) of **9**

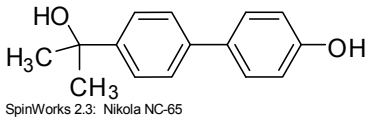

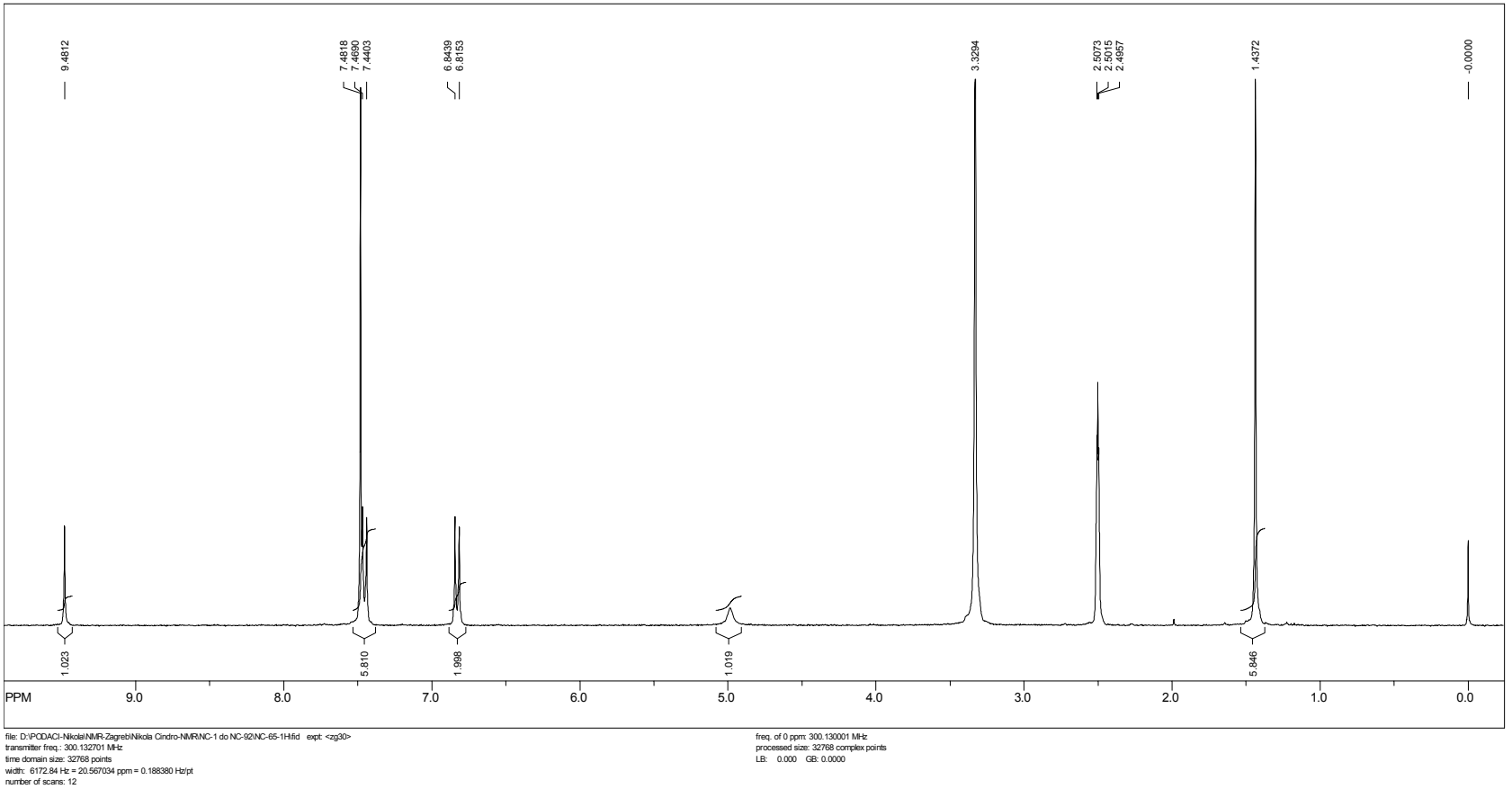

^{13}C NMR (DMSO-d_6, 75 MHz) of **9**

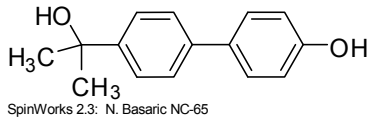

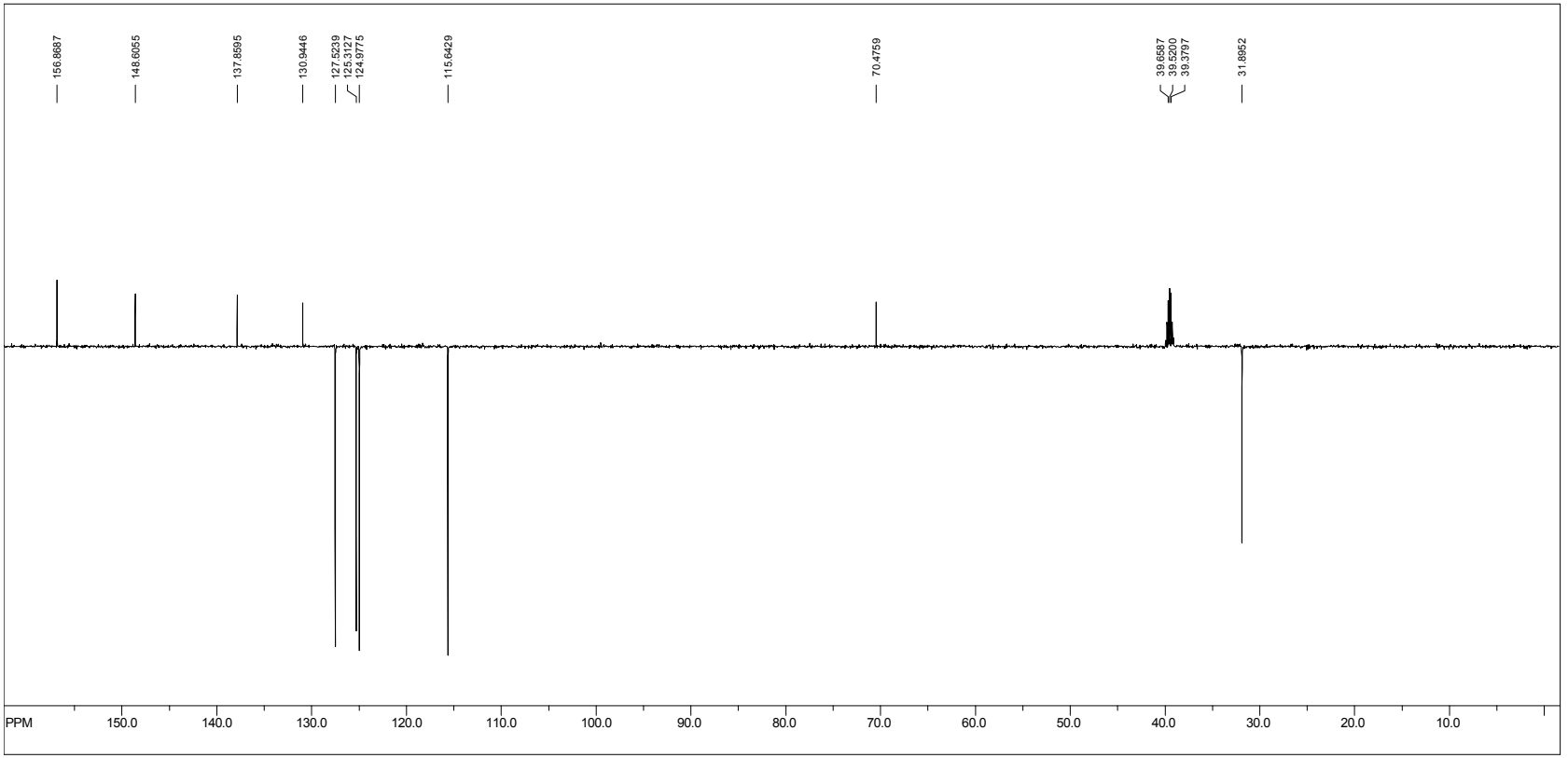

file: D:\PODACI-Nikola\NMR-Zagreb\Nikola Cindro-NMR\NC-1 do NC-92\NC-65-13C\fid expt: <jmod>
transmitter freq.: 150.917899 MHz
time domain size: 65536 points
width: 35971.22 Hz = 238.349615 ppm = 0.548877 Hz/pt
number of scans: 192

freq. of 0 ppm: 150.902882 MHz
processed size: 32768 complex points
LB: 0.000 GB: 0.0000

^{1}H NMR (DMSO-d_6, 300 MHz) of **10**

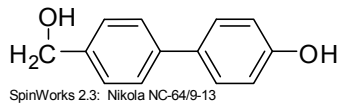

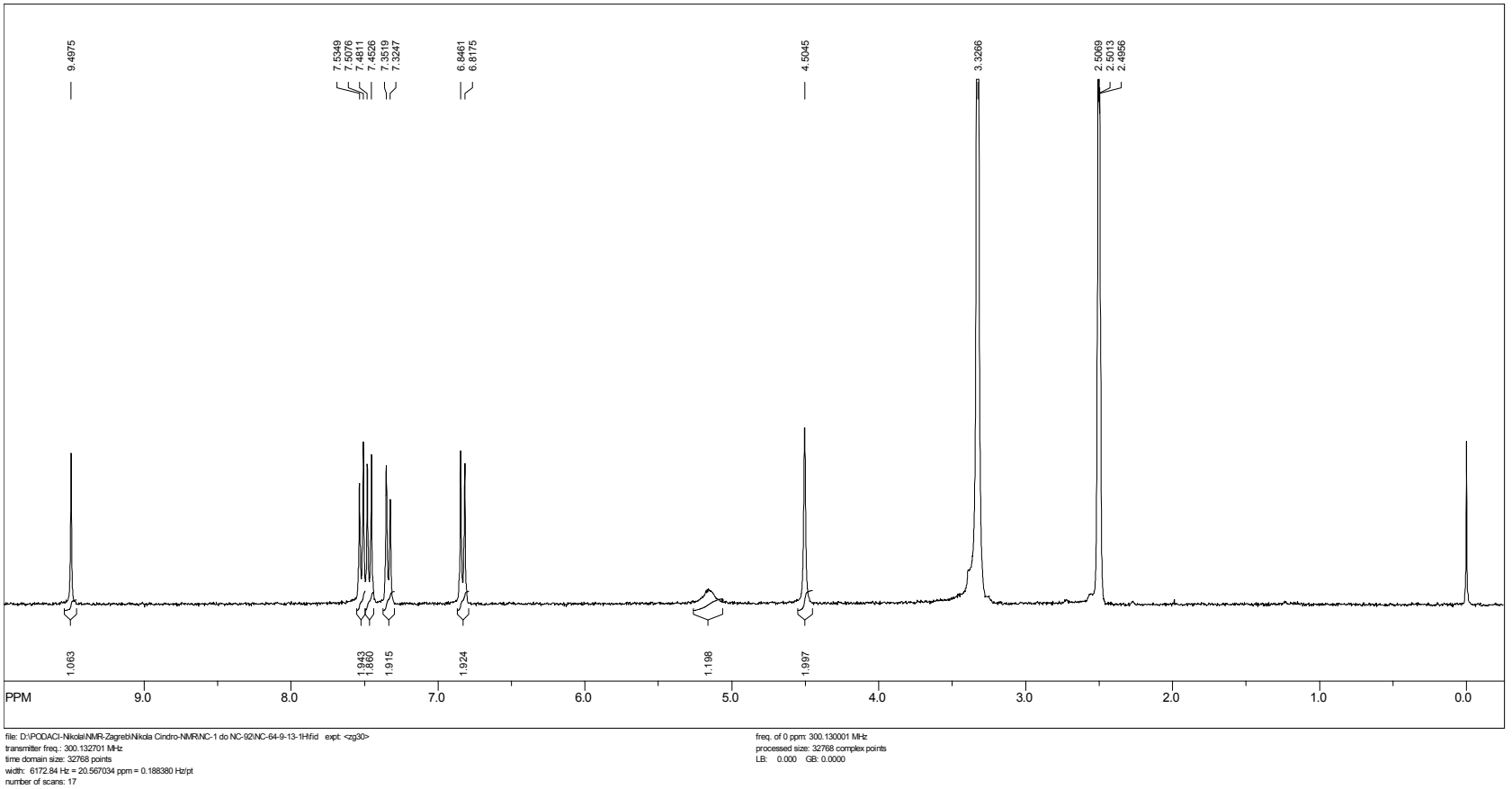

file: D:\PODACI-Nikola\NMR-Zagreb\Nikola Cindro-NMR\NC-1 do NC-92\NC-64-9-13-1H\fid expt: <zg30>
transmitter freq.: 300.132701 MHz
time domain size: 32768 points
width: 6172.84 Hz = 20.567034 ppm = 0.188380 Hz/pt
number of scans: 17

freq. of 0 ppm: 300.130001 MHz
processed size: 32768 complex points
LB: 0.000 GB: 0.0000

^{13}C NMR (DMSO-d_6, 75 MHz) of **10**

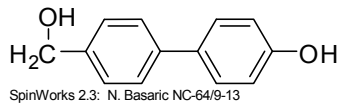

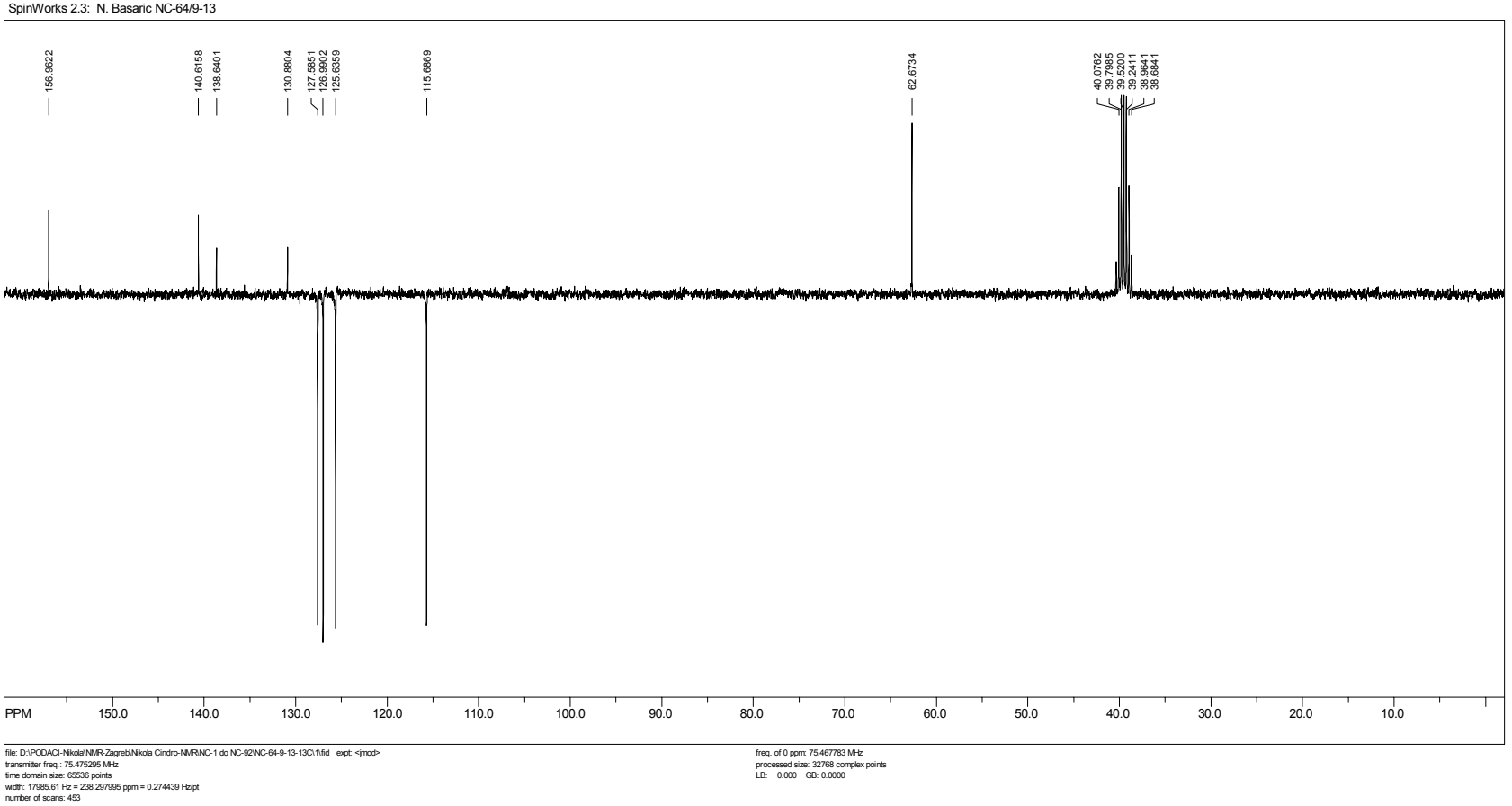

^{1}H NMR ($CDCl_3$, 300 MHz) of **11**

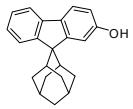

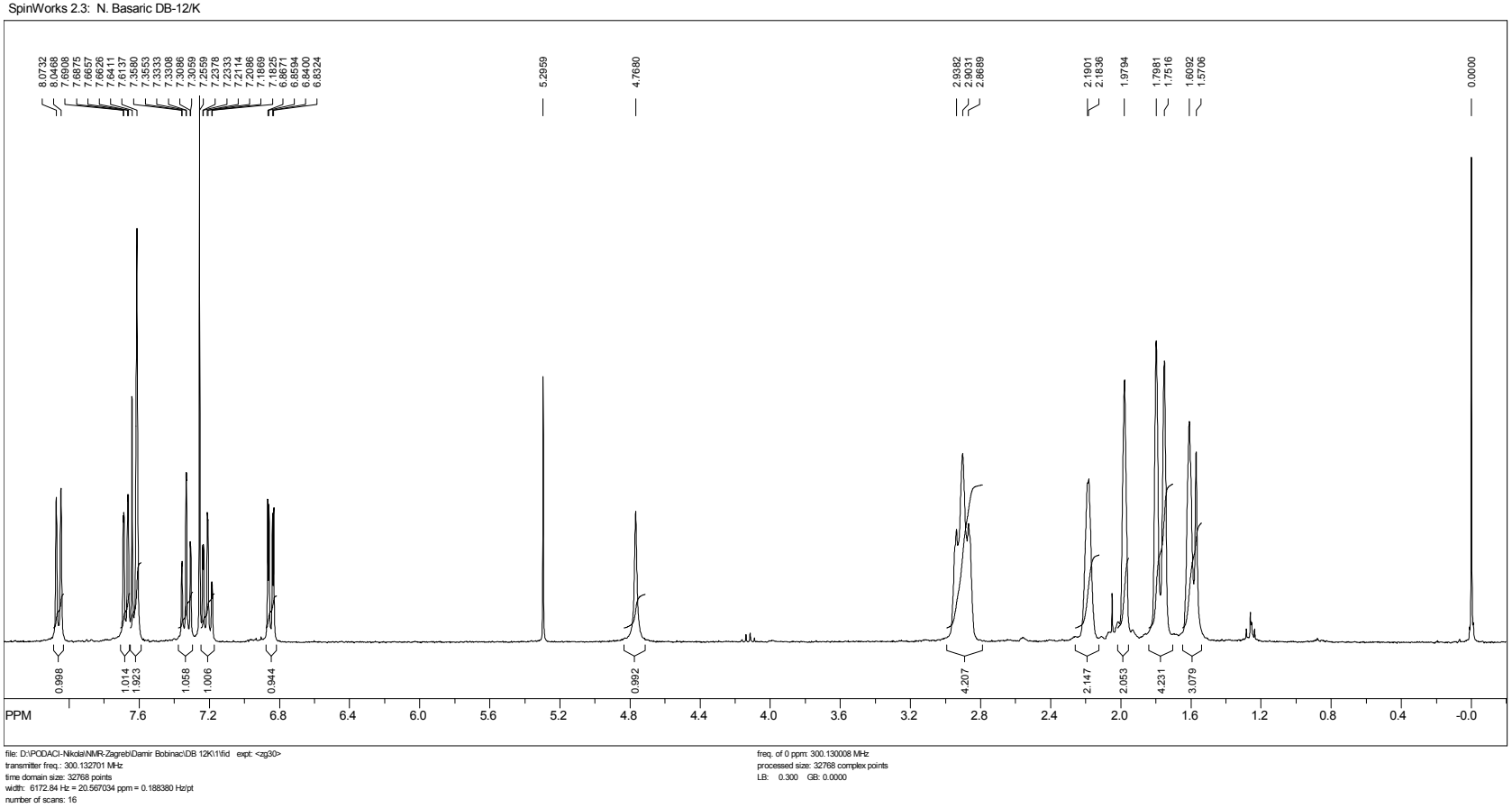

^{13}C NMR ($CDCl_3$, 125 MHz) of **11**

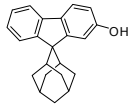

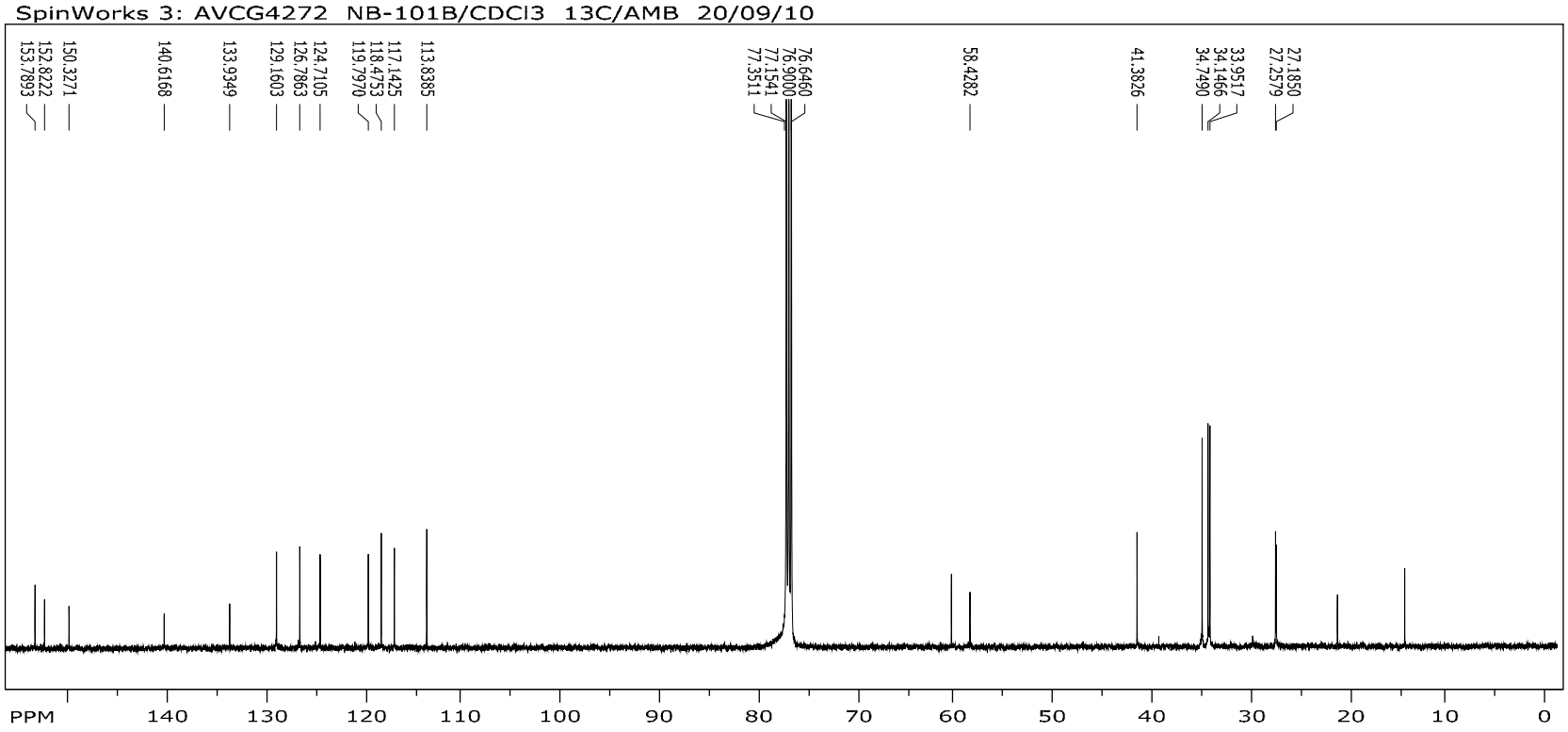

file: ...ck\500 MHz\NB-10 1B\avcg4272\1\fid expt: <zgpg30>
transmitter freq.: 125.771539 MHz
time domain size: 65536 points
width: 30864.20 Hz = 245.3989 ppm = 0.470950 Hz/pt
number of scans: 28024

freq. of 0 ppm: 125.757802 MHz
processed size: 32768 complex points
LB: 1.200 GF: 0.0000
Hz/cm: 796.201 ppm/cm: 6.33053

^{13}C NMR ($CDCl_3$, 125 MHz, DEPT) of **11**

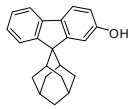

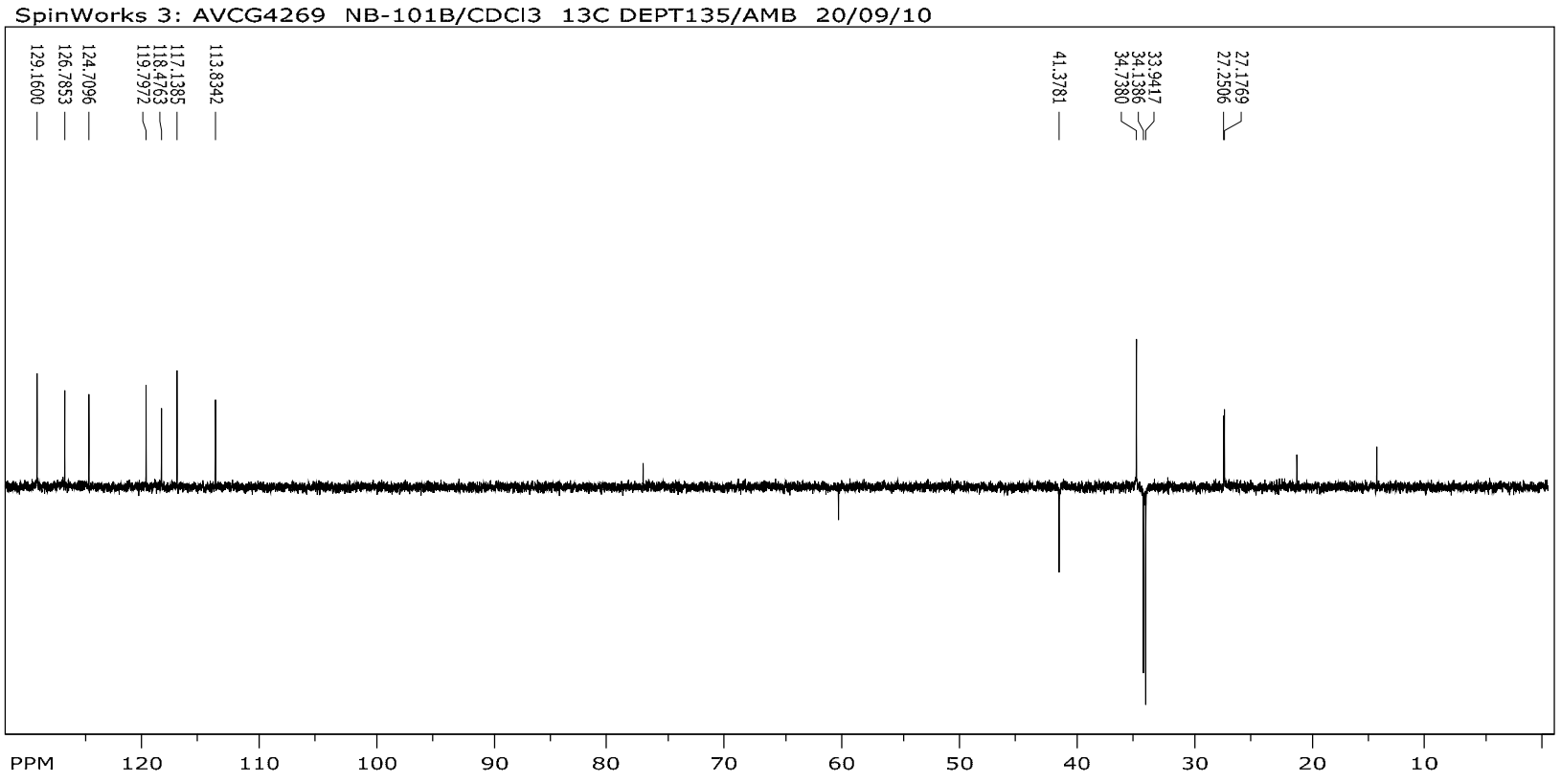

file: ...ck\500 MHz\NB-10 1B\avcg4269\1\fid expt: <dept135>
transmitter freq.: 125.771539 MHz
time domain size: 65536 points
width: 30864.20 Hz = 245.3989 ppm = 0.470950 Hz/pt
number of scans: 2048

freq. of 0 ppm: 125.757803 MHz
processed size: 32768 complex points
LB: 0.900 GF: 0.0000
Hz/cm: 666.683 ppm/cm: 5.30075

^{1}H NMR ($CDCl_3$, 300 MHz) of **6OMe**

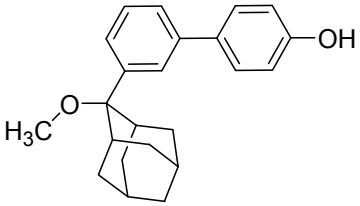

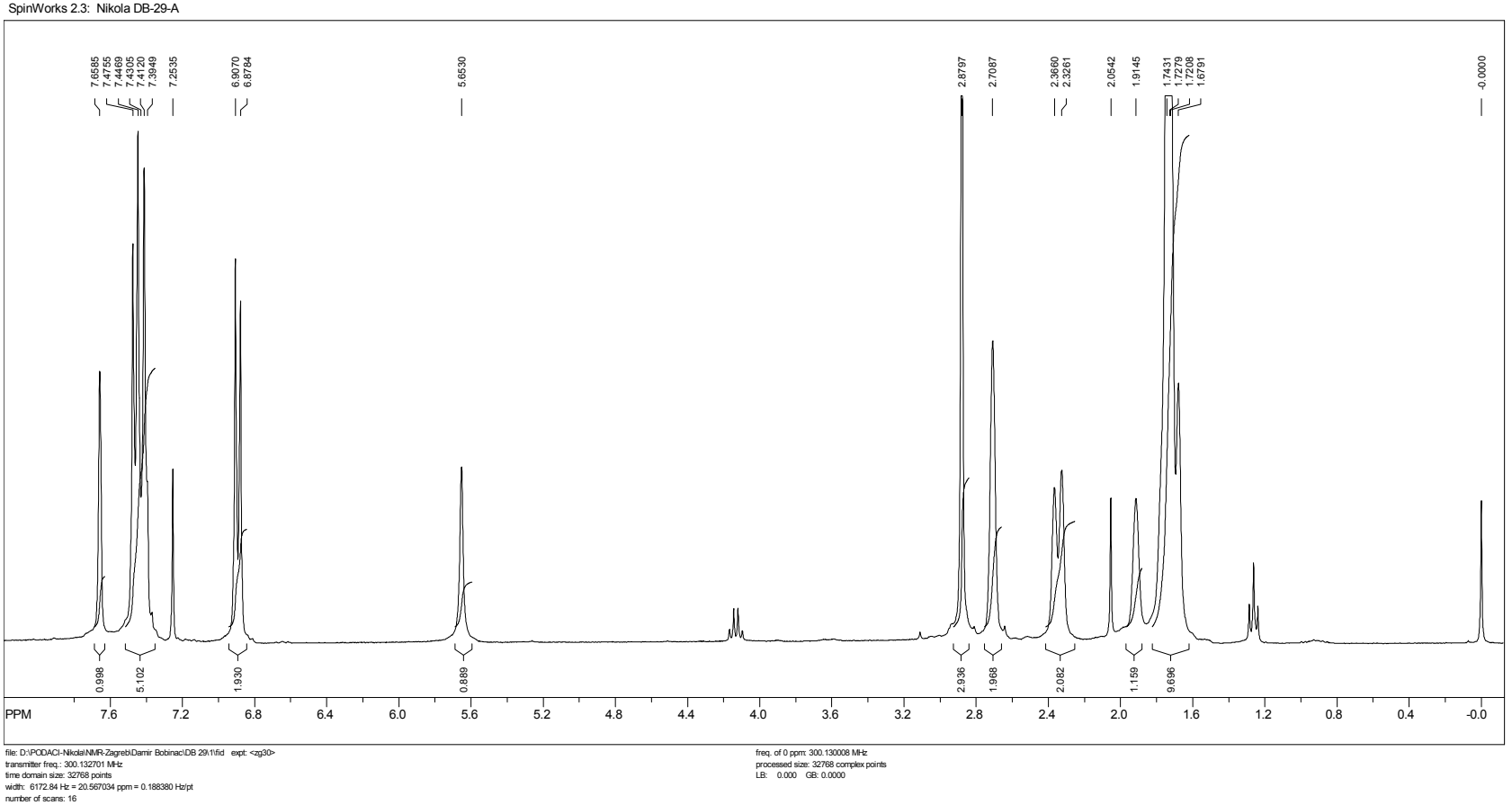

^{13}C NMR ($CDCl_3$, 75 MHz, APT) of **6OMe**

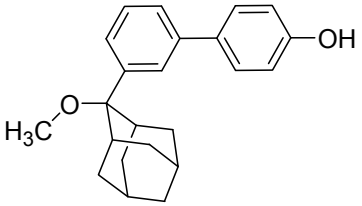

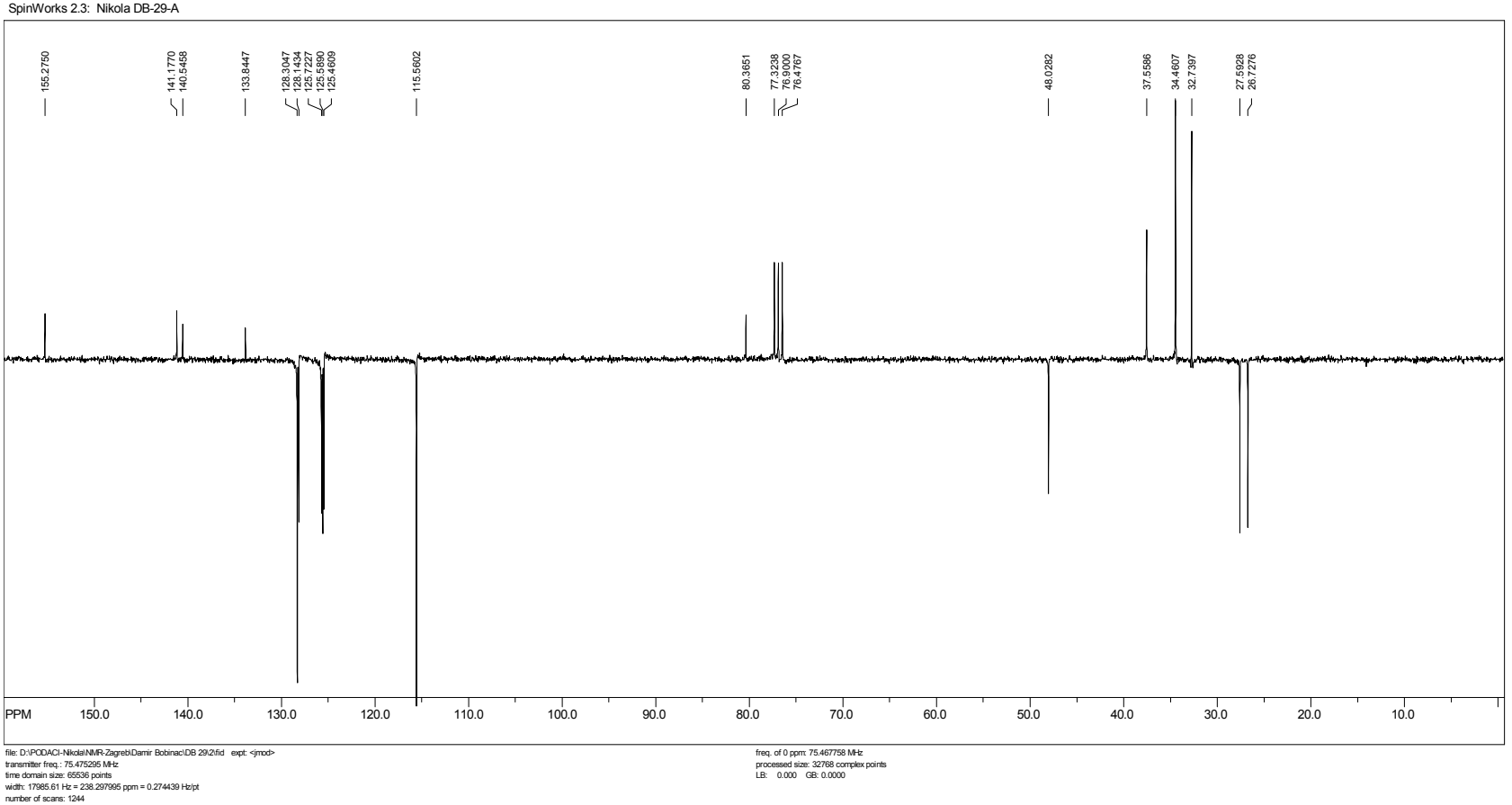

^{1}H NMR ($CDCl_3$, 300 MHc) of **7OMe**

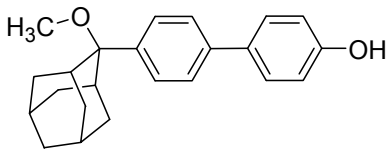

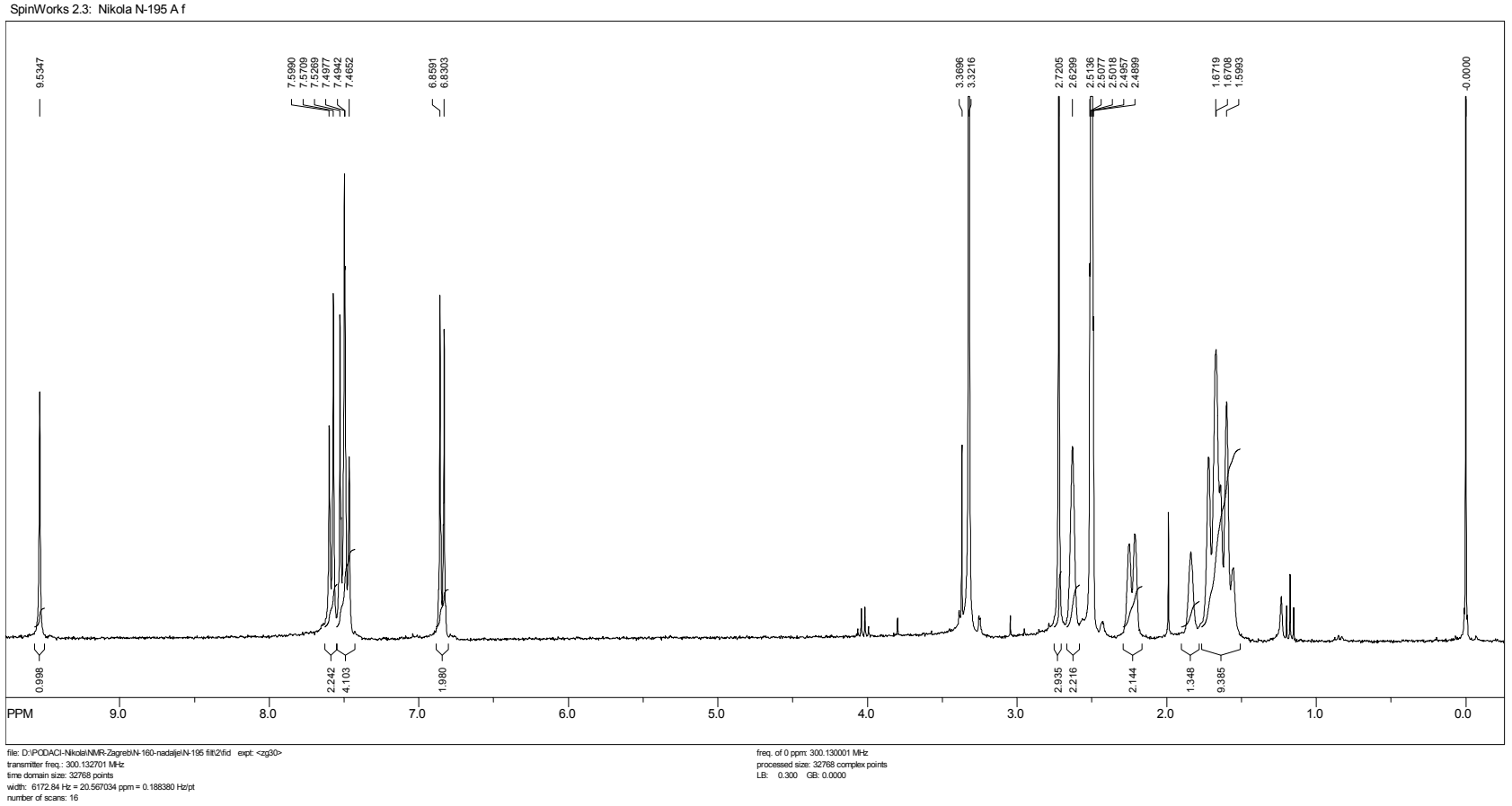

^{13}C NMR ($CDCl_3$, 300 MHz) of **7OMe**

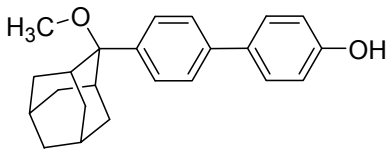

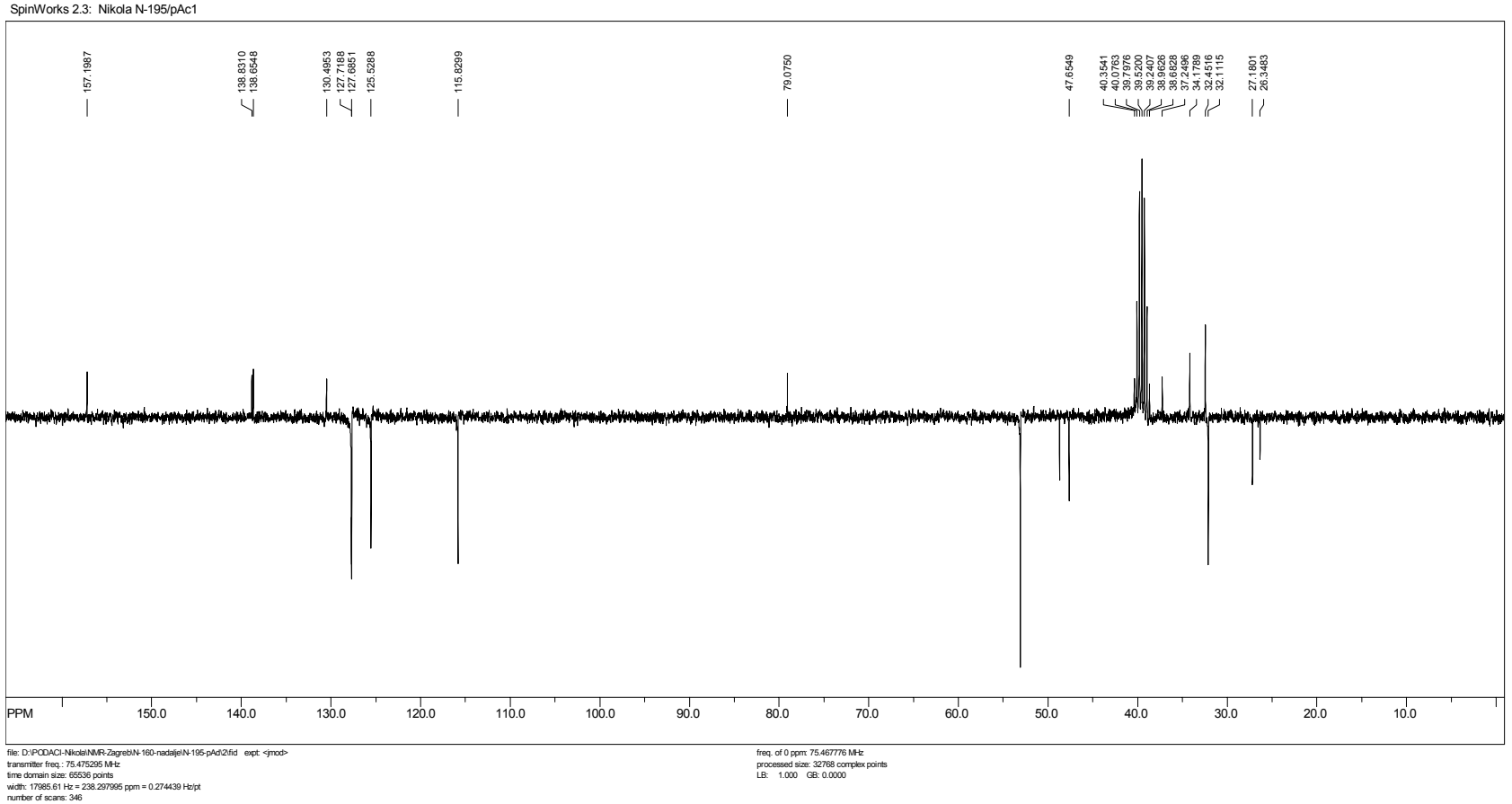

^{1}H NMR ($CDCl_3$, 500 MHz) of **8OMe**

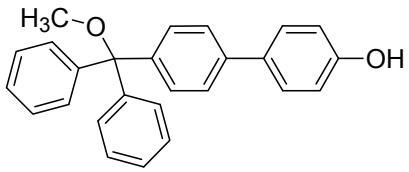

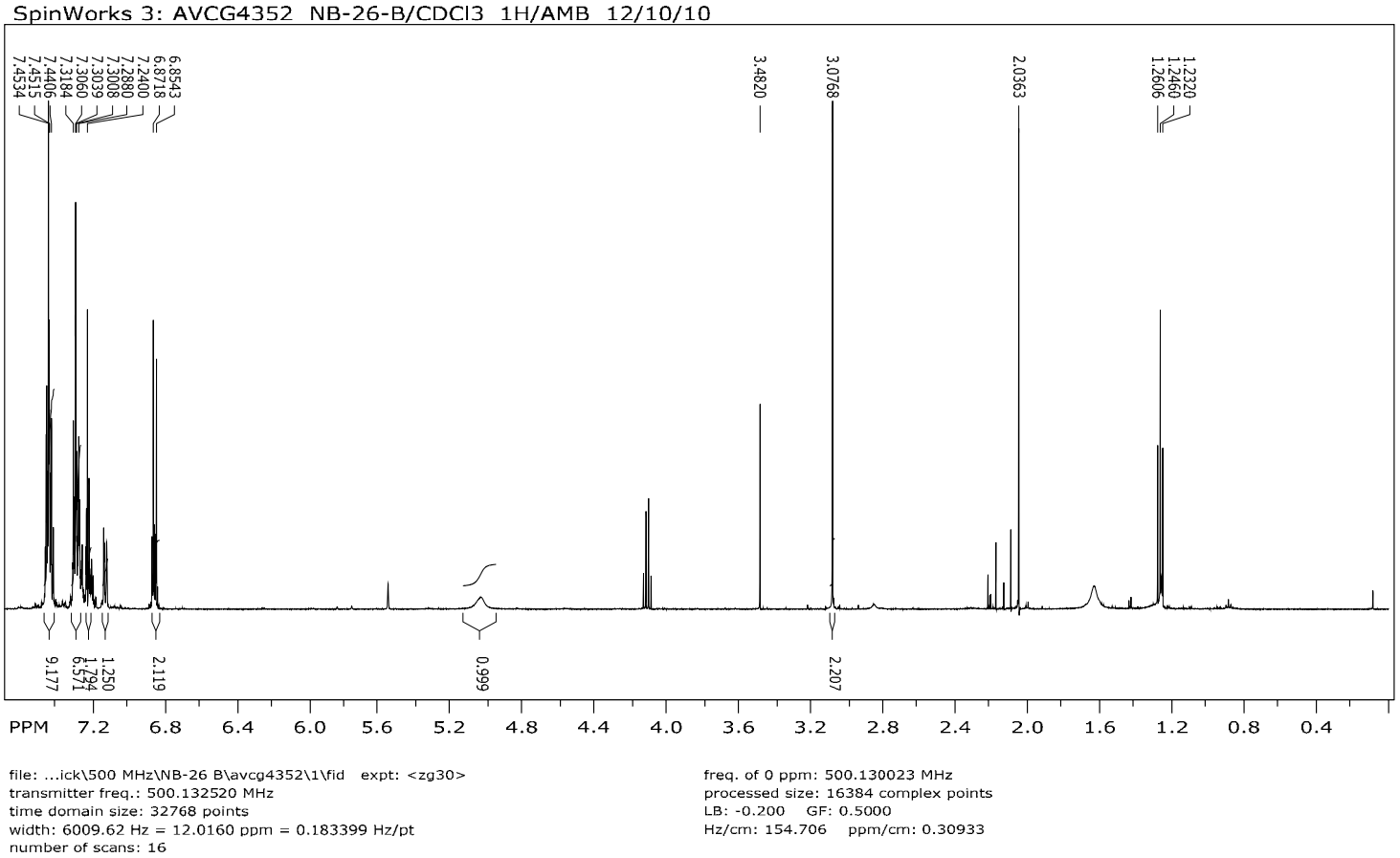

file: ...ick\500 MHz\NB-26 B\avcg4352\1\fid expt: <zg30>
transmitter freq.: 500.132520 MHz
time domain size: 32768 points
width: 6009.62 Hz = 12.0160 ppm = 0.183399 Hz/pt
number of scans: 16

freq. of 0 ppm: 500.130023 MHz
processed size: 16384 complex points
LB: -0.200 GF: 0.5000
Hz/cm: 154.706 ppm/cm: 0.30933

^{13}C NMR ($CDCl_3$, 125 MHz) of **8OMe**

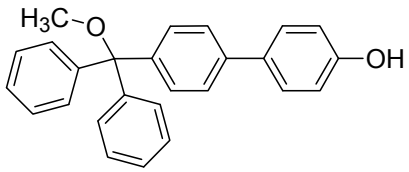

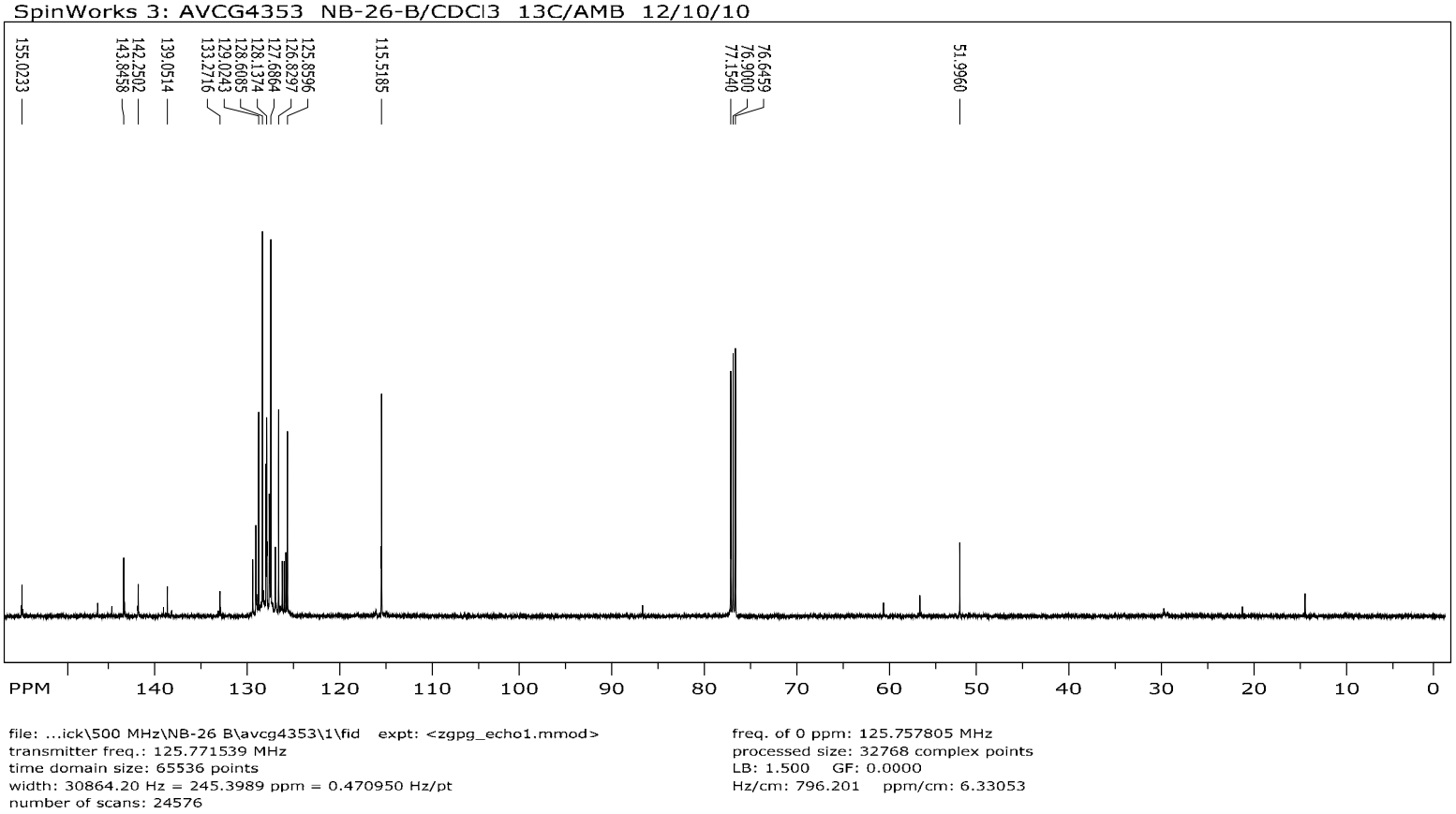

file: ...ick\500 MHz\NB-26 B\avcg4353\1\fid expt: <zgpg_echo1.mmod>
transmitter freq.: 125.771539 MHz
time domain size: 65536 points
width: 30864.20 Hz = 245.3989 ppm = 0.470950 Hz/pt
number of scans: 24576

freq. of 0 ppm: 125.757805 MHz
processed size: 32768 complex points
LB: 1.500 GF: 0.0000
Hz/cm: 796.201 ppm/cm: 6.33053

^{1}H NMR ($CDCl_3$, 500 MHz) of **12**

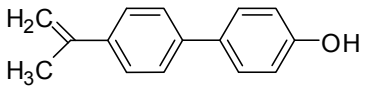

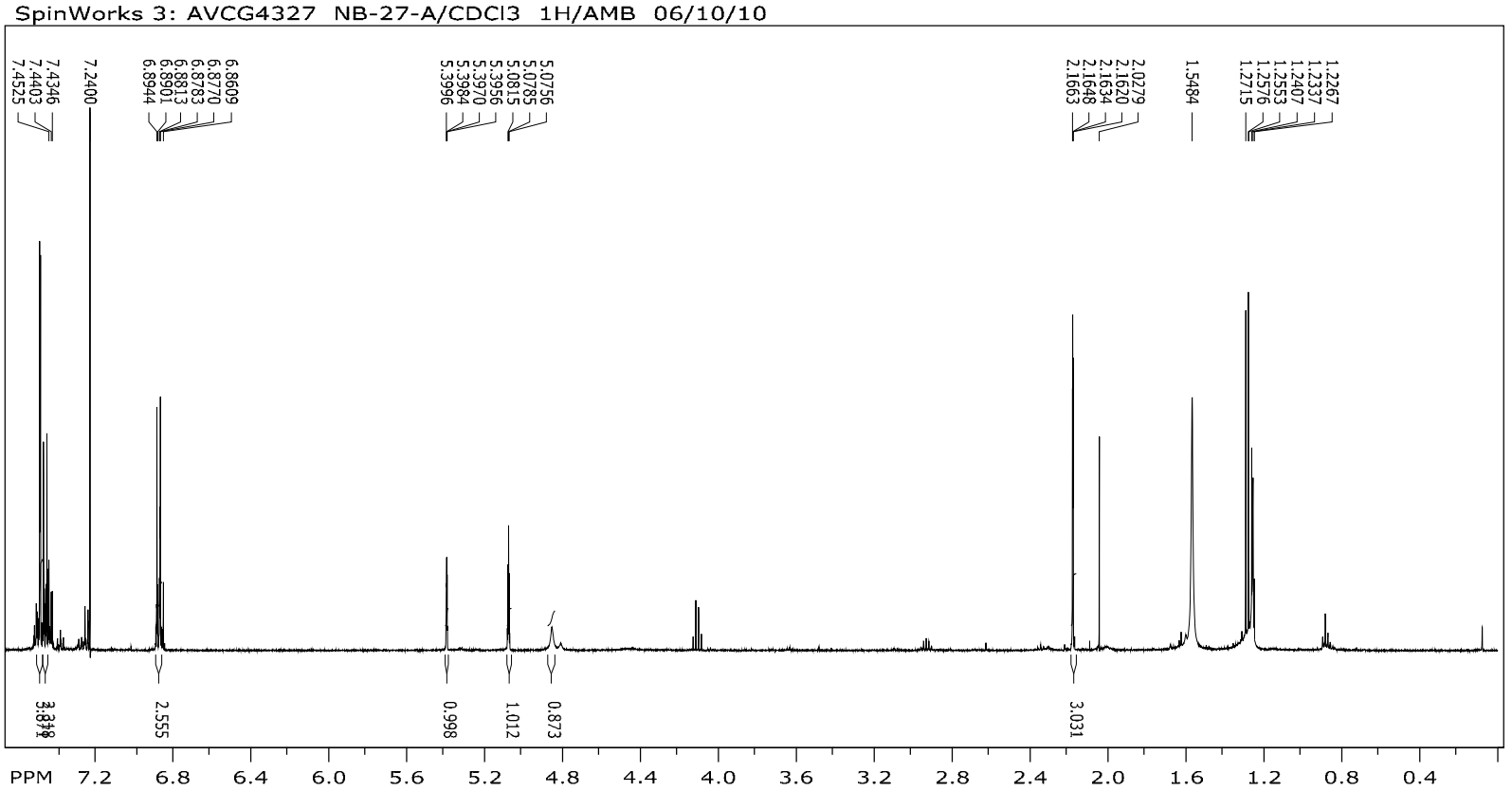

file: ...Nick\500 MHz\NB-27A\avcg4327\1\fid expt: <zg30>
transmitter freq.: 500.132520 MHz
time domain size: 32768 points
width: 6009.62 Hz = 12.0160 ppm = 0.183399 Hz/pt
number of scans: 16

freq. of 0 ppm: 500.130023 MHz
processed size: 16384 complex points
LB: -0.200 GF: 0.5000
Hz/cm: 154.221 ppm/cm: 0.30836

^{13}C NMR ($CDCl_3$, 125 MHz) of **12**

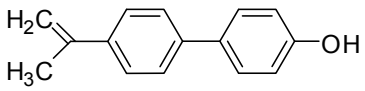

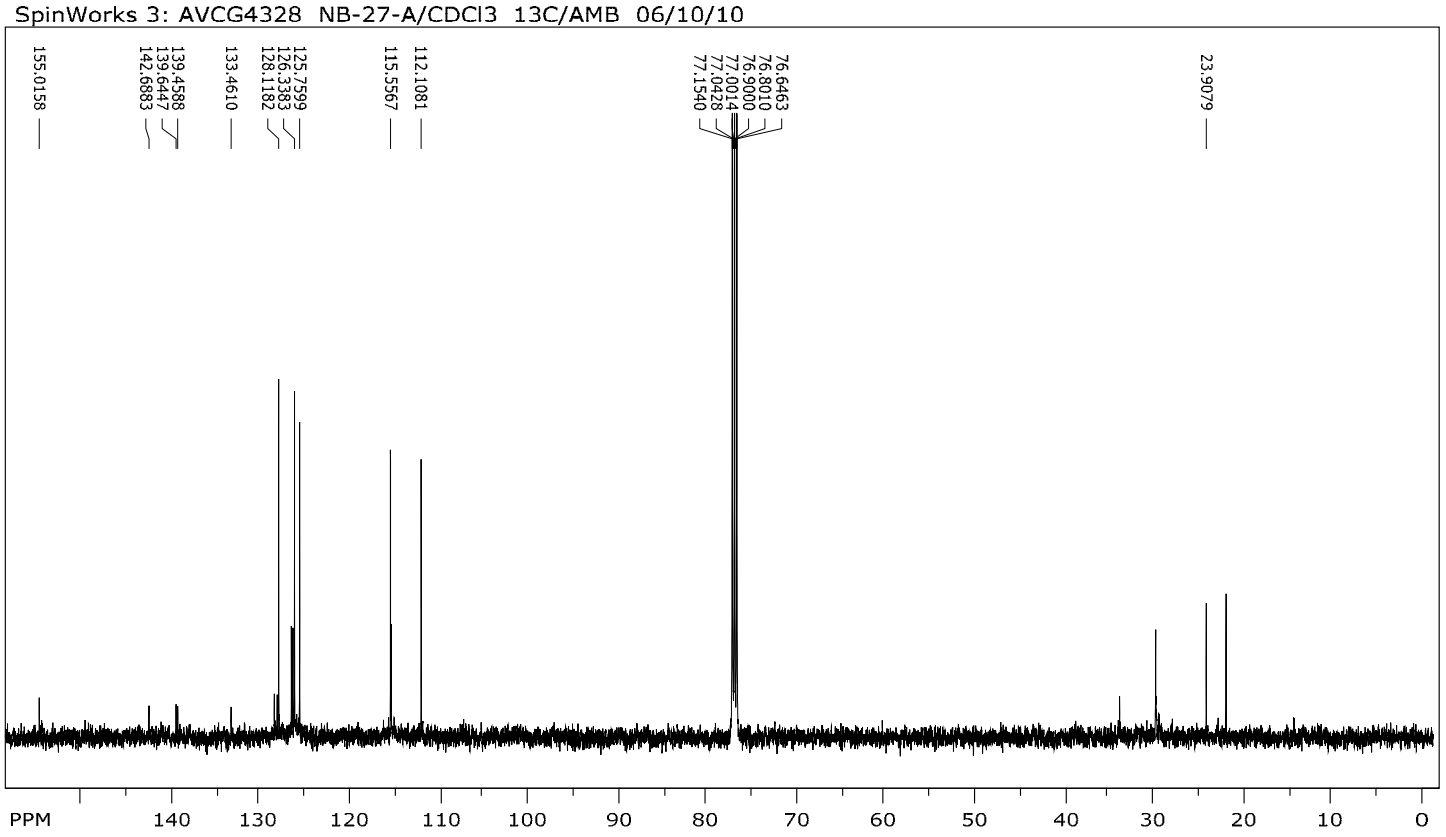

file: ...Nick\500 MHz\NB-27A\avcg4328\1\fid expt: <zgpg_echo1.mmod>
transmitter freq.: 125.771539 MHz
time domain size: 65536 points
width: 30864.20 Hz = 245.3989 ppm = 0.470950 Hz/pt
number of scans: 24576

freq. of 0 ppm: 125.757802 MHz
processed size: 32768 complex points
LB: 1.500 GF: 0.0000
Hz/cm: 806.994 ppm/cm: 6.41635

^{1}H NMR ($CDCl_3$, 500 MHz) of **9OMe**

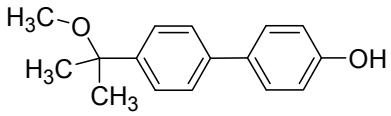

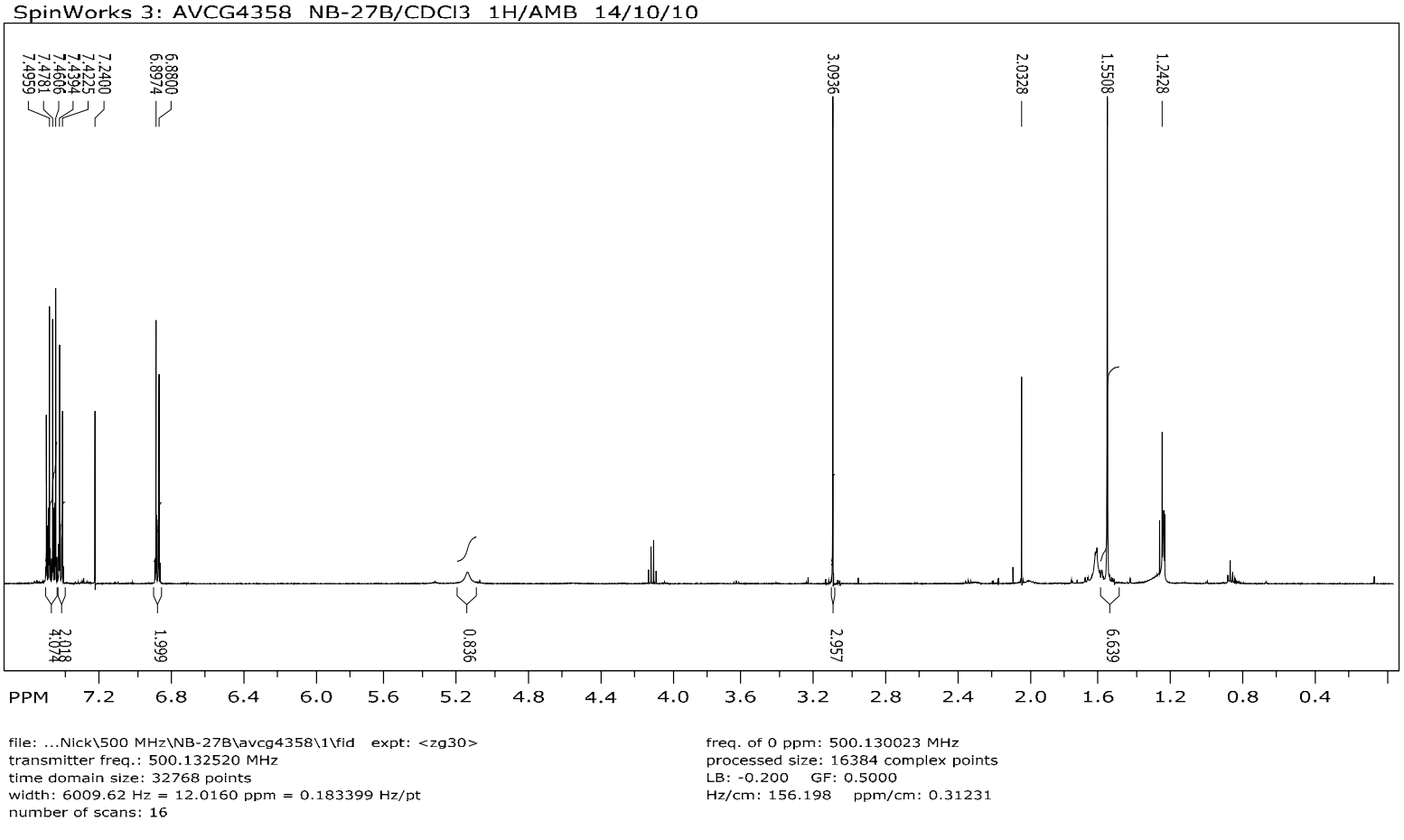

file: ...Nick\500 MHz\NB-27B\avcg4358\1\fid expt: <zg30>
transmitter freq.: 500.132520 MHz
time domain size: 32768 points
width: 6009.62 Hz = 12.0160 ppm = 0.183399 Hz/pt
number of scans: 16

freq. of 0 ppm: 500.130023 MHz
processed size: 16384 complex points
LB: -0.200 GF: 0.5000
Hz/cm: 156.198 ppm/cm: 0.31231

^{13}C NMR ($CDCl_3$, 125 MHz) of **9OMe**

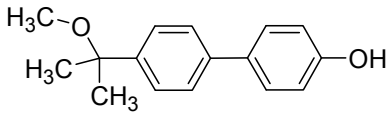

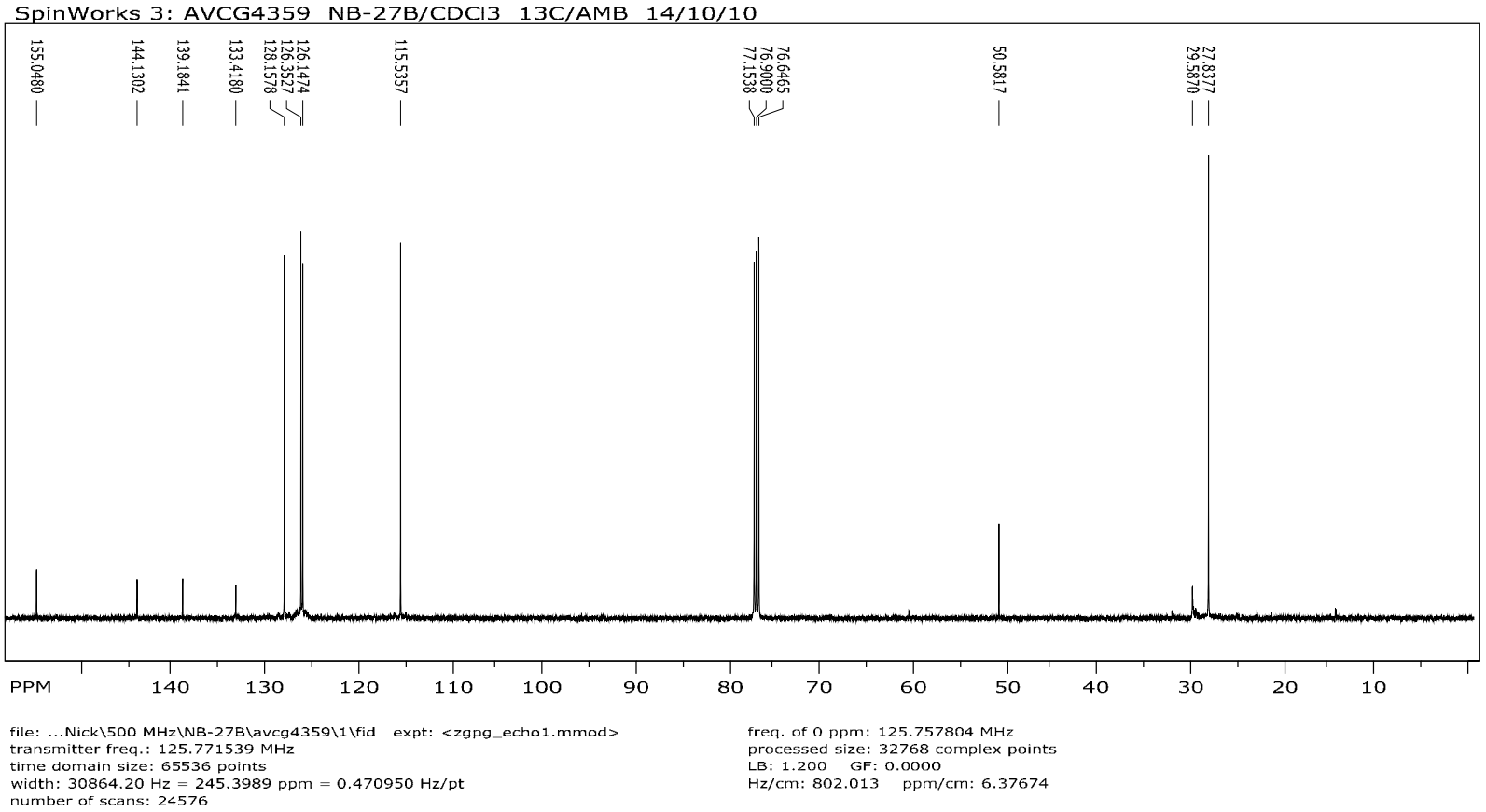

file: ...Nick\500 MHz\NB-27B\avcg4359\1\fid expt: <zgpg_echo1.mmod>
transmitter freq.: 125.771539 MHz
time domain size: 65536 points
width: 30864.20 Hz = 245.3989 ppm = 0.470950 Hz/pt
number of scans: 24576

freq. of 0 ppm: 125.757804 MHz
processed size: 32768 complex points
LB: 1.200 GF: 0.0000
Hz/cm: 802.013 ppm/cm: 6.37674